" THE TURBULENT MIXING OF A TWO-DIMENSIONAL JET OF FOREIGN GAS WITH A MOVING AIR STREAM "

By

A.A.M.M. El-Ehwany

B.Sc.(Eng.), D.I.C.

A Thesis submitted for the Degree of Doctor of Philosophy in the Faculty of Engineering of the University of London.

Aeronautics Engineering Department,
Imperial College of Science and Technology,
London.

September, 1965.

SUMMARY.

Experimental results are presented for the turbulent mixing of plane jets of air, helium and Arcton 12 issuing into a moving air stream. Only the diffusion of mass and momentum have been considered since both streams were of equal temperature. Transverse and centre-line velocity and concentration distributions are obtained for both jet and wake-like flows i.e. ($\frac{U_j}{U_m} > 1$) and ($\frac{U_j}{U_m} < 1$). Despite the large differences in density, the experimental free jet data ($U_j > U_m$) revealed, on the whole, that the assumption of an approximate self-preserving flow led to a quite reasonable prediction for the centre-line quantities and the jet growth. Measurements for the free wake ($U_j < U_m$) showed that the flow is self-preserving and that the wake model is relevant. It is found from the measurements of the centre-line concentration that none of these conditions $\frac{U_j}{U_m} = 1.0$, $\frac{\rho_j U_j}{\rho_m U_m} = 1.0$, $\frac{\rho_j U_j^2}{\rho_m U_m^2} = 1.0$ or even $\frac{H}{s} = 1.0$ (where H is the excess momentum flux ratio) gave the criterion for minimum mixing.

Measurements of the turbulent wall-jet showed that the assumption of a nearly self-preserving flow

(outside the wall-layer) leads to a reasonable prediction for the decay of the peak velocity and the wall-jet growth provided that ($H/s \geq 2$). The data for a weak wall-jet ($\frac{H}{s} < 2$) did not agree with Glauert's theory and the flow ceased to be self-preserving. For such weak wall-jets and film cooling flows, Stollery's boundary-layer model is more appropriate.

A C K N O W L E D G E M E N T

The Author wishes to record his indebtedness to Mr. J.L. Stollery, under whose supervision this work was carried out, for his continued interest, encouragement and guidance.

The author would also like to thank Dr. J.K. Harvey for his many helpful suggestions, concerning the experimental apparatus.

Thanks are also due to Mr. B.J. Belcher and the staff of the Electronics workshop, for their valuable assistance in the construction of some of the apparatus.

The author is grateful also to the members of the Departmental workshop who constructed the model; and to the Northern Research and Engineering Corporation, for their help in supplying some of the helium gas.

Finally, the author is very greatly indebted to the Government of the United Arab Republic, for the award of a scholarship which enabled him to carry out his studies in the United Kingdom.

CONTENTS.

LIST OF SYMBOLS

A	Cross-sectional area in^2
A^*	" " " at the throat of the metering Nozzle See figure (1-a) (in^2)
A_1, A_1'	Constants given by equations (6.4.2.10),(6.4.2.11)
a, b	Profiles constants (Mass-flux and Momentum-flux profiles)
B_1	Proportionality constant in the boundary-layer thickness formula.
C	Mass fraction concentration in percentage
C_1, C_2	Proportionality constants in equations (5.2.16),(5.2.18).
c, c'	Mixing length constants $c = l/\delta$ (e.g. Tollmien[16] $c' = l/x$ (e.g. Kuethe [35])
C_D	Drag Coefficient $\left(\frac{D}{\frac{1}{2}\rho U_m^2 A}\right)$
C_{Ds}	Drag Coefficient based on slot width = $\left(\frac{D}{\rho_m U_m^2 s}\right)$
C_p	Specific heat under constant pressure
D	Drag Force
D_{12}	coefficient of laminar diffusion of one gas into another.
E_2	Constant defined in the text as $\left[\Gamma\left(\frac{n+3}{n+2}\right)\right]^{n+2}$

f	Similarity function
H	Local excess momentum flux ratio $=\left(\frac{J}{\rho_m U_m^2}\right)$ (or jet momentum thickness)
h^o	Specific stagnation enthalpy BTU/lb
I	$\int_{-\infty}^{+\infty} e^{-a\eta^2} d\eta$
$I_{(U,P)}$	$\int_0^1 \left(\frac{\rho U}{\rho_m U_m}\right)\left(\frac{P - P_m}{P_w - P_m}\right) d\eta$
J	Jet excess momentum flux $= \left(\int_{-\infty}^{+\infty} \rho U(U - U_m)dy\right)$ away from the slot
K	Mole fraction concentration or concentration by volume in percentage.
k	Thermal conductivity.
l_o	The mixing length in Prandtl's theory of turbulence.
M	Molecular weight of the gas.
M^*	Mach Number
m	Mass flux parameter $(\rho_j U_j / \rho_m U_m)$
$m^\cdot$	Mass flow rate lb/ft^2/sec : $\int_{-\infty}^{\infty} \rho v dy$
m_e	Dimensionless mass flow rate $(m^\cdot / \rho_m U_m)$
N	Number of molecules of the gas
n	Power Law index
$P_{(x,y)}$	Conserved property (mass fraction concentration or specific total enthalpy)

P_r Prandtl Number $(C_p \mu / K)$ (dimensionless)

p pressure lb/in^2

R characteristic gas constant, $Pdal.ft/lb.F^\circ$

R_{ej} Slot Reynolds Number (dimensionless) $= \left(\frac{\rho_j U_j s}{\mu_j}\right)$

R_{ex} Freestream Reynolds Number " $= \int_0^x \frac{\rho_m U_m dx}{\mu_m}$

R_{em} Reynolds Number based on boundary-layer thickness (dimensionless) $= \int_0^\delta \frac{\rho_m U_m \, dy}{\mu_m}$

S_c. Schmidt Number $\left(\frac{\rho D_{12}}{\mu}\right)$ (dimensionless)

s slot height

T Temperature

U x-component velocity

u x-component turbulent velocity

U_τ Friction velocity $\sqrt{\tau_w/\rho}$

U_o Velocity difference on the jet or wake axis $= U_{max} - U_m$

U_{max} Centre-line velocity for jets and wakes and maximum velocity for wall jets

V y-component velocity

v y-component turbulent-velocity

x, y Cortesian coordinates

x_{pc} The potential core length of the jet

X Transform coordinate $= \int_0^x f(x)\, dx$

Z Transform Coordinate $= \int_0^y \rho/\rho_m \, dy$

GREEK SYMBOLS

α Similarity parameter in Glauert's profile

β , Molecular weight parameter $\left(\frac{M_j}{M_m} - 1\right)$

Γ Gamma function

γ , Specific heat ratio C_p / C_v

δ The characteristic width of the jet, wake or boundary-layer.

δ_m Half width at half depth of the jet, wake and wall-jet = y at $U-U_m = \frac{1}{2}(U_{max} - U_m) = .441\,\delta$

δ_i The width of the wall-layer in the wall jet = y at $U = 0.99\, U_{max}$

δ_o Velocity boundary-layer thickness = y at $U = .99\, U_m$

ϵ Eddy Kinematic viscosity (or eddy diffusivity)

$\bar{\epsilon}$ Used as Eddy Kinematic viscosity for incompressible flow (Sec. 4.2.1.)

ϵ^* Ratio of eddy kinematic viscosity to laminar kinematic viscosity = $(\rho\epsilon/\mu)$

η x-transform coordinate $\int_o^x \epsilon(x)\, dx$

η Similarity variable (y/δ) or (y/δ_m) , $\eta_i = (y/\delta_i)$

θ_j Initial momentum thickness at the slot = $\left[\frac{\rho_j}{\rho_m}\,\frac{U_j}{U_m}\left(\frac{U_j}{U_m} - 1\right)s\right]$

μ Coefficient of absolute viscosity (laminar)

ξ y/x

ρ Density of the fluid

ν Kinematic viscosity

σ Similarity parameter in the velocity profile

τ Shearing Stress

ψ Stream function

Suffices

c	concentration
j	jet values at exit
m	mainstream values
max	maximum or centre-line values
t	turbulent
u	velocity
w	wall values.

Other symbols which are not present in the above list should be adequately defined in the text.

I. INTRODUCTION

Many fluid flows of practical interest are of the turbulent type. Of all aerodynamic problems free turbulent shear flows are among the most important.

A well known type of free turbulent shear flow is the mixing layer flow, which occurs between two streams moving at different speeds in the same or opposite direction. A free jet occurs when a fluid is discharged from a slot or orifice into a large volume of stagnant fluid, or into a moving stream of relatively lower velocity. A free wake is normally formed behind a solid body which is being dragged through fluid at rest or behind a solid body which has been placed in a stream of fluid.

In the two dimensional field, most of the turbulent jet mixing work reported previously has been concerned with a jet of fluid issuing into a stagnant environment of the same fluid which is one example of a self-preserving flow. Most of the relevant references can be found in recent surveys by Abramovich[1] and Schlichting[2]. The sole experiment with a jet expanding into a moving stream reported by Weinstein[3] et al - used streams of the same density

with the jet velocity greater than the free stream velocity. No experimental results have been reported where the jet velocity is less than the free stream velocity. Such a flow is of great interest for combustion chamber cooling. For a jet issues into a moving stream self-preservation is only possible for the regions where ($U_o \gg U_m$) or ($U_o \ll U_m$) (e.g. Townsend [4]) where (U_o) is the difference between the centre-line velocity and the free stream velocity; i.e. for the plane jet and at far downstream for the wake.

The most important problem, however, arises when one gas is injected into an entirely different one moving in the same direction. The practical motivation for such an investigation has been the mixing of gas fuel in a combustion chamber, utilizing the diffusion flame (e.g. Ferri[5]).

The phenomena of turbulent mixing between two moving streams of gases of widely differing density is difficult to resolve and the analytical treatment of this problem is greatly impeded by the present limited knowledge of the fundamentals of turbulent transport of mass, momentum and energy. All the theories employ empirical constants which have

to be found from the experimental results. The work that has been done so far on this complex problem has concentrated entirely on the round jet into a quiescent or moving stream as indicated by the following Table.

Table 1.

Reference	type of jet	jet gas used	findings and remarks
Rundun[6]	Round jet $U_m=o$	hot air	energy diffused more rapidly than momentum.
Corrsin[7]	Round jet $U_m=o$	hot air	
Keagy & Weller[8]	Round jet $U_m=o$	H_e, CO_2, and N_2	Mass diffused more rapidly than momentum.
Forstall & Shapiro[9]	Round jet $U_m \neq o, U_j > U_m$	10% helium as tracer gas	($S_c < 1$) and was constant, independent of velocity ratios.
Vulis[10] (1955)	Round jet $U_m=o$	hot air, H_2 CO_2, O_2 and Steam	No concentration measurements.

Table cont...

Reference	type of jet	jet gas used	findings and remarks
Vulis[11] (1961)	Round jet $U_m \neq o$	hot air	$(\rho_j U_j^2 / \rho_m U_m^2)$ was the mixing parameter.
Regsdal[12] & Weinstein	Round jet $U_m \neq o$	Br	Concentration measurements only.
Ferri[13]	Round jet $U_m \neq o$	H_2	The free stream was supersonic
Zakkay[14]	"	H_2, H_e and Argon	" "
Alpinieri[15]	"	H_2, CO_2	High subsonic free stream, Sc = 0.5

According to the previous table, all the workers have agreed that both energy and mass diffuse more rapidly than momentum and the lighter the jet gas, the more rapid the centre-line decay. Despite the analytical studies presented by Tollmien[16], Schlichting [2] and Townsend [4] concerning the turbulent decay in incompressible self-preserving jets and wakes, relatively little has appeared regarding the more complicated problem of foreign gas injection.

The most recent attempts have concentrated on obtaining correlation of the experimental data; for instance, Cmax or Umax, using an eddy viscosity concept. Such work was reported by Ferri [13], Libby[17], Zakkay[18], Alpinieri[15] and Regsdal [12]. The semi-empirical formulae for the eddy viscosity used by these workers were all different in the sense that each formula assumes that the turbulent mixing process is due to a different flow parameter. Libby [17], for example, used a turbulent viscosity which was proportional to the maximum difference in the mass flux at a given station and has attributed the mixing process to be solely dependent on the mass-flux ratio. Minimum mixing at $\rho_j U_j = \rho_m U_m$ was therefore predicted. Regsdal's[12] eddy viscosity was proportional to the difference in velocity across the jet $(U_{max} - U_m)$, thus attributing the turbulent mixing to be dependent on the velocity ratio of both streams and from his own experimental results minimum mixing was found at $(U_j = U_m)$. Vulis,[11] from his own measurements of the centre-line temperatures, has reported that the sole parameter governing the turbulent mixing process was the momentum flux ratio and minimum mixing was found at $\rho_j U_j^2 = \rho_m U_m^2$. Recently Alpinieri[15] has reported that none of these parameters was correct.

Plane gas jets into a general stream, however, have not received as much attention and this was one of the reasons for the current set of experiments. A considerable part of this report is concerned with the development and the gross structure of two-dimensional free jets and wakes of a foreign gas. The main objectives were:-

To obtain experimental velocity and concentration profiles for air, helium and $Arcton_{12}$, jets immersed in a moving air stream; to compare the experimental results with simple asymptotic theoretical models for turbulent self-preserving jet and wake flows; to throw a better light on the understanding of the turbulent transport process between two parallel gas streams of widely differing density and to find, if possible, the most important flow parameter that governs the mixing process.

The remaining part of the present report is concerned with the mixing of a turbulent wall jet of a foreign gas with an air mainstream. This process occurs in film cooling or heating and also finds application as a method of boundary-layer control.

This latter problem, however, has been the subject of considerable analytical and experimental

study during the past few years and these investigations, in fact, can be divided into two groups:- The first group of workers were mainly interested in uniform density streams, in which the injection velocity was very much greater than the free-stream velocity. Most of their analytical treatments were based on the assumption that, except for the small wall-layer, the flow is approximately self-preserving (e.g. Glauert[19]). The agreement between their experimental results and this theory was only satisfactory when $U_j \gg U_m$. No experimental data have been reported, in which the jet velocity is only slightly in excess of the freestream velocity (weak wall jet); or when the jet velocity is less than the freestream velocity (wall jet with initial momentum deficit or wall wake).

The second group of workers were investigating the film cooling problem to an adiabatic wall under constant pressure. The density of the stream was nearly uniform and the sole experiment which dealt with dissimilar gases has been reported by Hatch and Papell[20], who injected helium as a coolant into a hot air stream. The experimental results for film cooled adiabatic walls, together with a survey of previous

analytical treatments, can be seen in the report by Stollery and the author [21] (to be found in a pocket to this thesis.). In this note it is suggested that far downstream from the slot the flow should behave like a fully developed turbulent boundary-layer. A simple theoretical model was developed and extended to cover the case of foreign gas injection. According to the flow parameters and the density ratios examined in this note, the utility of Stollery's boundary-layer model is limited to $m \leqslant 1.50$. The present report generalizes this model for any conserved property at the wall (e.g. concentration) and investigates its utility over a wider range of density ratios.

2. Apparatus and test facilities.

All the tests were carried out in two of the low speed wind tunnels in the Aeronautics department, Imperial College.

2.1 Wind Tunnel.

2.1.1 Test with streams of the same density.

a. The Primary Stream.

The 3'x2' closed circuit low speed wind tunnel was used. The tunnel has 12' long working section and has a maximum test section velocity of 160ft./sec. Bleed slots at the end of the working section ensure a constant mass flow rate through the test section during the run.

b. The secondary stream

The secondary air was supplied to the tunnel through an aerofoil shaped injection slot, shown in fig. (1a). The slot width was $\frac{1}{2}$" and spanned the 2' wide tunnel working section, as shown in figure (1b). The basic elements of the injection slot were as follows:-

1. The plenum chamber:- 1" diameter steel pipe 42" long, fitted with a series of 1/16" diameter holes, spaced at 1/4" intervals. The working pressures inside the pipe were such that the small holes were choked. The pressure was between 55-75 p.s.i.a. The plenum chamber was connected to the high pressure supply, available in the laboratory, by means of rubber hosing through a pressure regulator and controlled by a throttle valve.
2. The Diffuser:- 4" long and had a 24" span, with a total diffusing angle of 12°. Three gauze screens of 12 mesh were fitted at equal spaces along the diffuser to

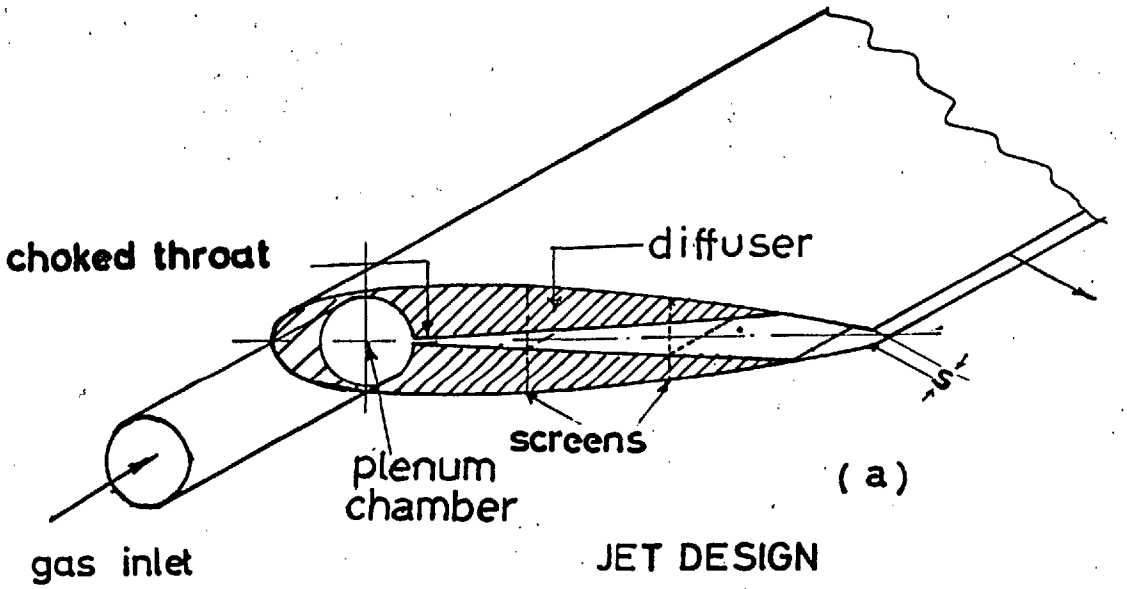

(a)

JET DESIGN

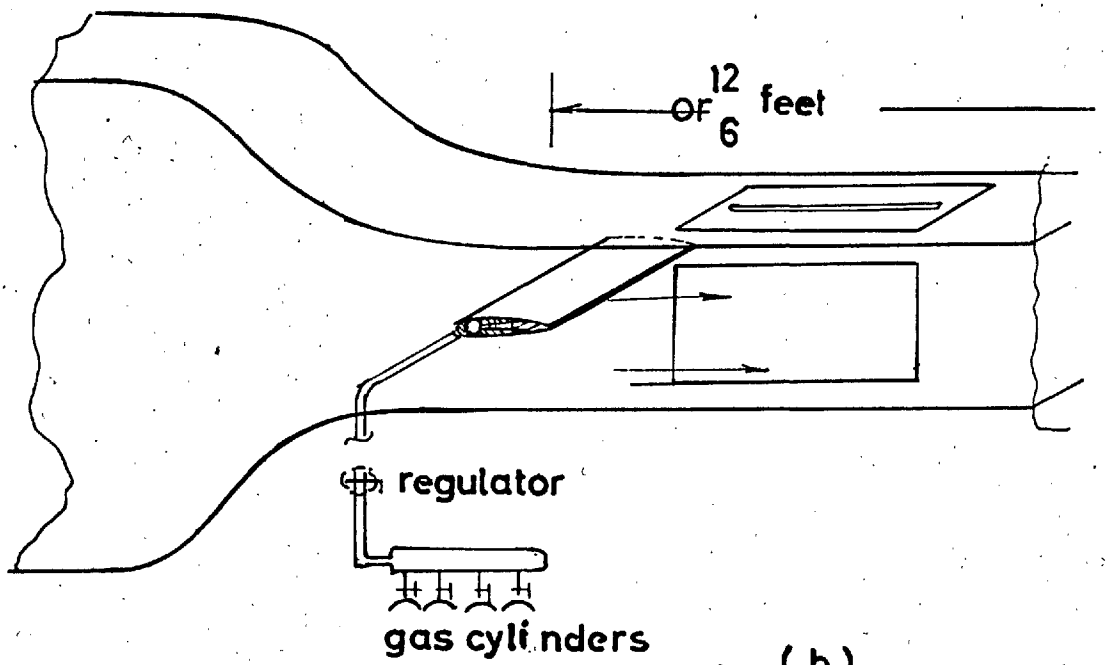

(b)

JET IN THE TUNNEL

FIG. (1)

obtain a uniform total pressure along the span of the slot. For this particular design (using a choked throat), the velocity distribution at the slot exit was found to be two dimensional to $\pm$ 3% except within one inch of the tunnel side walls. The maximum jet Reynolds' number based on slot width was 12,000.

2.1.2 Test with dissimilar gas streams.

a. Primary stream

The 18"x18" open circuit low speed wind tunnel was used. The tunnel has a 6 ft. long, square working section and a maximum test section velocity of 104 ft./sec. at full throttle. Speed control was achieved by throttling the air at inlet to the tunnel fan. Hence the turbulent intensity in the working section was probably higher at the lower tunnel speeds.

b. Secondary gas stream (Helium and $Arcton_{12}$)

The secondary gas stream was supplied to the tunnel through a two-dimensional slot similar to that shown in figure (1a). The slot width was 1/16". The secondary jet of either helium or $Arcton_{12}$ was supplied from high pressure bottles available commercially.

Helium bottles contain a gas volume equivalent to 200 cu. ft at N.T.P., at a maximum pressure of

2000 p.s.i.g. The chemical name of the refrigerant Arcton$_{12}$ is dichlorodifluoromethane and its chemical formula is (C Cl_2 F_2), the physical data can be obtained from reference (22).

The Arcton $_{12}$ cylinders contained 126 lb. wt. of liquid under 57 p.s.i.a at 70° F. An arrangement was made to utilize more than one bottle at a time (see figures 1c and 1d). This was done by introducing a common manifold connecting 4 cylinders through high pressure rubber hosing. The gas (helium or Arcton$_{12}$) was then supplied to the slot plenum chamber from this common header through a pressure regulator valve. A pressure gauge was fitted to the low pressure circuit, to check the regulator pressure gauge reading. Again, the working pressures were sufficiently high so that choking occured at the throat.

The maximum jet Reynolds' numbers were 1000 for helium and 7,000 for the Arcton$_{12}$ jet.

2.2. Instrumentation and traversing gear

Measurements consisted of total head, static pressure, and concentration by volume.

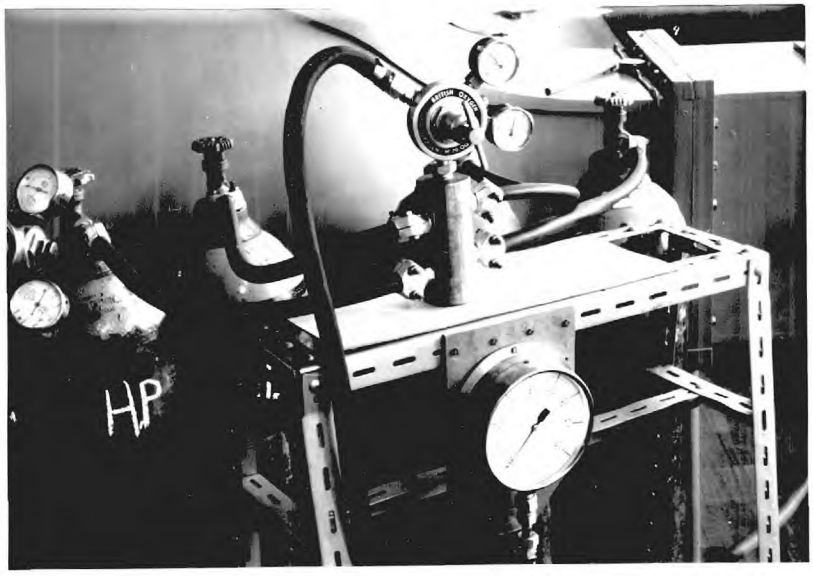

Fig.(1-c) The pipe connection for helium bottles

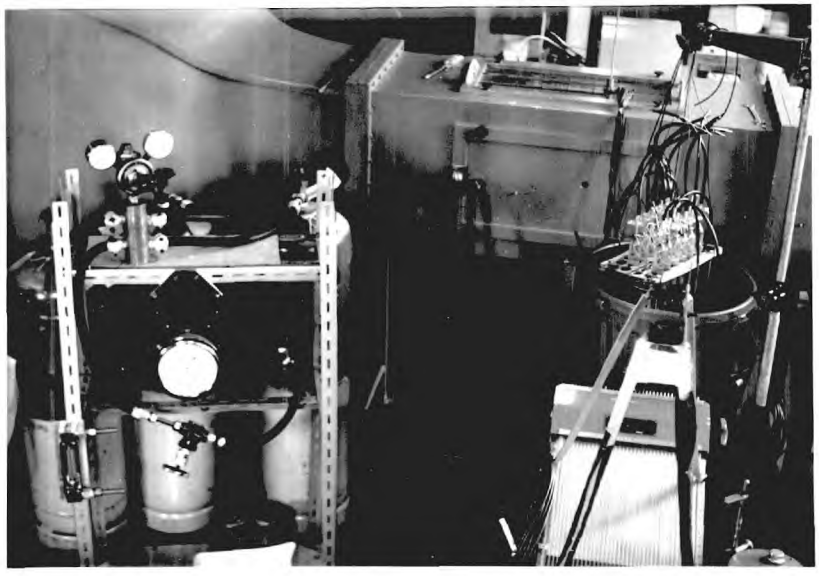

Fig.(1-d) The sampling bottles (on the right) and the pipe connection for the $Arcton_{12}$ bottles.

2.2.1 Similar density stream

Velocity traverses were made, using a probe assembly, consisting of a total head and static pressure tubes, placed ½" apart. The total head tube was 0.045 int. diameter, the static pressure tube was 1/16" external diameter with four equi-spaced radial holes of 0.005" diameter. The probe assembly was mounted on the micrometer head of the traverse gear mechanism installed on the tunnel roof; see figs. (1-e , 1-f) The probes could be positioned to an accuracy of ± 0.01" in the y direction and ± 0.03" in the other directions. The pressures were measured by means of a multi-tube alcohol monometer. The tunnel speed was measured from the reference pressure using the Betz monometer.

2.2.2 Dissimilar gas streams.

The mixing region was surveyed at various downstream locations to obtain the velocity and concentration profiles, using a pitot-static rake, (as shown in fig. 1-g). The rake consisted of four 1/16" external diameter stainless steel static pressure tubes. The total pressure tubes were 1/16" internal diameter and were also used to collect gas samples for the concentration measurement. There are

Fig.(1-e) The traverse gear mechanism of the 5'x2' wind tunnel (side view)

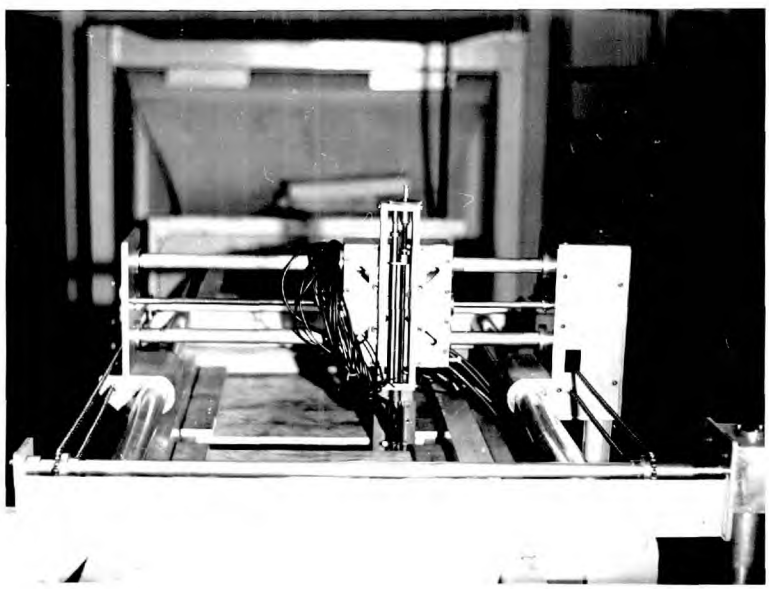

Fig.(1-f) The traverse gear mechanism (plane view)

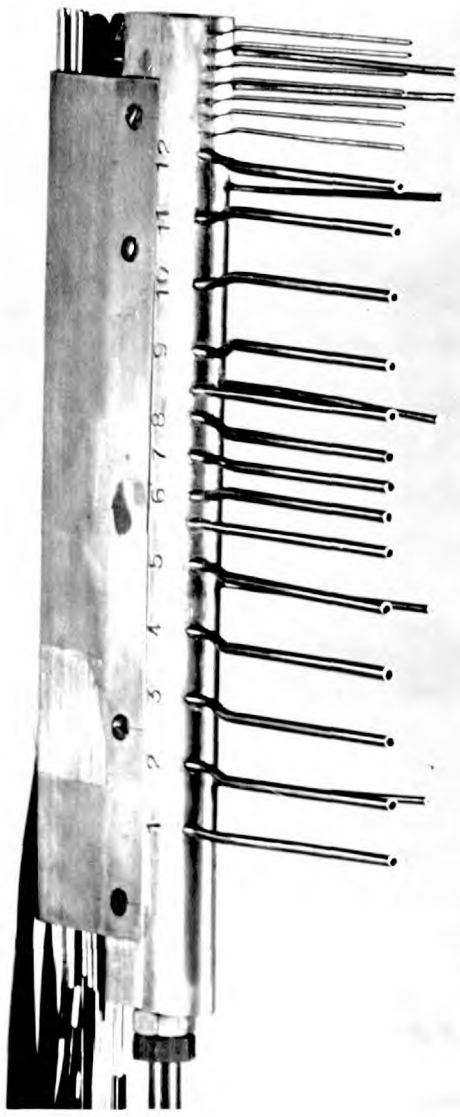

Fig.(1-g) Pitot-static pressure take, used also to withdraw the gas samples.

few detailed experimental data concerning the design of the sampling probes, therefore no special probe has been used. The flat-nosed tubes with constant inside diameter have proved satisfactory see section(2.6.1). The total head and the static pressures measurements were recorded photographically, by mounting the camera on the inclined alcohol manometer; thus the actual running time was minimized.

2.3. Sampling and concentration measurements.

Gas samples were withdrawn from the mixing region and collected in a series of sampling bottles each of 150 c.c. capacity. The bottles were immersed in a large tank of water and were connected to the sampling probes by means of rubber leads as shown in figure (1-d). The bottles were perfectly sealed and the volume of the rubber leads was very small compared with the bottles' volume. The sampling procedure was carried out under vacuum created by the difference in the water level in the tank and in the sampling bottles when the bottles were raised upwards. The possibility of air escaping into the sampling bottles was not likely, as the vacuum created was a few millimeters of water. It should be worth noting that the degree of solubility of helium in water is approximately

zero, and that of the $Arcton_{12}$ about 0.012% by weight. The "underwater" method is more practical than using evacuated bottles. The sampling procedure was repeated each run to make sure that the gas samples withdrawn were sufficiently representative. At the conclusion of the test run, these samples were introduced to a double range thermal conductivity cell, whose out-put was proportional to the concentration of the jet gas in the sample. The proportionality between the cell out-put and concentration was determined by a calibration. The construction and calibration of the gas analyser are given in section 2.4

2.4 "Gas Analyser"

Of the many physical properties of gases employed in analysis - thermal conductivity is the simplest and most economical to use, though it is only applicable to two component mixtures (though each component can itself be a mixture of gases e.g. air or $Arcton_{12}$)

2.4.1 General principles

If a constant electric current is passed through a platinum wire surrounded by gas in a chamber, the temperature of the wire will rise until a point of

equilibrium is reached. At this point, the electrical energy supplied to the wire will be equal to the thermal energy lost. Provided radiation, convection and direct conduction effects are minimised or remain constant, the temperature of the wire will depend on the heat lost by thermal conduction through the gas. Since the electrical resistance of a wire is proportional to its temperature, a measurement of the former may be used to determine the latter. These are the general principles of the gas analyser, or "Katharometer" (Cambridge Inst. Co.).

2.4.2 "Katharometer" basic principles:

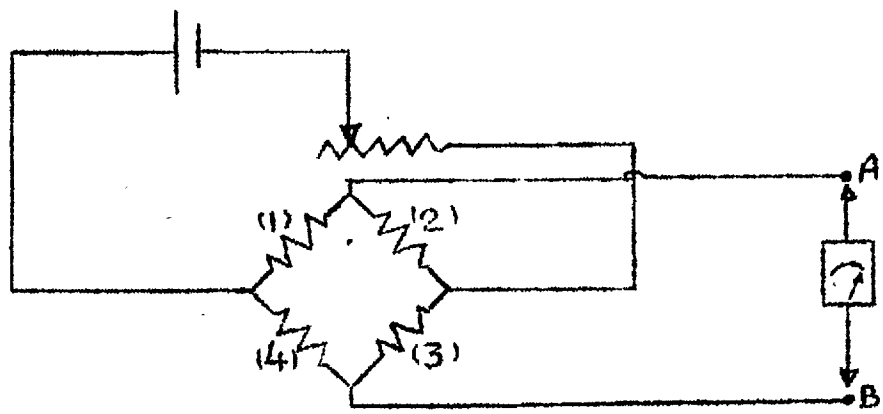

Consider the above figure; the four platinum wires 1, 2, 3 and 4 have identical electrical and thermal characteristics and are enclosed in separate cells within the Katharometer metal block (see fig. 2). Each wire forms one arm of a simple Wheatstone bridge. With constant bridge current and all four cells are open to the same gas; each wire will attain the same temperature and resistance. There will be no potential difference between points A and B i.e. the bridge is balanced and no current flows through the galvanometer. If, for example, pure air is introduced into two cells, (containing wires 2 and 4) and a helium-air mixture introduced into the remaining cells, (containing wires 1 and 3) then wires 1 and 3 will lose more heat to the walls of their cells than wires 2 and 4, since the thermal conductivity of helium is greater than that of the air. In consequence the difference in temperature, and therefore in electrical resistance of the wires, will throw the bridge out of balance causing a deflection of the galvanometer. The difference of potential between A and B and hence, the current flowing through the galvanometer, depends upon the difference between the thermal conductivity of the air and that of the helium-air mixture. The galvanometer can thus be calibrated to give directly

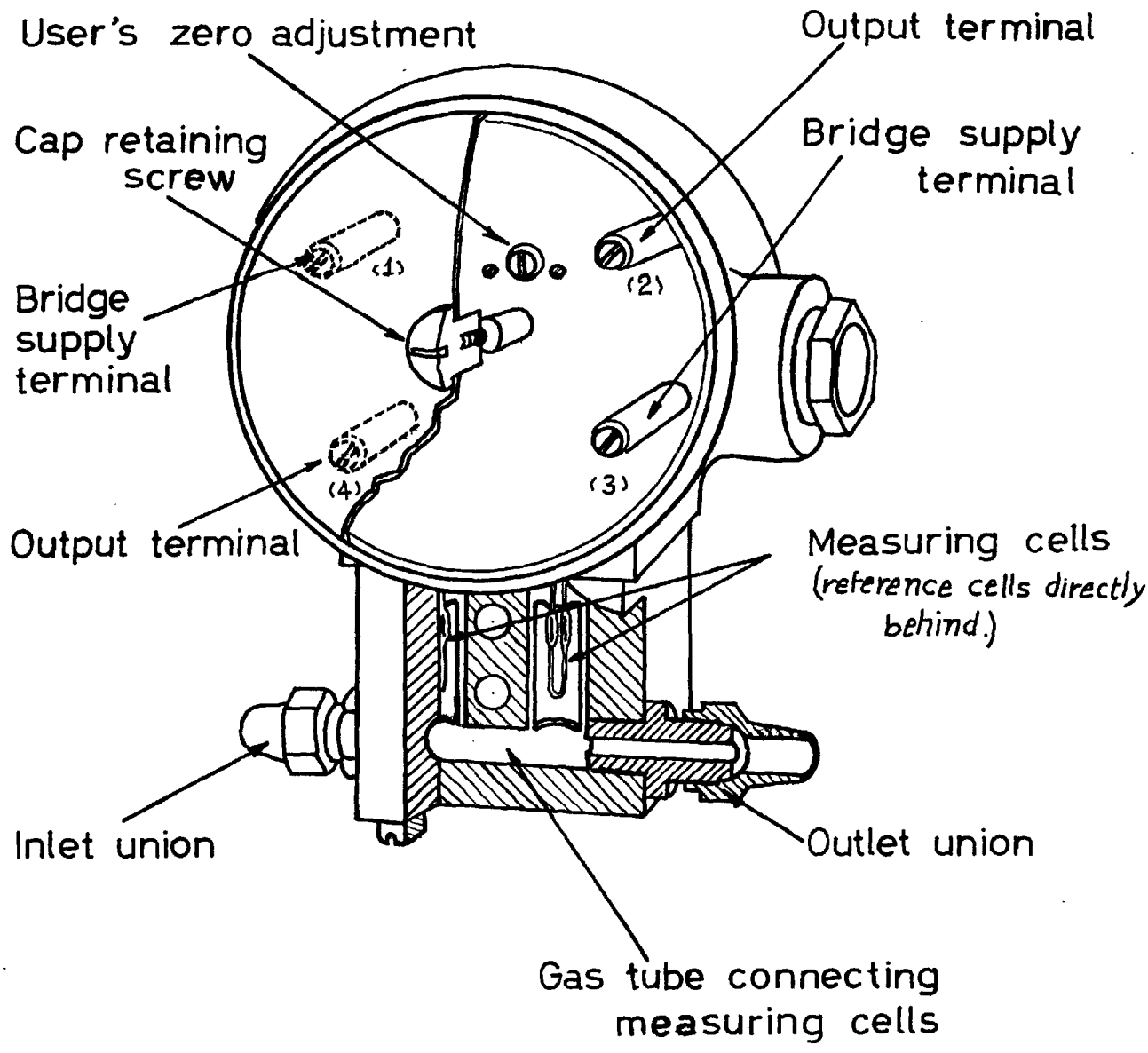

FIG. 2. Cross sectionend katharometer metal block used in the test.

the percentage of helium or of other gas in the mixture. Usually two cells are sealed with a known reference gas, and are known as reference cells, whereas the remaining two (measuring cells) are open to the sample gas. The constructional detail is shown in figure (2) as given by the Cambridge Instrument Co. The reference cells were sealed with pure air and the measuring cells were calibrated to detect both helium and $Arcton_{12}$ concentrations from 0-100%.

2.5 Gas analyser circuit and accessories

2.5.1 The electrical circuit

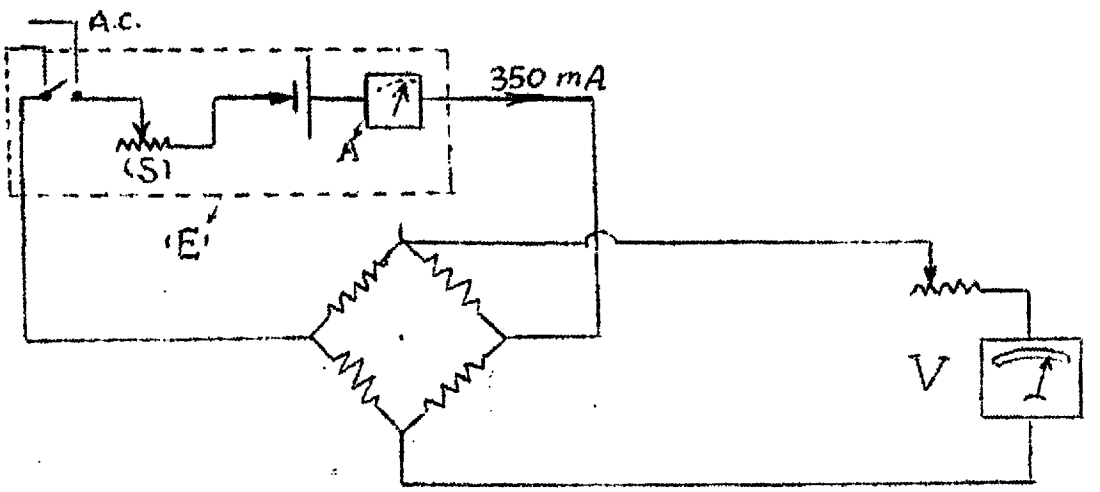

The above diagram is a simplified "Katharometer"-bridge circuit; its main components are:-

E:- is the main current supply unit, consisting of a rectifier, variable resistance (rheostat) (s) and

current indicator. This unit supplies 350 milliamps to the circuit within ± 1%. Current adjustment was by means of the rheostat (s) connected in series with the supply. A galvanometer (V) was connected in parallel to the circuit for the out-put measurements. A small variable resistance was connected in series to the galvanometer circuit to adjust the full scale reading:-

2.5.2 Gas sample circuit.

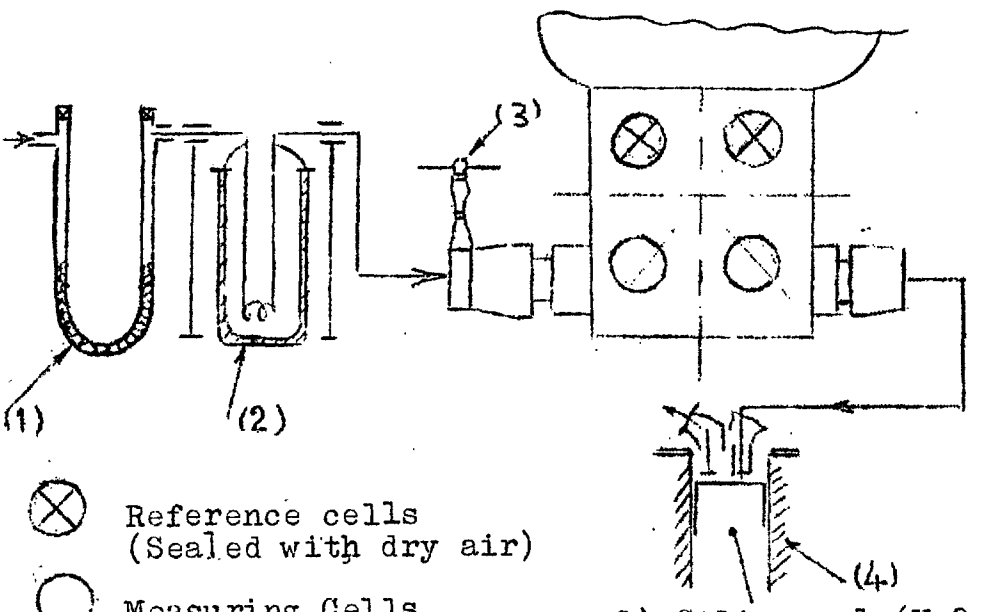

The above figure is a diagramatic sketch, outlining the gas sample circuit through the "Katharometer". The sample was first introduced to the absorption chambers, which consisted of:-

1. U glass tube, containing silica gel for H_2O absorption.
2. An insulated vessel containing liquid nitrogen for CO_2 absorption.

Though the amount of water vapour present in the sample was very small, it was felt that the water vapour might condense and block the narrow gas passages in the "Katharometer".

A small (single acting) reciprocating vacuum pump (speedivac) was used to circulate the gas sample through the "Katharometer" circuit, the amount of gas sample flow through the cell was controlled by a regulator valve, mounted at the inlet to the "Katharometer". Although thermal conductivity does not vary significantly over a wide range of mass flow rates, the best result was obtained when the mass flow rate was adjusted to 200 ml./min.

2.6 Gas analyser calibration.

This is normally in percentage by volume calibration curves were supplied by Cambridge Inst. Co

for both helium-air mixtures, and for $Arcton_{12}$ -air mixtures, as shown in figures (3a) and (3b) respectively. The following procedures were made to check these curves.

1. The zero of the meter was frequently corrected either during the test or during calibration. This was done by introducing a stream of pure, dry air into the measuring cells of the "Katharometer". The zero of the indicator was then adjusted by means of the screw head between terminal (1) and (2) of the meter, see figure (2).

2. The full scale reading was checked by introducing a stream of the pure gas (H_e and $Arcton_{12}$) and the 100% indicator deflection was checked. The small variable resistance in the output circuit was available to adjust the full scale deflection. It should be worth noting that the thermal conductivity of the $Arcton_{12}$ gas is less than that of air, hence when dealing with the $Arcton_{12}$-air mixture the output voltage terminals were reversed as the current direction was reversed. The absolute value of the voltage output was 300 millivolts for both gases at full indicator deflection. The calibration of the gas analyser was then carried out after the zero reading had been

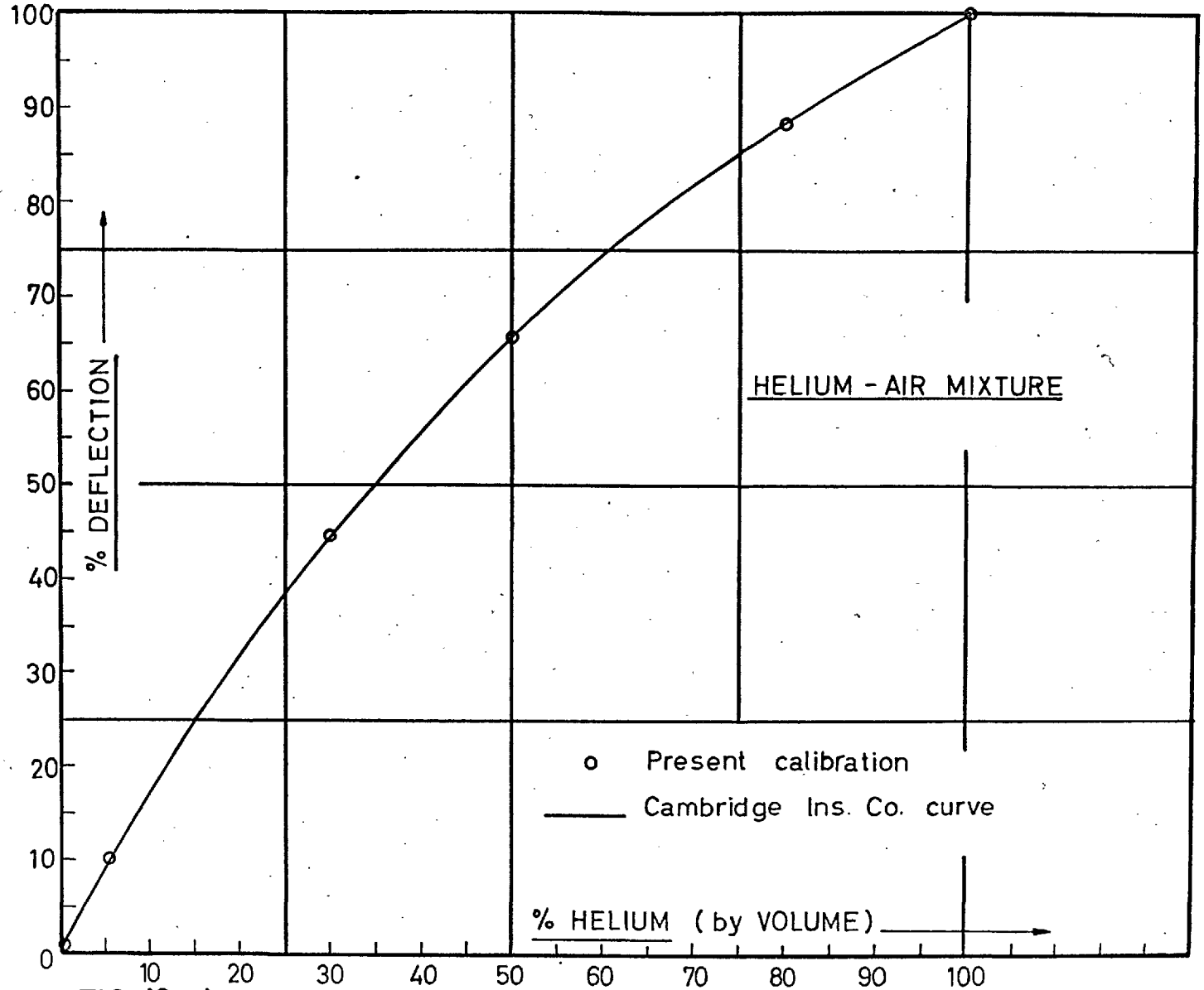

FIG. (3-a) Katharometer's calibration curve.

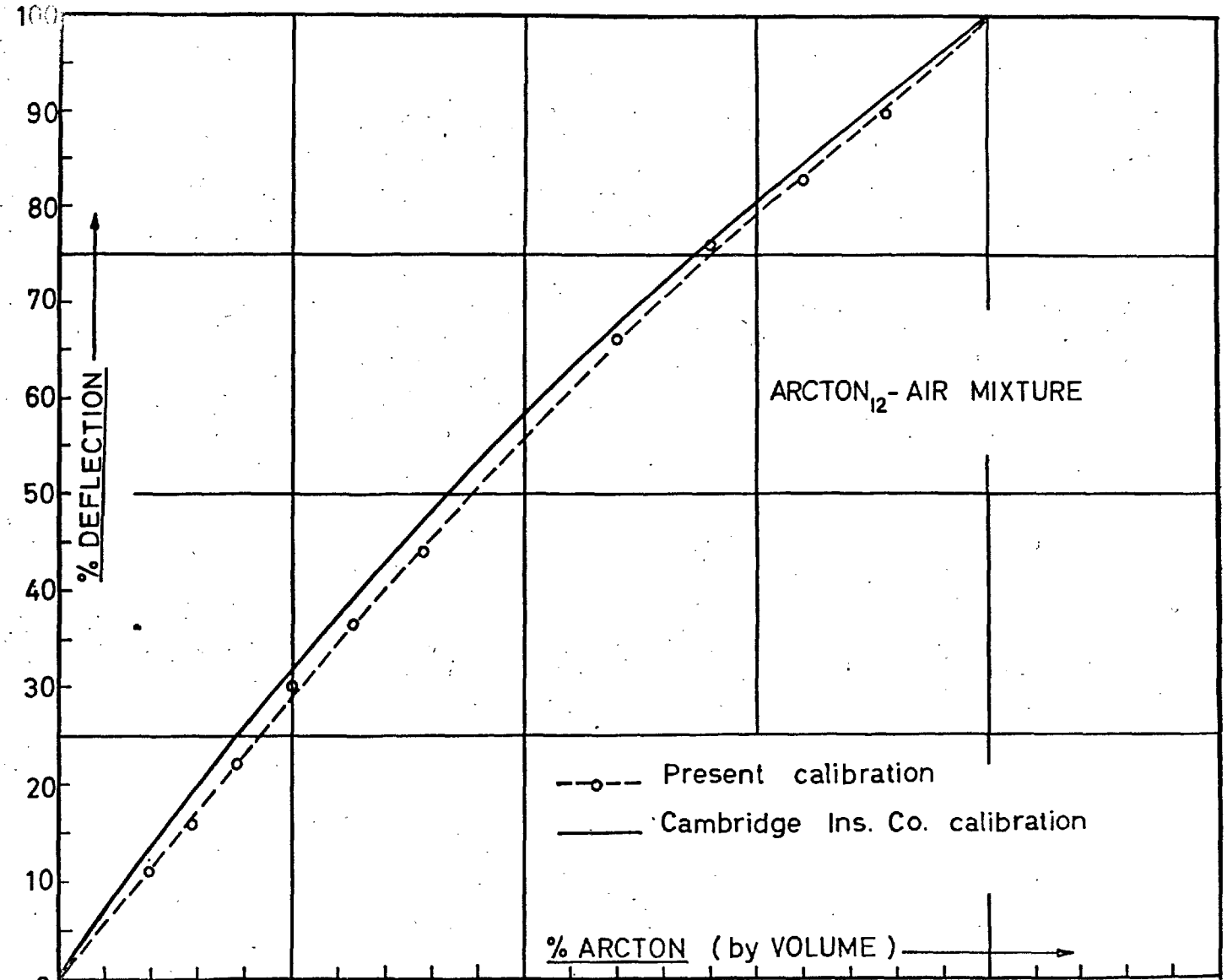

FIG.(3-b) Katharometer's calibration curve.

adjusted and the full scale deflection had been checked.

2.6.1 Calibration test procedure:-

A calibration test consisted of introducing a samples of known valumetric composition and measuring the indicator deflection. Care was taken that the samplesfed into the "Kathorometer" were under similar conditions to those of the actual test. An Orsat apparatus was employed to produce these samples of known composition. Each gas sample was thoroughly mixed with the air before it was introduced to the meter. Each point was repeated several times; and an average value was taken. The results were consistent with the supplied calibration curves, except a slight discrepancy in the $Arcton_{12}$-air mixture data, as shown by figure (3-b). Since the helium result was consistent with the Cambridge one and since the composition of the Arcton can vary widely, it was therefore decided to use our calibration data for the $Arcton_{12}$. The sensitivity of the gas analyser was such that a concentration of less than 0.01% by volume, could be detected. The accuracy of the concentration measurements was checked by an integration of the jet mass flow contained in the measured transverse

profiles and compared with the initial mass flow rate, i.e.

$$\dot{m}_j = \int_{-\infty}^{+\infty} (\rho UC)dy = \text{const.}$$

The equation was satisfactory to within ± 5%.

2.7. Tunnel calibration.

2.7.1 Tunnel speed correction.

In order to measure the free stream velocity during the experiment, it is necessary to have a calibration curve which gives the mean wind speed in the tunnel from reading of a reference pressure. This was done in the usual way by calibrating the tunnel when empty, and correcting for blockage.

2.7.2 Tunnel blockage correction.

The Tunnel blockage correction was calculated following Lock [23] for the wing section slot symmetrically placed in a rectangular closed working section tunnel and completely spanning its breadth. This correction was found to be negligible.

2.8. The Wall-jet Tests.

2.8.1 Similar density streams

A wooden plate 10'x7'-½" thick was installed

at the middle of the 3'x2' tunnel test section, immediately below the slot trailing edge, (see figure (3-o). The plate's leading edge was rounded and the curvature was such that the slot trailing edge was completely tangential to the plate. In order to detect any variation in the static pressure along the plate, it was equipped with a series of pressure taps. A small flattened pitot tube was used for surveying the boundary-layer.

2.8.2 Dissimilar density streams

A 6'x1½'x1/16" steel plate was placed in the middle of the 18" tunnel. The static pressure taps were used for measuring the static pressure along the wall, and for collecting the gas samples to measure the concentration at the wall. Smaller pitot (1 mm. diam.) and static tubes were added to the bottom of the rake shown in figure (1-g) for surveying the boundary-layer.

2.8.3 Summary of the test conditions.

Table (2) summarises all the test conditions covered in the experiments.

The range of velocity ratios were mostly obtained by changing the tunnel speed while keeping the jet velocity constant. The exception was the

Fig. (3-c) Wall jet model and the boundary-layer probe assembly .

TABLE (2)

SUMMARY OF THE TEST CONDITIONS

FLOWS	Gas Injected / Conditions	AIR					HELIUM					ARCTON$_{12}$					
		S''	$\frac{U_j}{U_m}$	$\frac{\rho_j U_j}{\rho_m U_m}$	$\frac{\rho_j U_j^2}{\rho_m U_m^2}$	Re_j	S''	$\frac{U_j}{U_m}$	$\frac{\rho_j U_j}{\rho_m U_m}$	$\frac{\rho_j U_j^2}{\rho_m U_m^2}$	Re_j	S''	$\frac{U_j}{U_m}$	$\frac{\rho_j U_j}{\rho_m U_m}$	$\frac{\rho_j U_j^2}{\rho_m U_m^2}$	Re_j	
FREE FLOW	Free Jet	↑	3.0 1.5	3.0 1.5	9.0 2.25	↑	↑	6.05 4.5 2.76	(0.825) 0.615 0.378	5.0 2.76 (1.0)	↑	↑					
	Free Wake	$\frac{1}{2}''$	0.67 0.50	0.67 0.50	0.44 0.25	12,000	$\frac{1}{16}''$	1.04	0.137	0.147	350 — 500	$\frac{1}{16}''$	0.950 0.650 0.485 0.245 0.157	4.0 2.74 2.0 (1.0) 0.66	3.84 1.75 (1.0) 0.252 0.104	↑	← no velocit data
SEMI BOUNDED FLOW	Wall Jet	↓	5.20 3.0 1.48	5.20 3.0 1.48	27.0 9.0 2.2	10,000	↓				↓	↓	∞ 1.45	∞ 6.1	∞ 8.8	7000 — 6000	← " " "
	Wall Wake		0.667 0.50	0.667 0.50	0.444 0.25	↓							(1.0) 0.80 0.485 0.245	4.2 3.36 2.0 (1.0)	4.2 2.68 (1.0) 0.252	↓	← " " "

( ) represent the unit parameter or closely related to unity

helium air series where both the jet velocity and the tunnel speed were changed simultaneously. Measurements were taken as far as 210 slot widths for air/air tests, while measurements up to 1000 slot widths were made for the other gases.

2.8.4 Measurements of the jet velocity (U_j)

The jet velocities were calculated using the one-dimensional gas dynamic equations. P_o is the plenum chamber pressure, adjusted so that choking condition was maintained at the throat, using

$$\frac{p^*}{P_o} = \left(\frac{2}{\gamma+1}\right)^{\left(\frac{\gamma_i}{\gamma_i-1}\right)} \qquad (2.8.4.1)$$

$$T_j^*/T_o = (2/\gamma_i+1) \qquad (2.8.4.2)$$

where γ_i is the specific heat ratio of the particular gas.

$= 1.4$ for air

$= 1.136$ " $Arcton_{12}$

$= 1.67$ " helium

hence, $U_j^* = \sqrt{\gamma_i R_j T_j^*} = \left(\frac{2\gamma_i}{\gamma_i+1}\frac{P_o}{\rho_o}\right)^{\frac{1}{2}}$ (2.8.4.3)

The jet exit velocity was subsonic, then the continuity of mass flow rate is

$$\rho_j U_j A_j = \rho_j^* U_j^* A_j^* \qquad (2.8.4.4)$$

from (2.8.4.3)

$$U_j = \left[\left(\frac{2\gamma_i}{\gamma_i + 1} \right)^{\frac{1}{2}} \left(\frac{P_o}{\rho_o} \right)^{\frac{1}{2}} \frac{A^*}{A_j} \frac{\rho_j^*}{\rho_j} \right] \qquad (2.8.4.5)$$

In terms of P_o, T_o rather than ρ^*, equation (2.8.4.5) can be written as

$$U_j = \left[\left(\frac{\gamma_i}{R_j T_o} \right)^{\frac{1}{2}} \left(\frac{2}{\gamma_i + 1} \right)^{\frac{\gamma_i + 1}{2(\gamma_i - 1)}} \frac{P_o}{\rho_j} \frac{A^*}{A_j} \right] \qquad (2.8.4.6)$$

The mass flow rate $\dot{m}_j$

$$= \left[\left(\frac{\gamma_i}{R_j T^o} \right)^{\frac{1}{2}} \left(\frac{2}{\gamma_i + 1} \right)^{\frac{\gamma_i + 1}{2(\gamma_i - 1)}} P_o A^* \right] \qquad (2.8.4.7)$$

Since A^*/A_j is fixed by the slot design, therefore the jet velocity was calculated for any given plenum chamber pressure P_o, temperature T_o, exit pressure P_j and exit temperature T_j using equation (2.8.4.6.) The velocity was checked experimentally at various locations across the span of the slot the results were consistent with equation (2.8.4.6) to within $\pm$ 3%.

3. Data reduction.

The static pressure and temperature were essentially constant throughout the flow field. The local measurement of the concentration (K) of the injected gas in the mixture will give the local value of the number density according to the following equations (e.g. Jean [24])

$$K = \frac{N_j}{N} \qquad (3.1) \qquad 1-K = \frac{N_m}{N} \qquad (3.2)$$

where N is total number of molecules of the mixture of the jet gas and the air per unit volume under the pressure P and the temperature T.

i.e. $$N = N_j + N_m \qquad (3.3)$$

Considering a steady state of the mixture of the two gases, then the mass density ϱ of the mixture under pressure P and temperature T for a binary gas mixture is:-

$$\varrho = M_j N_j + M_m N_m \qquad (3.4)$$

from (3.1) and (3.2) equation (3.4) can be written as:-

$$\varrho = \varrho_m (\beta K + 1) \qquad (3.5)$$

where $\beta = (\frac{M_j}{M_m} - 1)$ is molecular weight parameter. The velocity is found from the measurement of (ρU^2) using the pitot-static probes.

3.1 Results of the profiles measurements

The figure presenting the results are arranged in the order in which they are discussed.

3.2 Discussion of the profile measurements for the free jet and wake flows.

3.2.1 The velocity profiles.

The experimentally measured velocity profiles are normalized by plotting $\left|\frac{U - U_m}{U_{max} - U_m}\right|$ vr. (y/δ_m) where (δ_m) is the individual half width at half velocity difference, measured from the jet centre-line. Though various length scales are defined in the literature, (δ_m) has the great advantage that is, can be measured accurately. Unless otherwise stated (δ_m) is used here as the characteristic scale length. The results are shown in figures 4 (a, b, c and d) The profiles except those in the 'potential core' $(o < x/s < 30)$ for the whole range of velocity ratios for all gas combinations tested; air/air, helium/air and $Arcton_{12}$/air are approximately similar and could

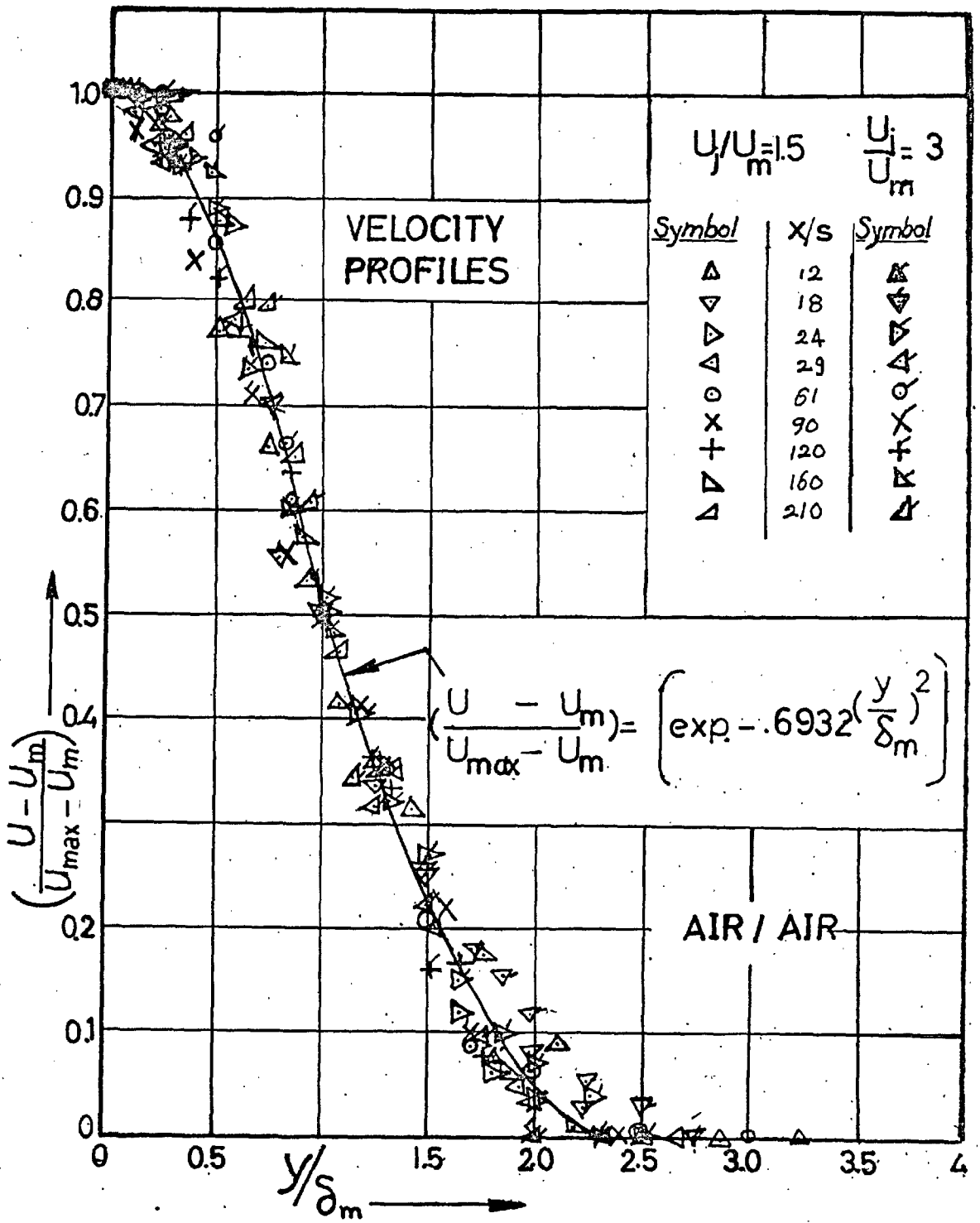

FIG.(4-a) Correlation of normalized velocity profiles for turbulent free jet flow. ($U_j/U_m > 1$)

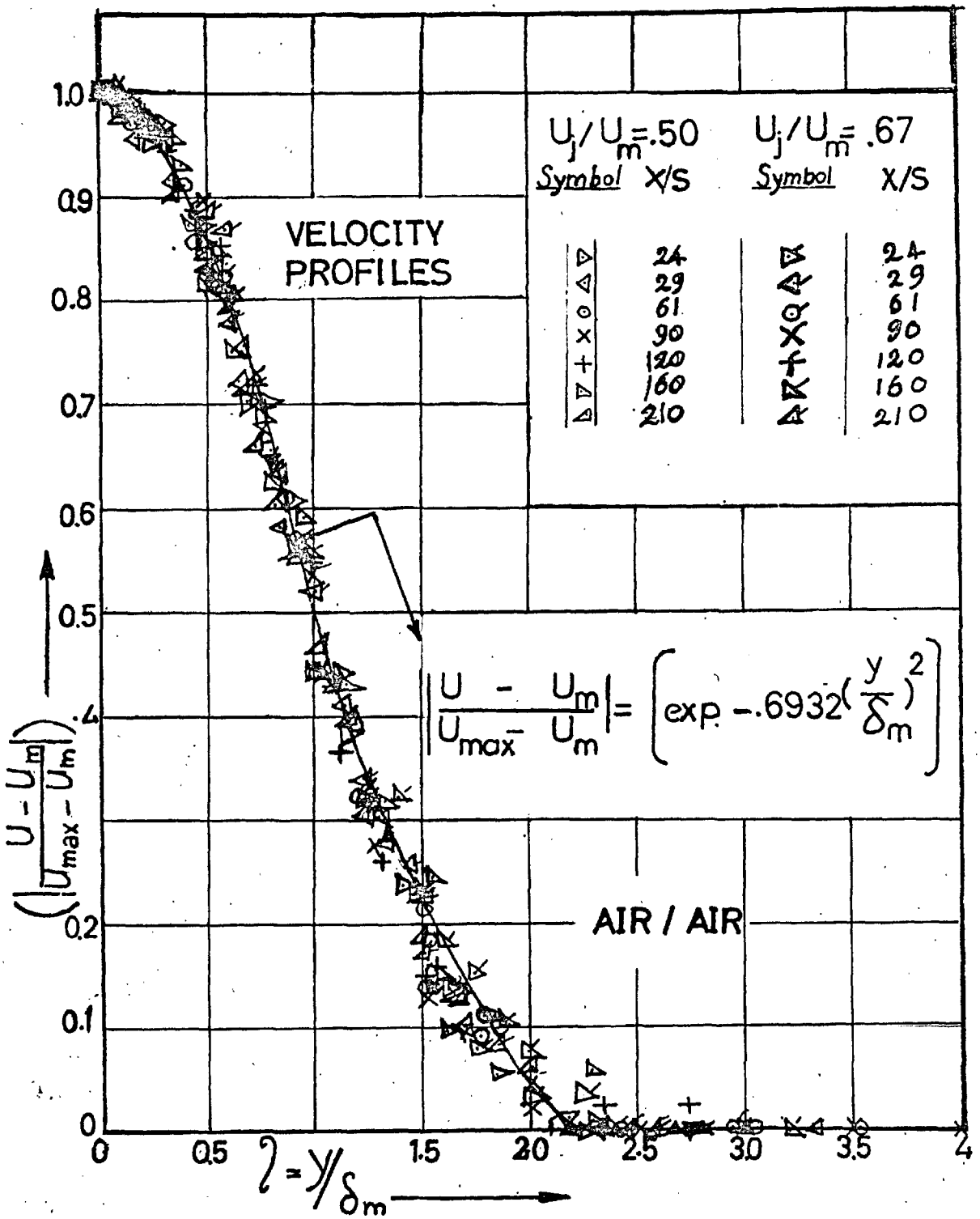

FIG.(4-b) Correlation of normalized velocity profiles for turbulent free wake flow.($U_j/U_m < 1$)

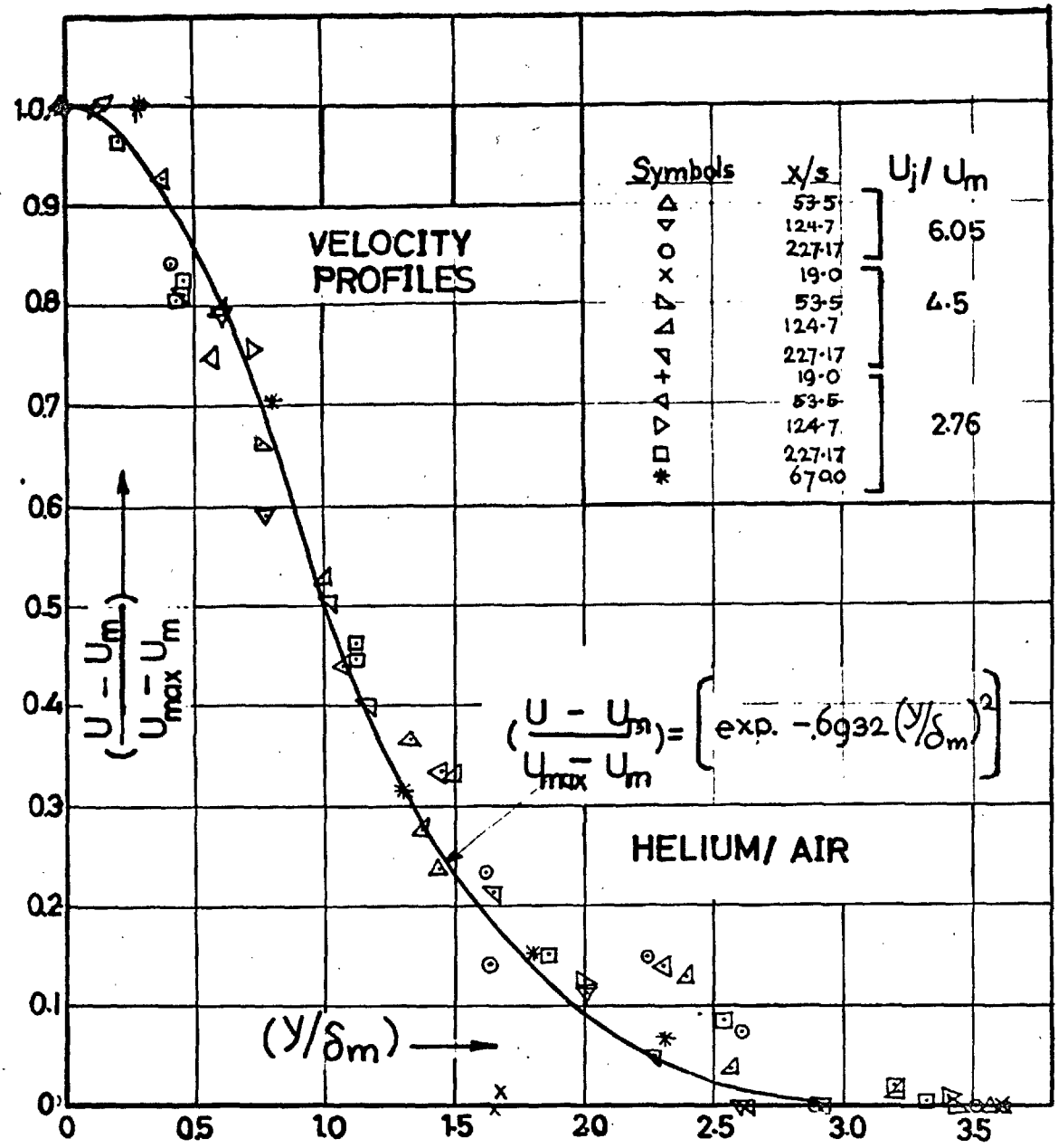

FIG.(4-c) Correlation of normalized velocity profiles for helium air mixing in a turbulent free jet flow. ($U_j/U_m > 1$)

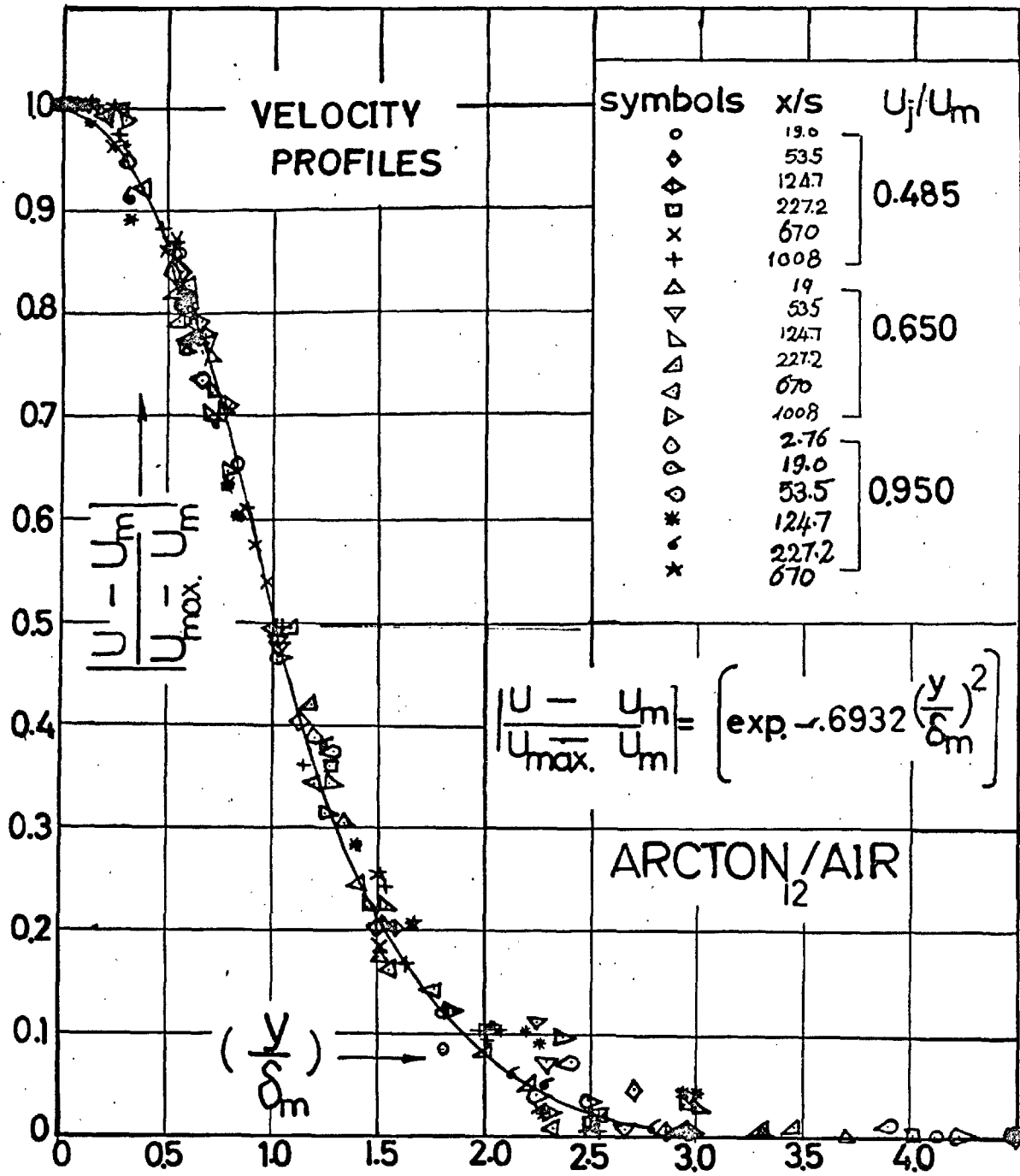

FIG.(4-d) Correlation of normalized velocity profiles for Arcton air mixing in a turbulent free wake flow. (Uj/Um < 1)

be reasonably well expressed by the "Gaussian distribution function", that is,

$$U = U_m + (U_{max} - U_m)\left[\text{Exp. } -.6932\ (y/\delta_m)^2\right] \quad (3.2.1.1.)$$

This function is, in fact, very useful and has been used by many workers, for example, Weinstein [4] for a two-dimensional jet issuing into a moving stream by Eskinazy [25] when correlating the data of Schlichting[2] Forthman [26] and Corrsin [7] and by Keogy and Weller for a jet of gas issuing into a still atmosphere of widely different density.

3.2.2 The concentration profiles.

The concentration measurement was carried out immediately downstream of the potential core to about 1000 slot widths downstream. The concentration profiles were normalized as,

$$K/K_{max} = f\ (y/\delta_{m_c})$$

where (δ_{m_c}) is the individual length scale defined as y at $K = \frac{1}{2} K(max)$. The data again show that the Gaussian distribution is a fair description of the concentration profiles i.e.

$$K/K_{max} = \text{exp.} \left[-.6932\ (y/\delta_{m_c})^2\right] \quad (3.2.2.1)$$

as found by Keagy and Weller.[8] The correlation of the normalized concentration profiles are shown in figures (4-e) and (4-f) for helium and $Arcton_{12}$ jets respectively.

3.2.3 Mass Flux and Momentum flux profiles

The fact that the momentum and the mass fluxes are conserved and independent of (x) suggests that both mass and momentum profiles will be similar downstream of the core region. These profiles are illustrated in figures 4 (g, h, i and j). From which it is seen that, except for some of the helium data, the momentum and mass flux profiles are similar and can also be represented by the Gaussian distribution that is,

$$\rho U = \rho_m U_m + (\rho_{max} U_{max} - \rho_m U_m) \text{ Exp.} \left[-.6932 (y/\delta_m^*)^2 \right] \quad (3.2.3.1)$$

$$\rho U^2 = \rho_m U_m^2 + (\rho_{max} U_{max}^2 - \rho_m U_m^2) \text{ Exp.} \left[-.6932 (y/\delta_m^{**})^2 \right] \quad (3.2.3.2)$$

where (δ_m^*) and (δ_m^{**}) are the respective individual half width defined as the usual way. Similar results for the (ρU^2) profiles were obtained by (Valis[10]) for a round jet of gas into a still surrounding

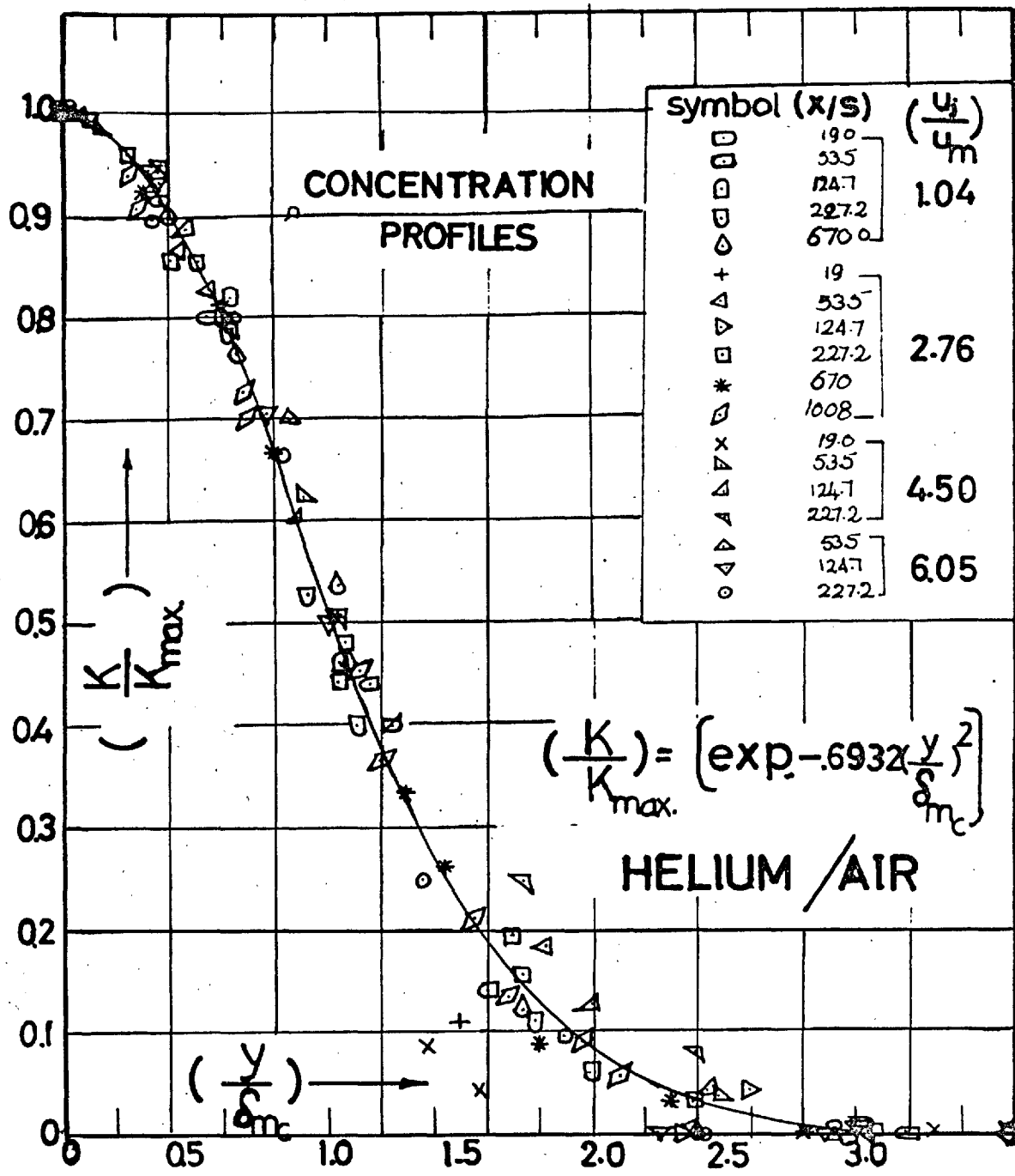

FIG. (4-e) Correlation of normalizd concentration profiles for helium air mixing in a turbulent free jet flow. ($U_j/U_m > 1$)

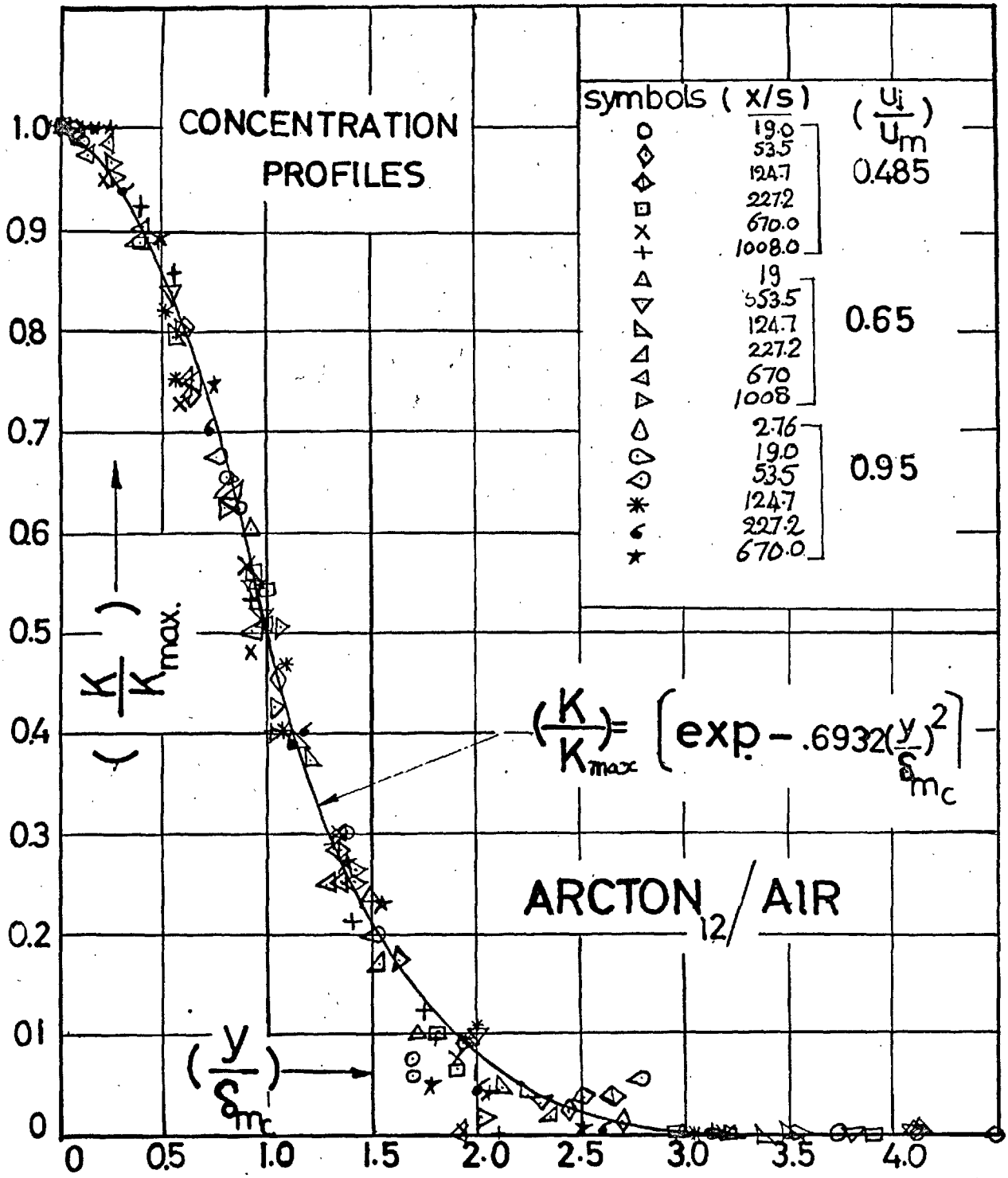

FIG.(4-f) Correlation of normalized concentration profile for Arcton air mixing in a turbulent free wake flow. (Uj/Um <1)

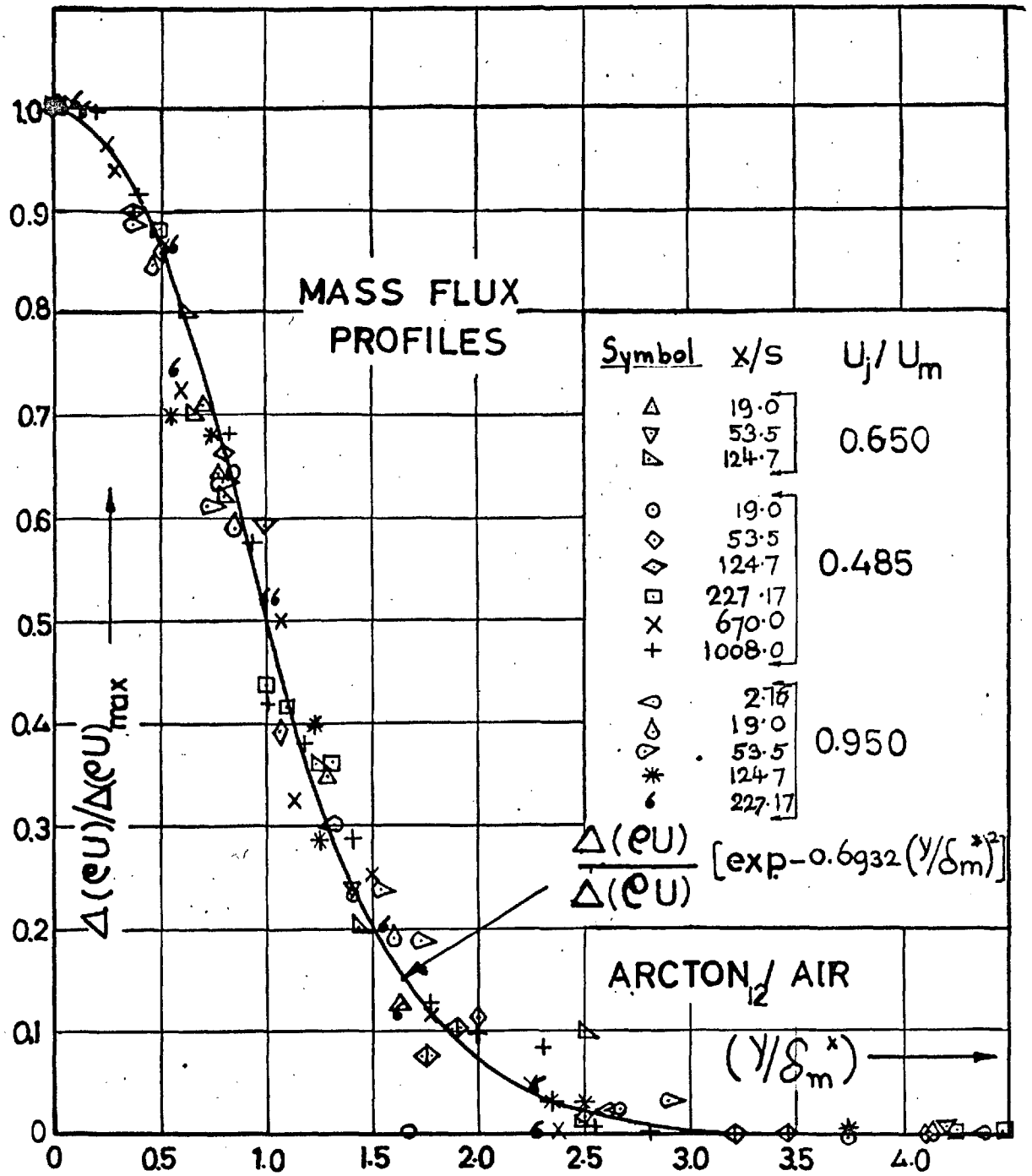

FIG. (4-9) Correlation of normalized mass flux Profiles for Arcton air mixing in a turbulent free wake flow. (Uj/Um <1)

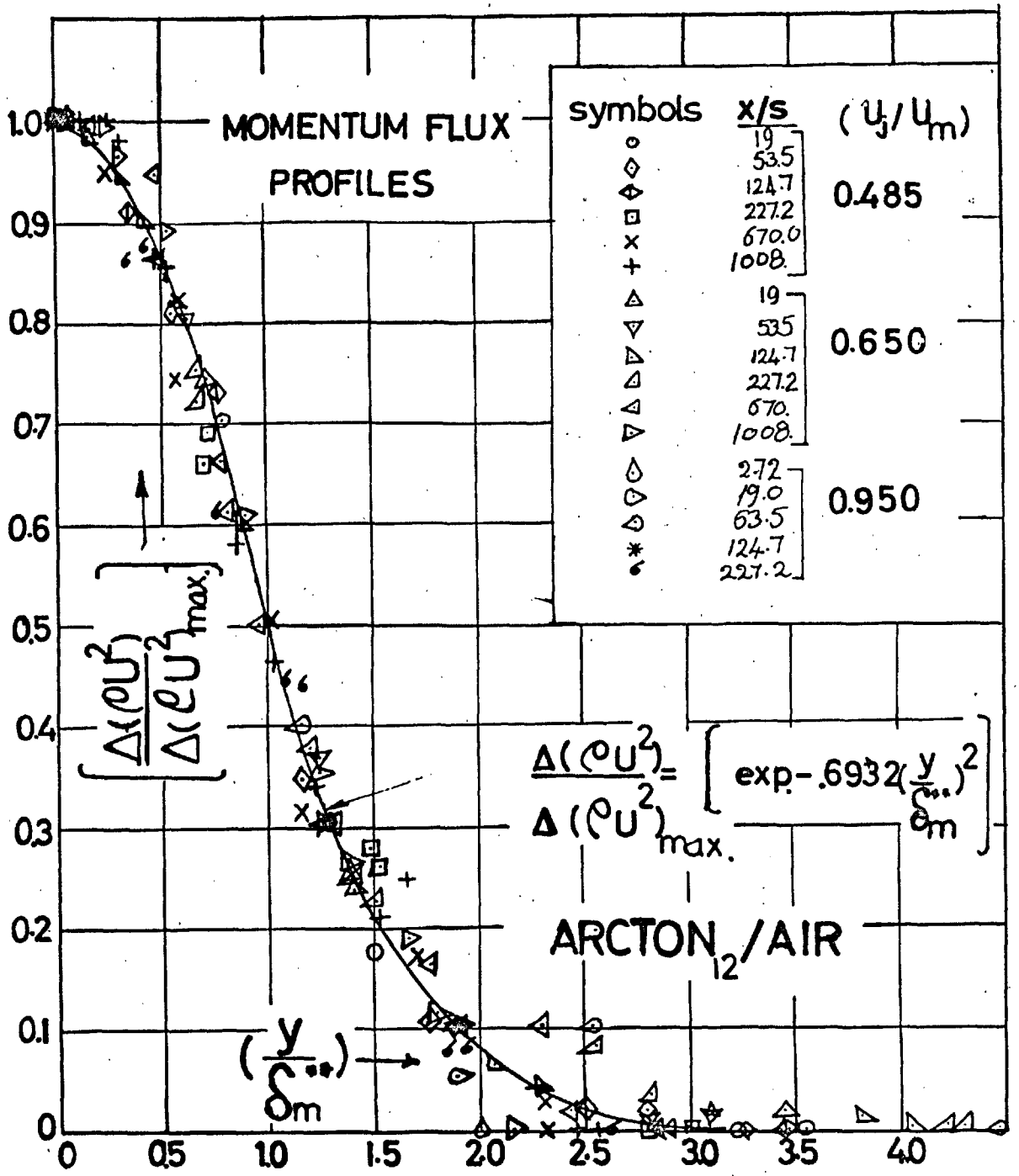

FIG. (4-h) Correlation of normalized momentum flux Profiles for Arcton air mixing in a free turbulent wake flow. ($U_j/U_m < 1$)

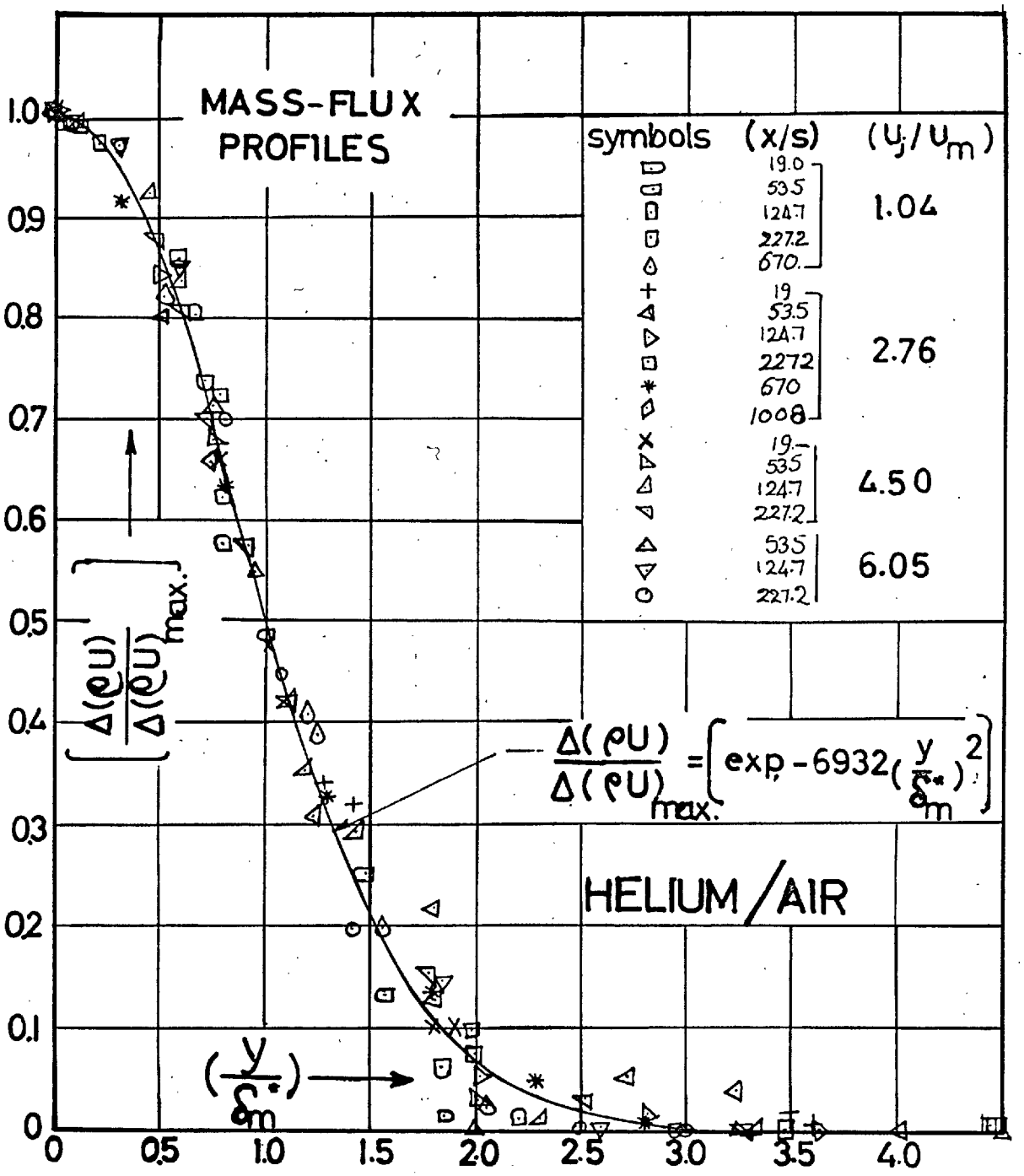

FIG. (4- i) Correlation of normalized mass flux Profiles for helium air mixing in a free turbulent jet flow. (Uj/Um > 1)

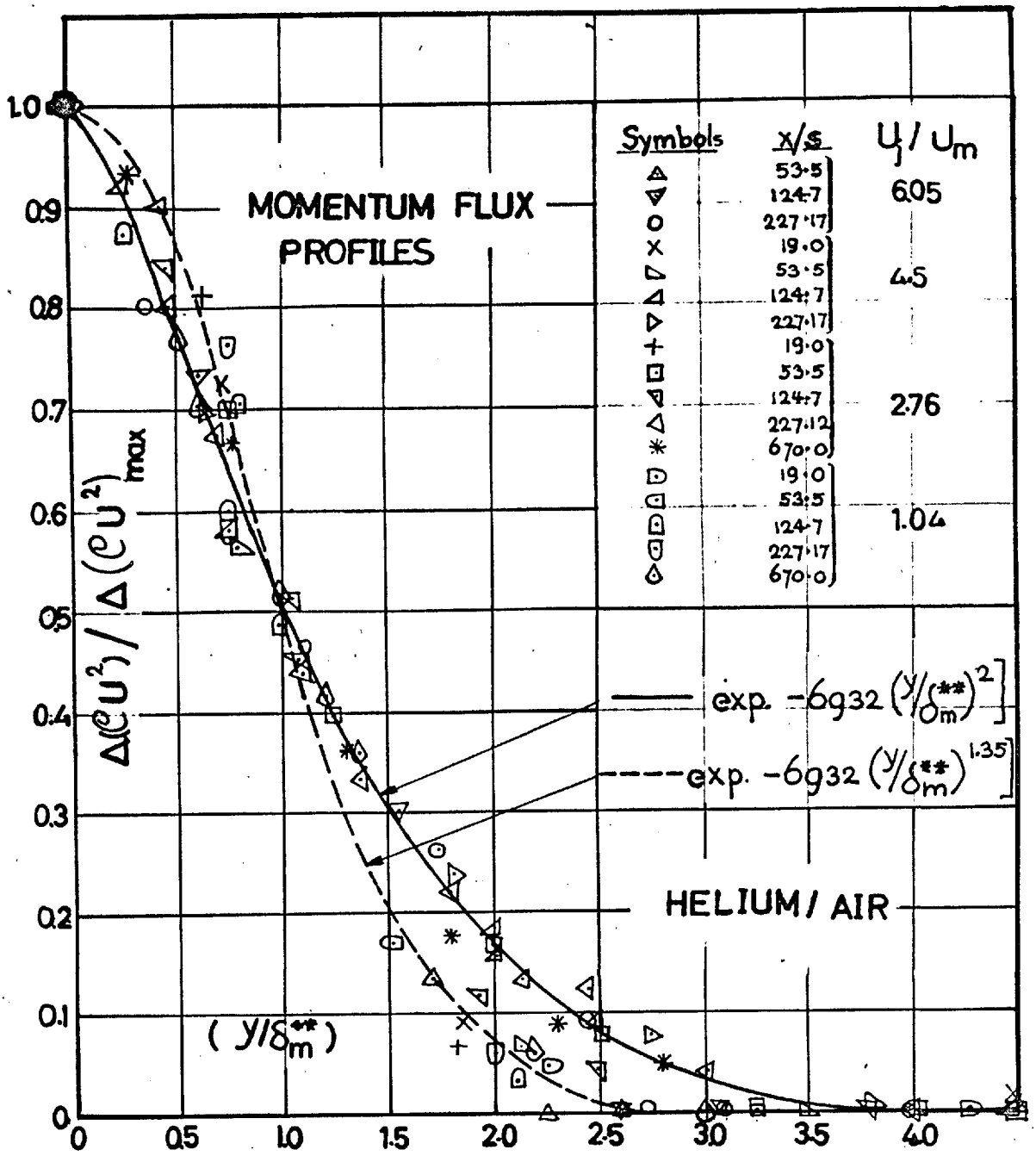

FIG. (4-j) Correlation of normalized momentum flux Profiles for helium air mixing in a turbulent free jet flow. (Uj/Um > 1)

($\rho \neq$ constant) and by Maczynski [27] for a round jet into a moving air stream (ρ = const). Referring to figure (4-j) the consistency between the experimental measurements of the helium and the Gaussian distribution function is not satisfactory. The explanation of this discrepancy, might possibly be attributed to the experimental error in measuring the total head. Helium is a very light gas so that the measured pitot pressure was very small. It is probably worth noting that Keagy and Weller have found a similar problem when dealing with the helium; though their jet velocity was higher (400 ft/sec.) than the present one ($\cong$150 ft/sec.)

Having shown the experimental profiles to be following the Gaussian distribution, it would be appropriate to compare between this function and the other theoretical profiles, which have been written, according to the different assumptions in the mechanism of mixing. This comparison is shown in figure (4-k). The present experimental velocity profiles are represented by a mean line through the data. A short account of the theoretical profiles shown in figure (4-k) is given in section 4.

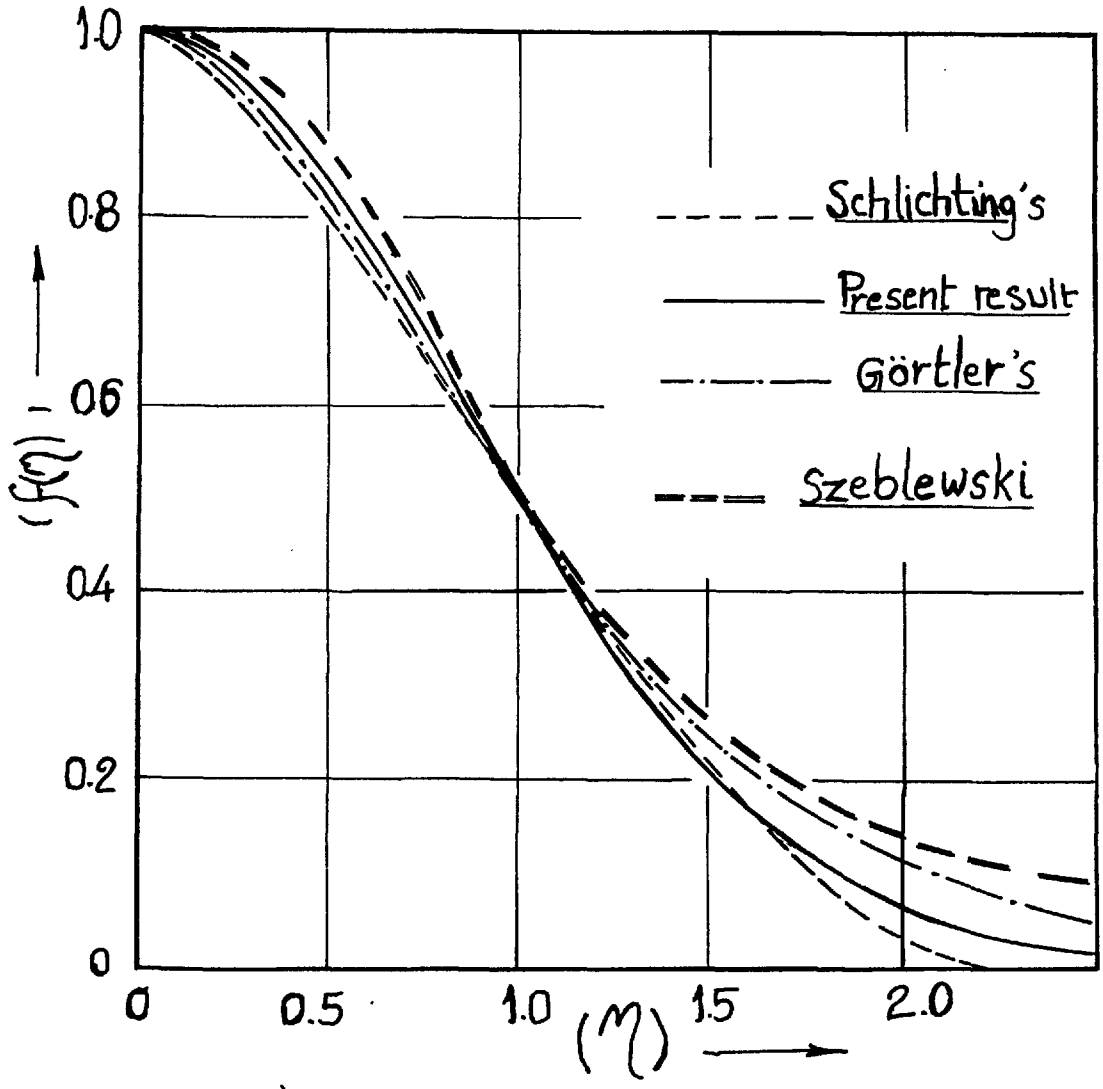

FIG.(4-K)

COMPARISON OF VARIOUS THEORETICAL CURVES FOR THE MEAN VELOCITY PROFILES IN TURBULENT FREE FLOWS.

3.3 The Wall-jet and the wall-wake profiles

3.3.1 The wall-jet velocity profiles:

The development of the wall jet velocity profiles at various stations downstream of the slot are shown in figures (5-a), (5-b) and (5-c) for the range of velocity ratios examined (5.2:,3 and 1.48) with air injection. In figure (6-a) an attempt is made to correlate the overall velocity profiles for $(\frac{U_j}{U_m})$ 5.2 and 1.48, Glauert's [19] theory is present for comparison. The correlation indicates that both velocity ratios have similar profiles but only the 5.2 one is similar to Glauert, though the agreement becomes poor as (y) increases.

As Glauert [19] pointed out the entire flow of the wall jet cannot conform to an overall similarity solution. He divided the flow into an inner and outer portion on either side of the peak velocity and chose an eddy viscosity based on Blasius turbulent pipe flow near the wall (inner layer) and Prandtl's hypothesis further out (outer-layer). The value of eddy viscosity was selected to obtain a velocity profile in agreement with Bakk's[28] measurements. Dividing the wall jet profile into two layers would indicate that the shear stress is zero at the position

(FIG.5-a) Turbulent Wall Jet Velocity Profile development along the plate

$(U_j/U_m = 5.2)$ $(\rho_j/\rho_m = 1.0)$ (Air/Air)

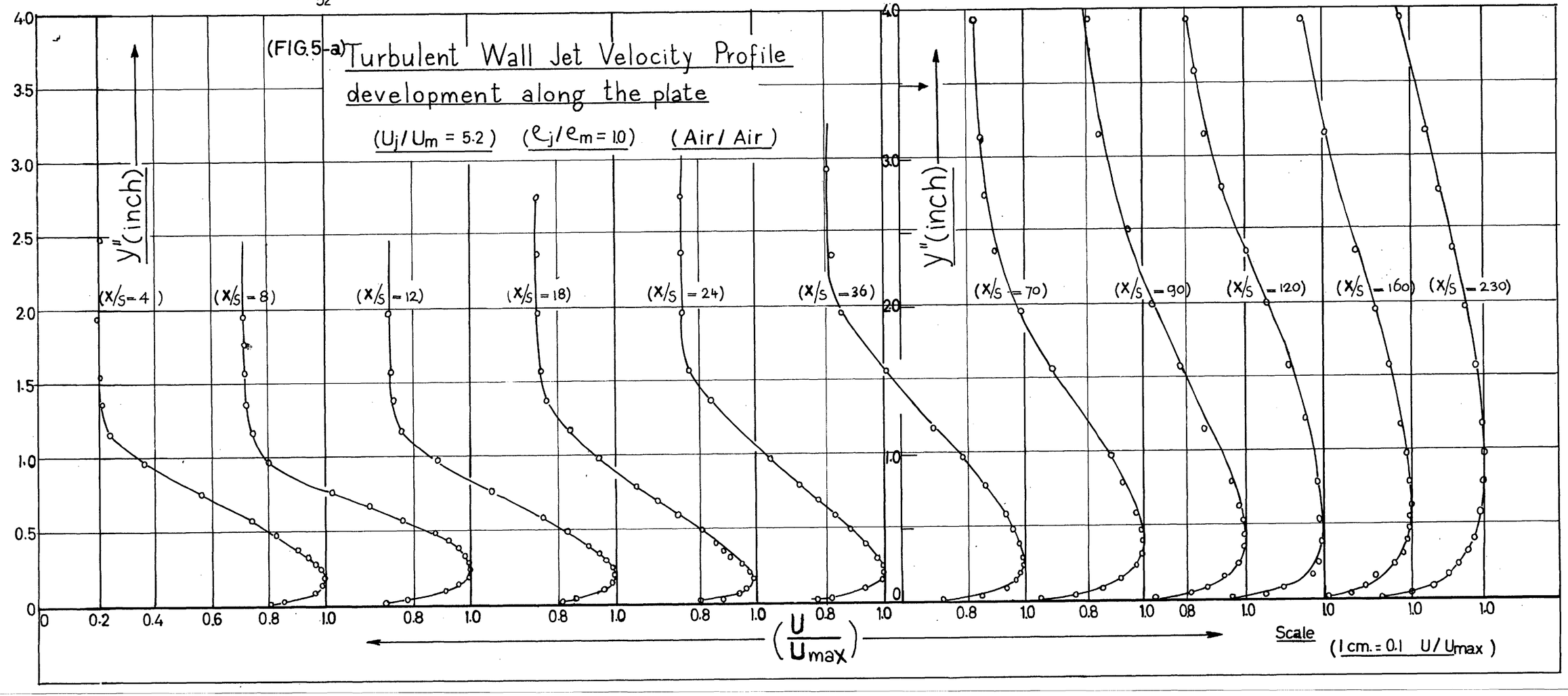

(FIG.5-b) Turbulent Wall Jet Velocity Profiles development along the plate

($U_j / U_m = 3$) ($e_j / e_m = 1.0$) (Air/ Air)

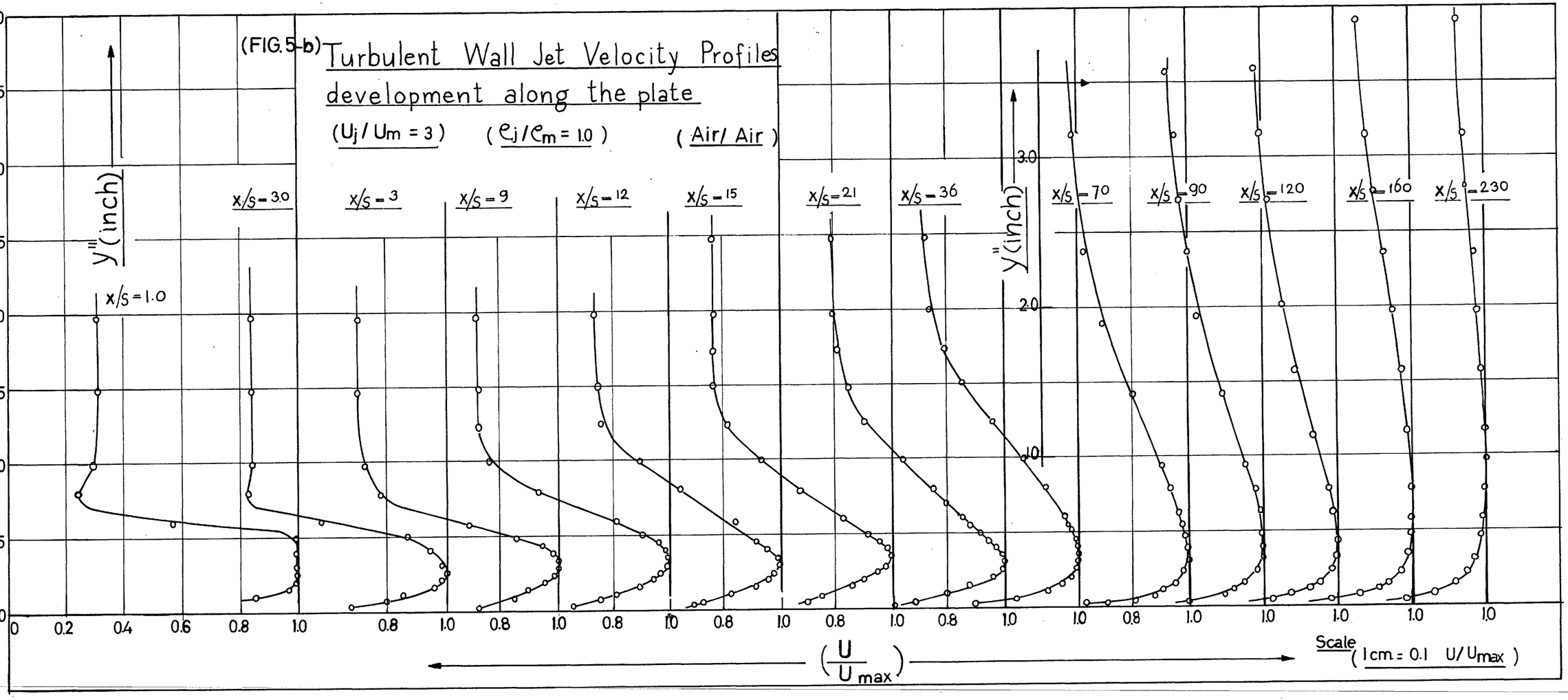

(FIG. 5-c) Turbulent Wall Jet Velocity Profiles Development along the Plate

$\left(\frac{U_j}{U_m} = 1.48\right)$ $\left(\frac{\rho_j}{\rho_m} = 1.0\right)$ (Air/Air)

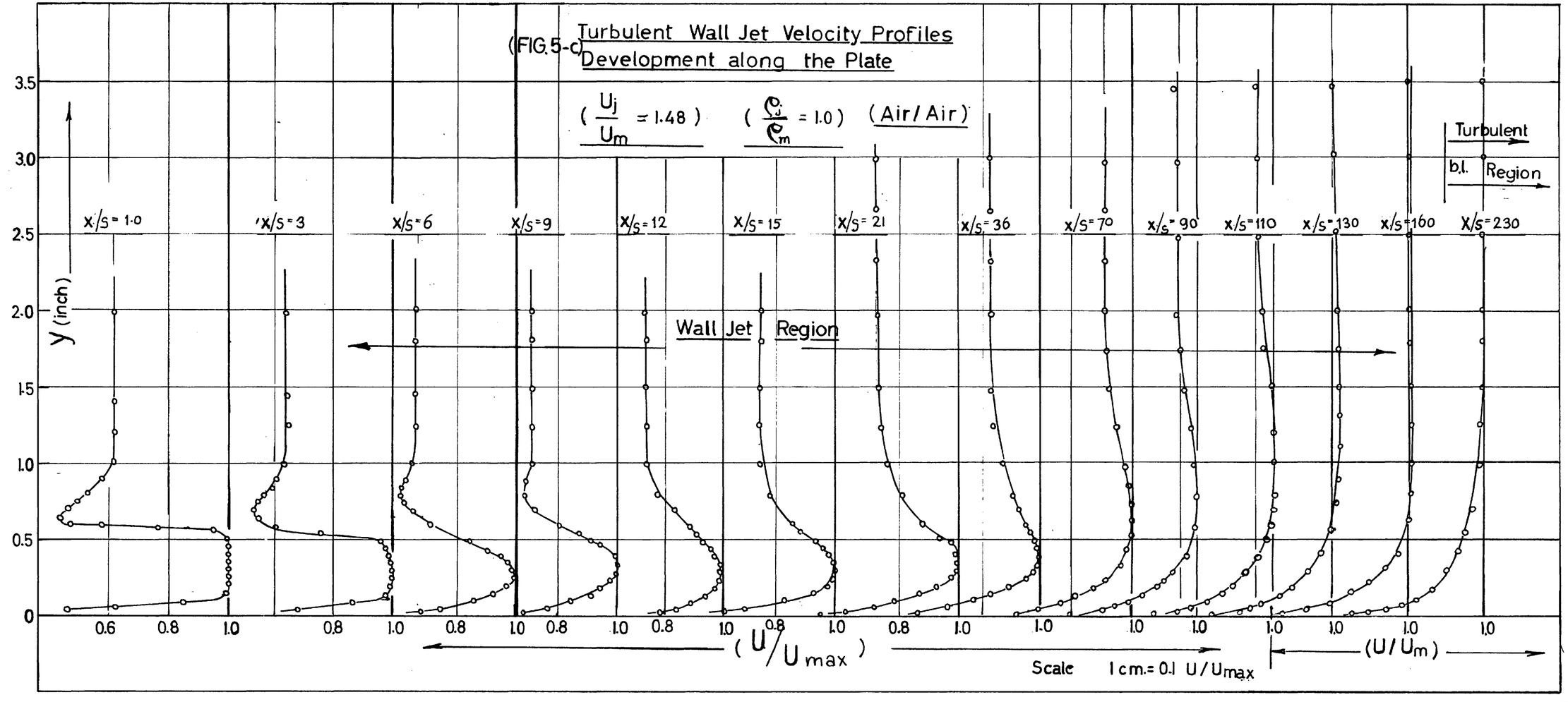

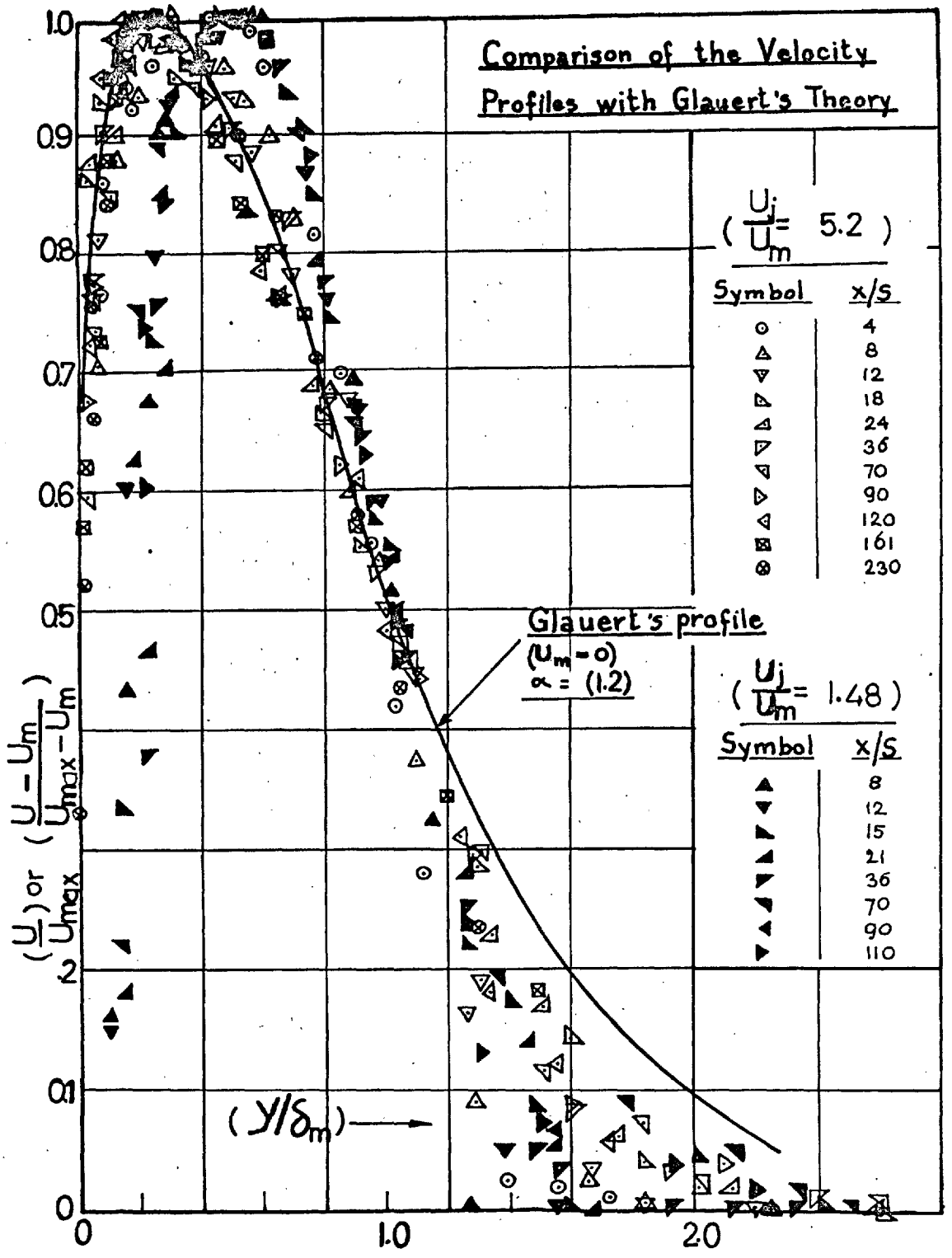

FIG.(6-a) Correlation of normalized turbulent wall-jet velocity Profiles.

of maximum velocity. However as we shall discuss later on, the correspondence of the point of zero shear stress with the peak velocity location has been shown experimentally to be false by Verhoff[29], Bradshow[30], and very recently Kruka [31]. In the present experimental profile, however, for values of (x/s) where $\frac{U_{max}}{U_m} > 1$, the profiles are split into two parts, at a distance y where U = 0.99 U_{max} measured from the wall, into an outer and inner layer profiles.

3.3.1.1 The Outer-layer profiles.

The outer layer profiles are normalized as

$$\left(\frac{U-U_m}{U_{max}-U_m}\right) = f\ \frac{(y-\delta_i)}{(\delta_m-\delta_i)}$$

where, (δ_i) is the inner layer width = y at U = 0.99 U_{max} and (δ_m) is defined as usual, measured from the wall. Fig. (6-b) shows these profiles when they are well described by the exponential function, that is ,

$$\left(\frac{U-U_m}{U_{max}-U_m}\right) = \text{Exp.}\left[-.6932\ \left(\frac{y-\delta_i}{\delta_m-\delta_i}\right)^2\right] \qquad (3.3.1.1.)$$

The correlation is very satisfactory except those profiles beyond (x/s) = 160 for the "weak" wall jet ($\frac{U_j}{U_m}$ = 1.48) This disagreement is expected, since

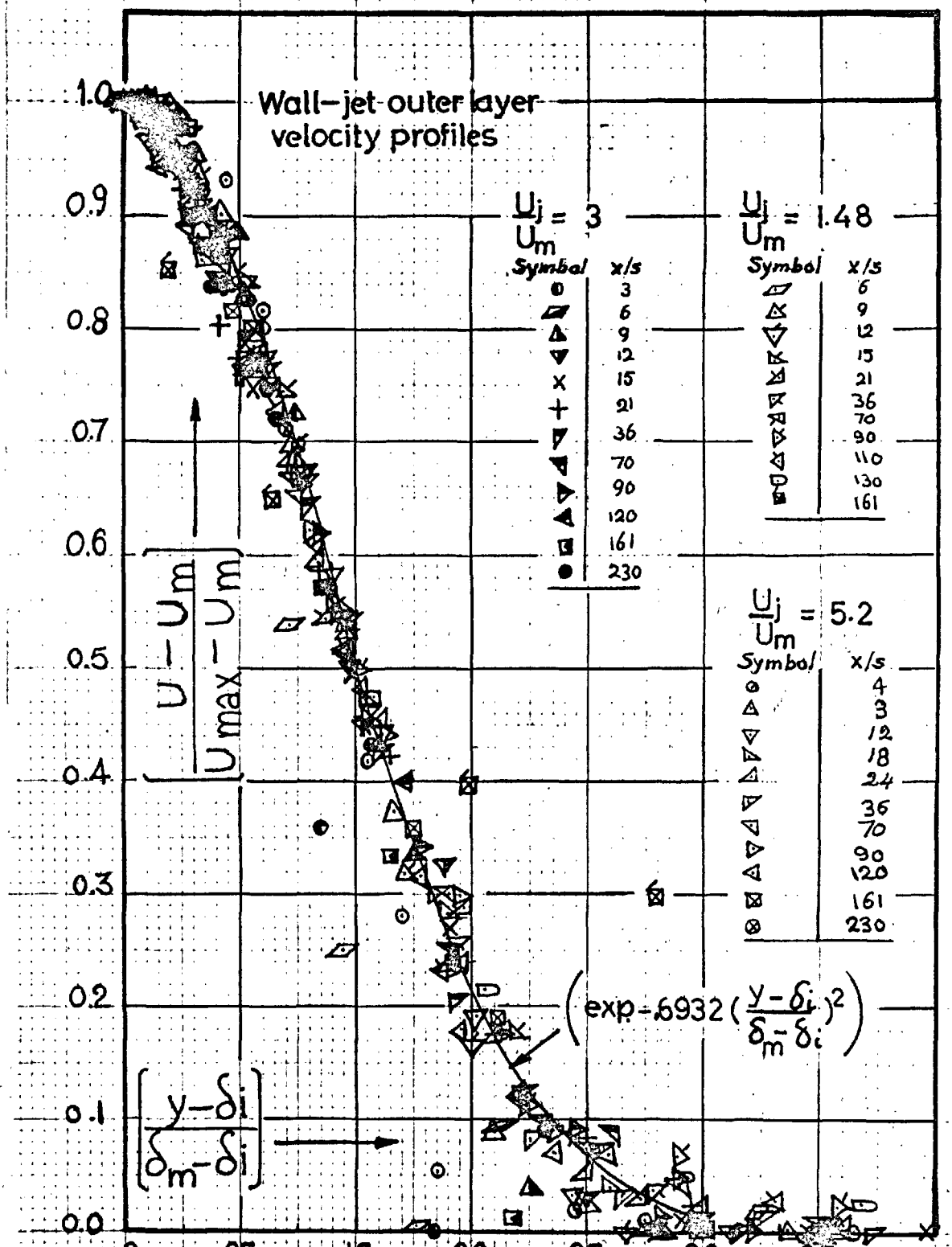

FIG. (6-b) Correlation of normalized velocity Profiles in the outer layer of a turbulent wall-jet.

at (x/s) is large (U_{max}) approaches (U_m) and at the same time the wall boundary-layer becomes thicker (see figure 5-c). Eventually, as $U_{max} = U_m$, the velocity profiles become similar to that of a fully developed turbulent boundary-layer (§ 3.3.2 figure (8)). It has been reported by George [32] that a fully developed boundary-layer velocity profile was found at 170 slot widths for $\frac{U_j}{U_m} = 1.5$. Unfortunately the present experimental measurements were limited to 230 slot widths which is the actual working length of the 3` x 2` tunnel test section, so it was impossible to examine the asymptatic behaviour of the wall jet results with higher velocity ratios (3 and 5.2).

3.3.1.2 The inner layer.

The velocity profiles in the inner layer are shown in figure (6-c) when they are normalized according to the conventional power law as,

$$\left(\frac{U}{U_{max}}\right) = \left(y/\delta_i\right)^{\frac{1}{n}} \qquad (3.3.1.2.1)$$

The data showed that (n) is slightly varying with $(\frac{U_j}{U_m})$. According to figure (6-c) an average value of (10) is appropriate, which is similar to that assigned by Patel [33], and the average value of Kruka [31], but it

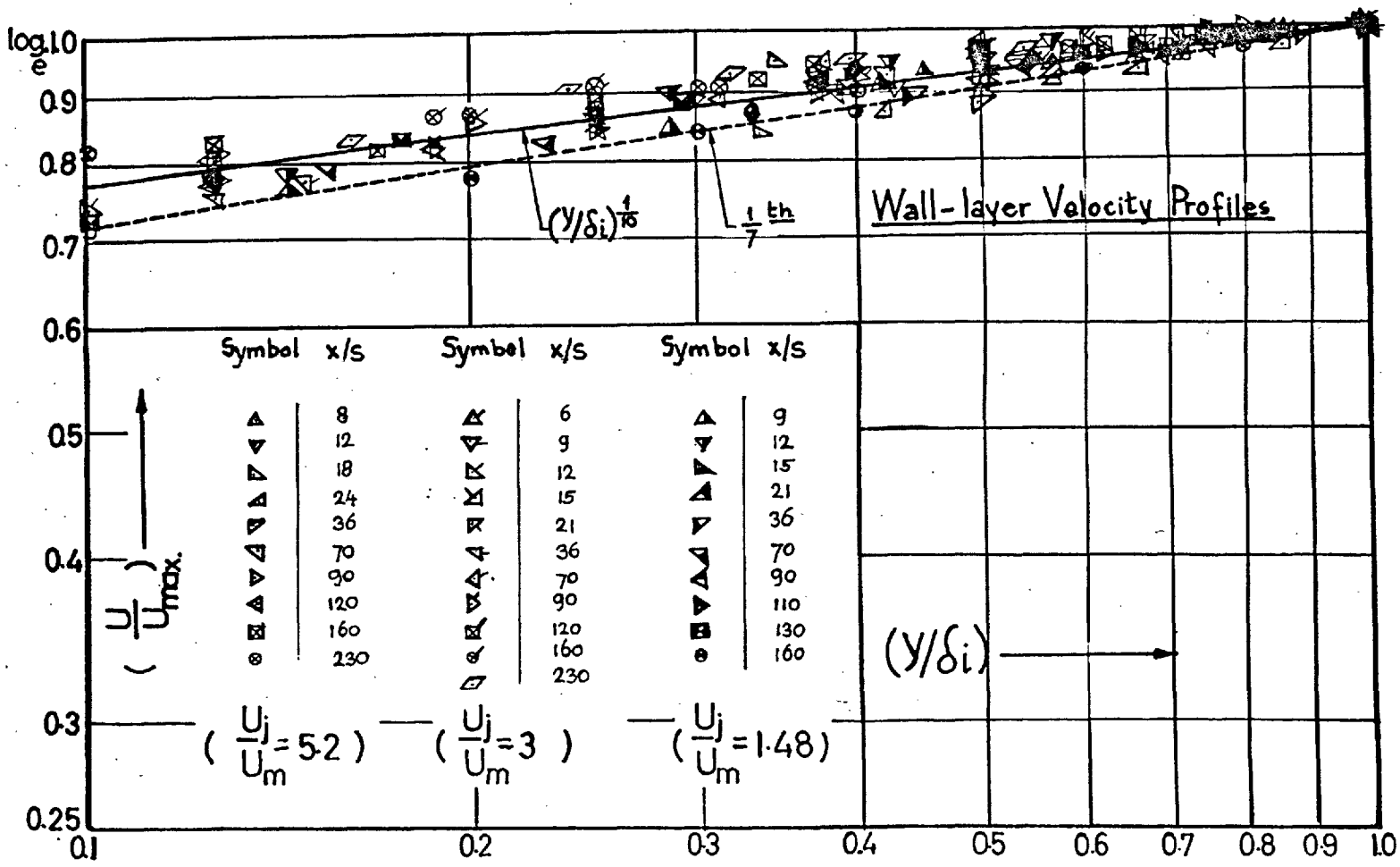

FIG. (6-c) Correlation of the normalized wall layer velocity Profiles

is rather less than Schwarz's [34] value which was (14).

3.3.2 Wall wake flow.

3.3.2.1 The velocity profiles

The development of the velocity profiles for the wall wake are shown in figures (7-a), (7-b) for air/air, (7-c) (7-d) and (7-e) for Arcton $_{12}$/air, $\frac{U_j}{U_m}$ =0.67, 0.5 (air/air), 0.80, .485 and .245 (Arcton $_{12}$/air). These profiles have no velocity maximum and downstream of the potential core region it can be seen that each profile consists of an outer wake component and an 'inner boundary layer'. This mixing region, however, is terminated quite rapidly for air/air (figure 7-a and 7-b, $x/s \geqslant 50$) but rather less rapidly for the Arcton $_{12}$/air (figures 7-c and 7-d, $x/s \geqslant 250$). When the velocity profile of the free shear layer (wake component) merges with the inner boundary layer the profile becomes similar to that of a fully developed turbulent boundary layer. These fully developed velocity profiles are normalized according the universal power low. The air/air data asymptote to 1/7th power low as shown in figure (8) while the Arcton$_{12}$/air results asymptote to 1/6th

(FIG.7-a) Turbulent Boundary-layer Velocity Profiles Development over a flat Plate with fluid injection.

$\left(\frac{U_j}{U_m} = 0.667\right)$ $\left(\rho_j/\rho_m \simeq 1.0\right)$ Air / Air

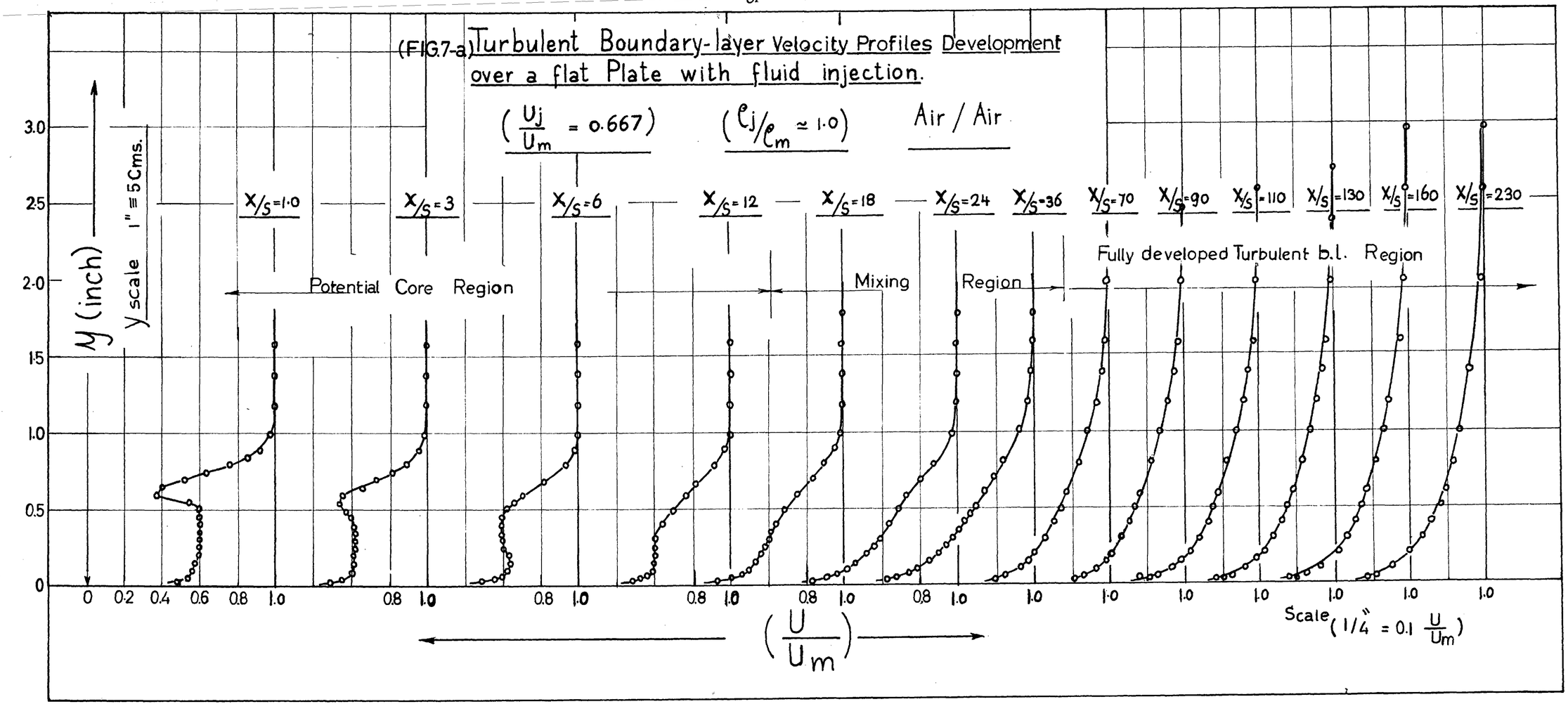

(FIG.7-b) Turbulent boundry layer Velocity Profiles Development Over a flat plate With fluid Injection

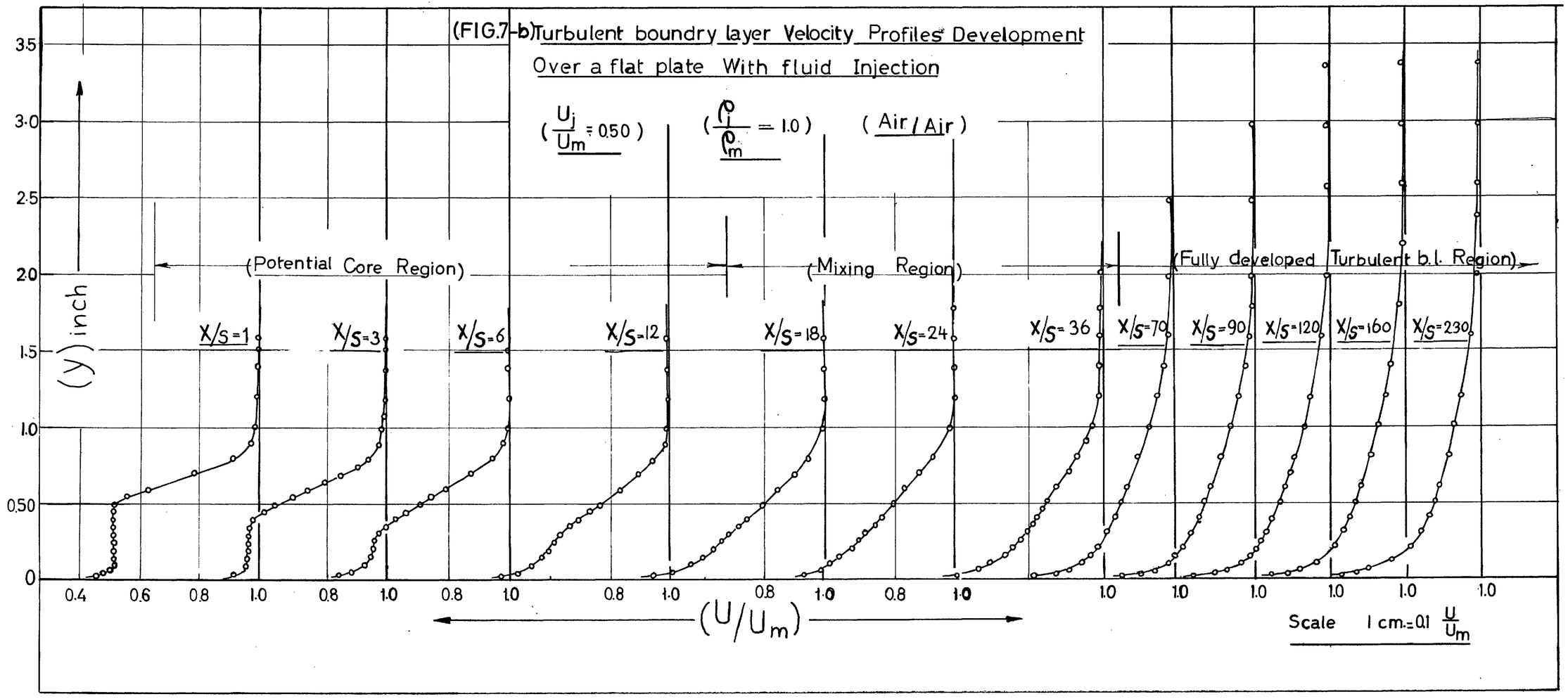

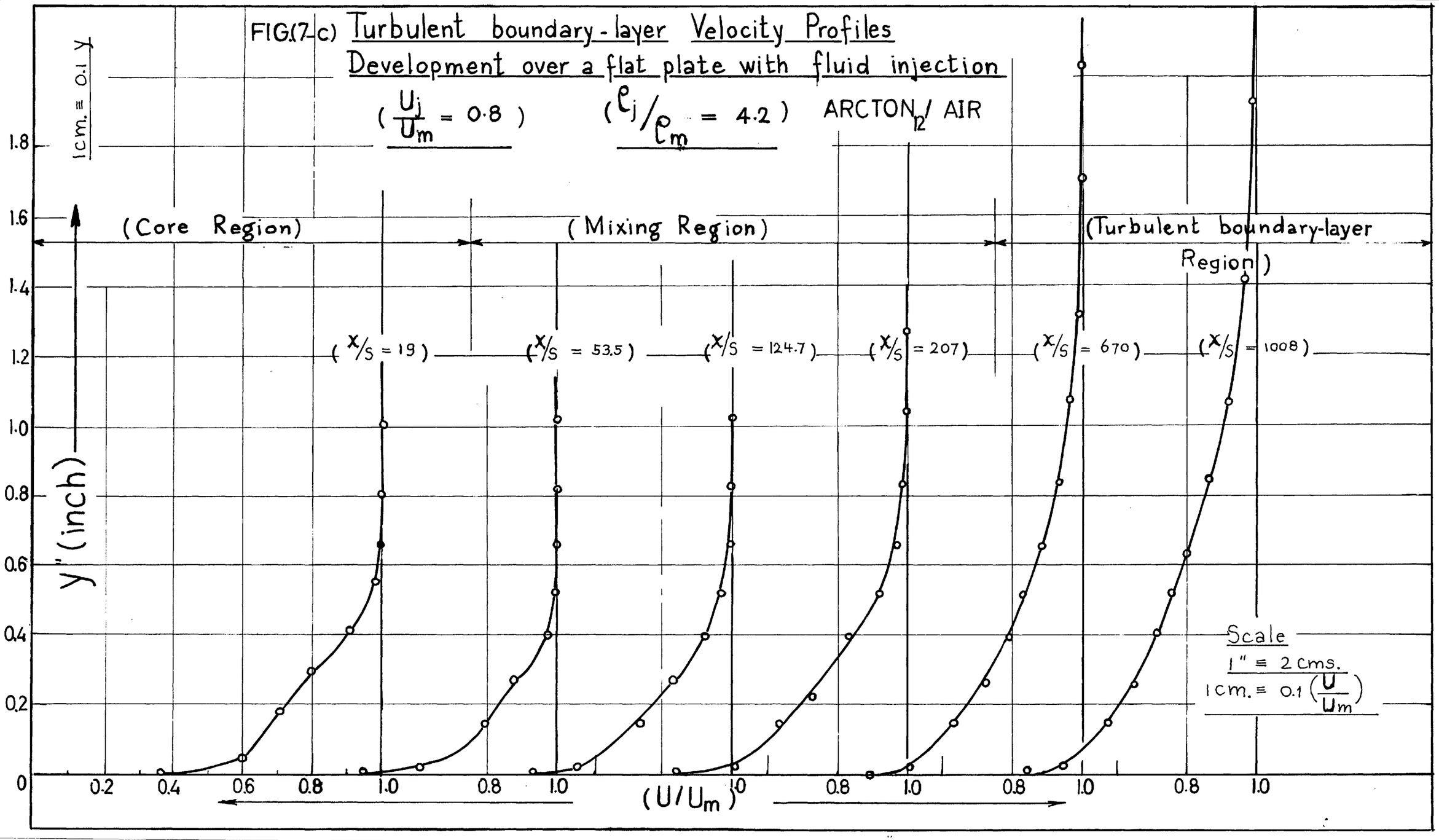
FIG.(7-c) Turbulent boundary-layer Velocity Profiles
Development over a flat plate with fluid injection
($\frac{U_j}{U_m}$ = 0.8) (ρ_j/ρ_m = 4.2) ARCTON 12 / AIR
1cm. ≡ 0.1 y
y" (inch)
(Core Region)
(Mixing Region)
(Turbulent boundary-layer Region)
(x/s = 19)
(x/s = 53.5)
(x/s = 124.7)
(x/s = 207)
(x/s = 670)
(x/s = 1008)
0
0.2
0.4
0.6
0.8
1.0
1.2
1.4
1.6
1.8
(U/Um)
Scale
1" ≡ 2 cms.
1cm. ≡ 0.1 (U/Um)

FIG.7. Turbulent boundary-layer Velocity Profiles Development over a flat plate with fluid injection

$\left(\frac{U_j}{U_m} = 0.485\right)$ $\left(\frac{\rho_j}{\rho_m} = 4.2\right)$ ARCTON$_{12}$/AIR

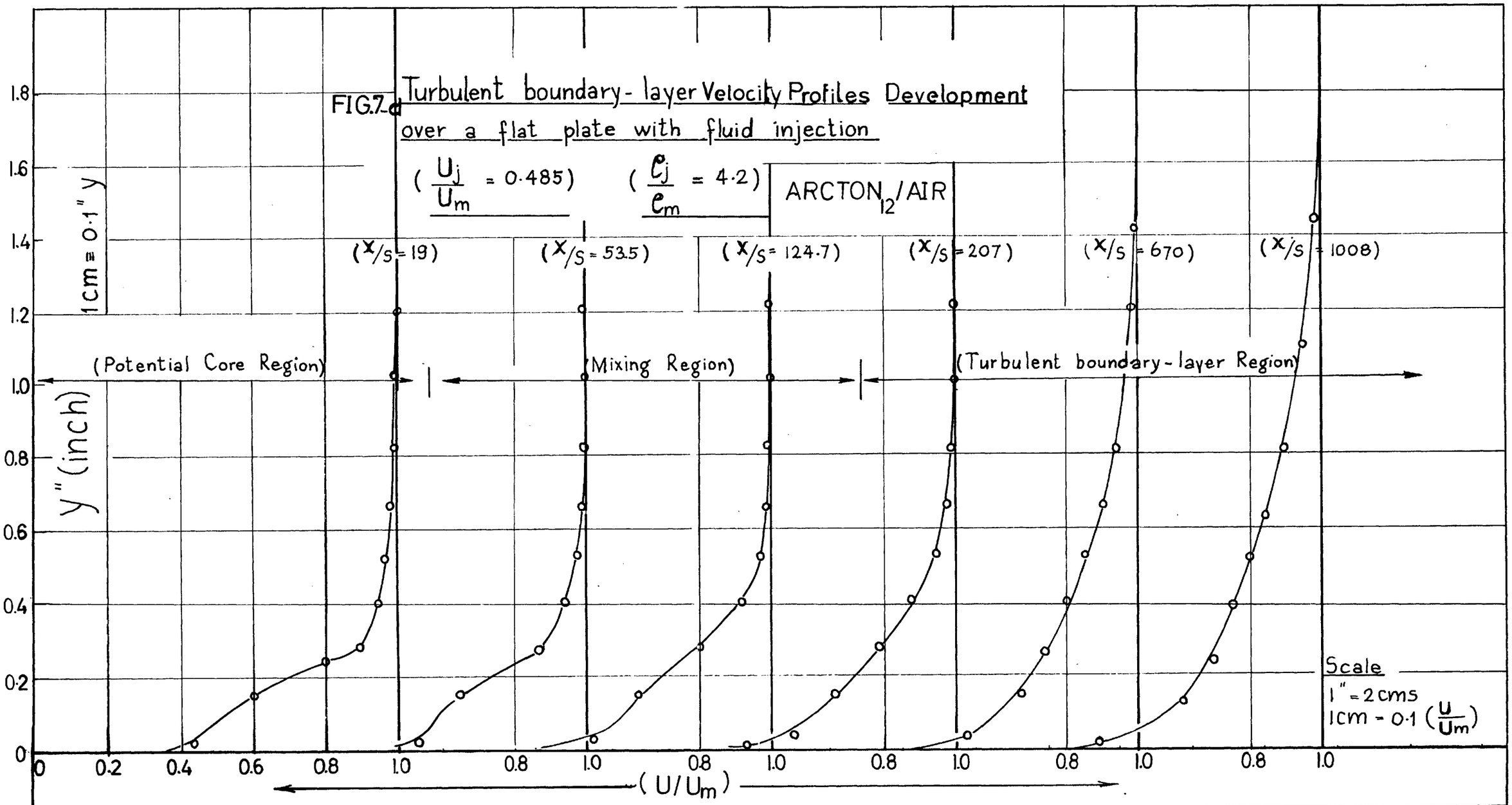

(FIG.7-e) Turbulent boundary-Layer Velocity Profiles Development over the flat plate with fluid injection

$\frac{U_j}{U_m} = 0.245$ $\frac{\rho_j}{\rho_m} = 4.2$ ARCTON$_{12}$ / AIR

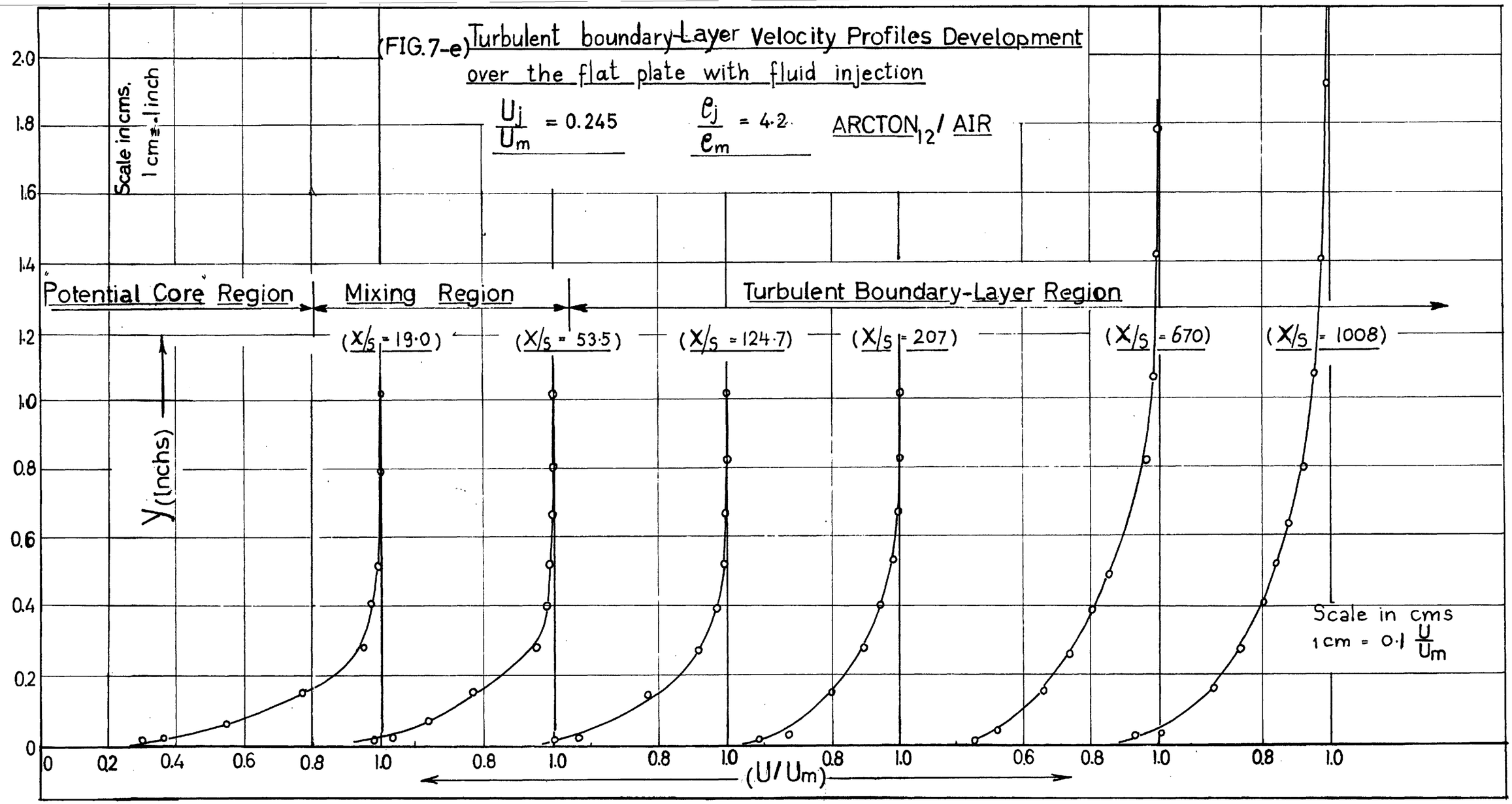

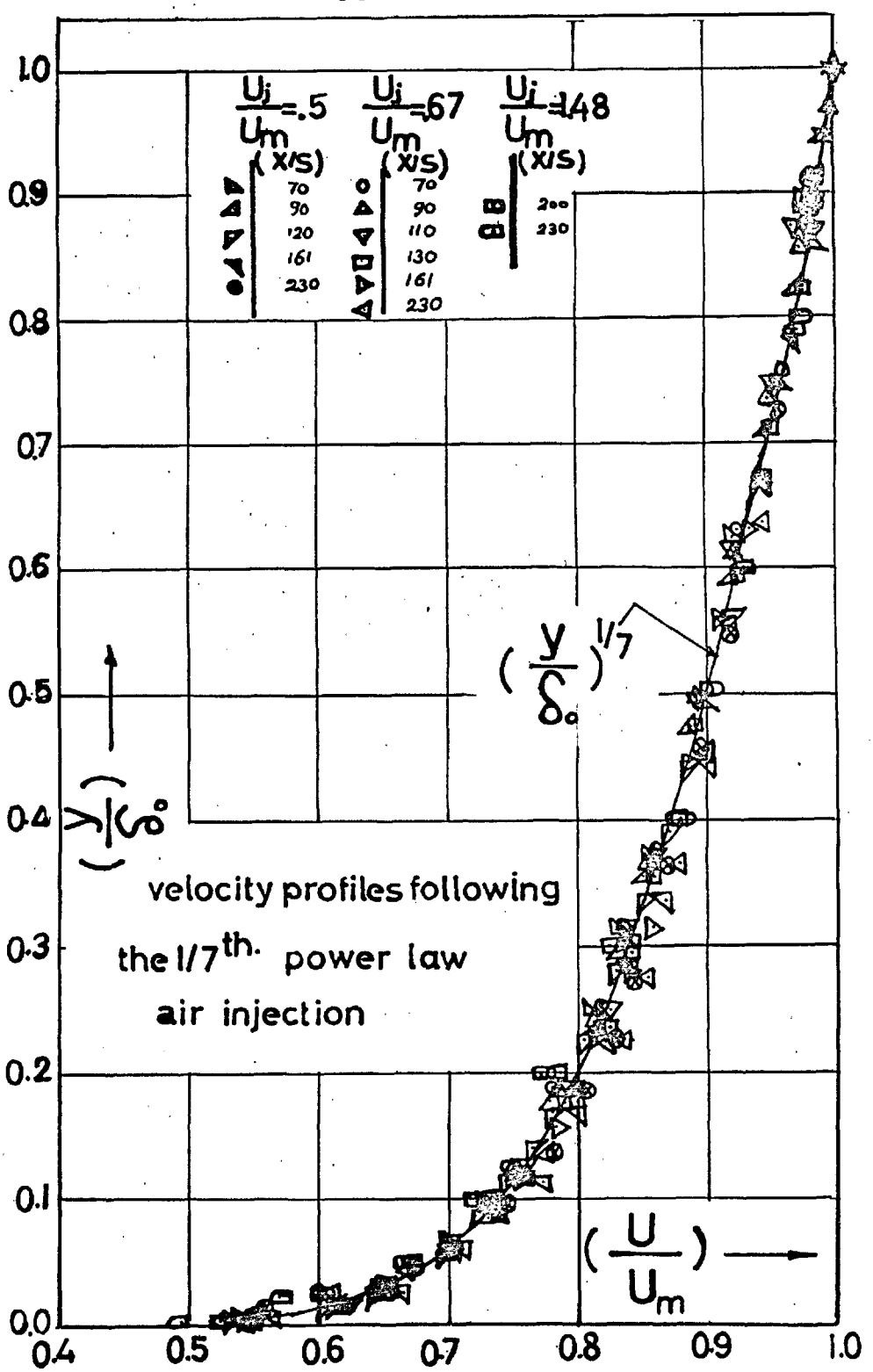

FIG. (8) Correlation of normalized velocity Profiles in the fully developed turbulent boundary layer region.

power law as given by figure (9-a). Figure (9-b), however, shows that the mass velocity profiles, in fact, asymptote to 1/7th power law.

3.3.2.2 The concentration profiles

The concentration profiles across the boundary layer are obtained at the same locations at which the velocity profiles are obtained. Figure (10) shows that the concentration profiles are similar and can be well represented by the exponential function downstream of the potential core region ($x/s \geqslant 30$) that is,

$$(K/K_w) = \text{Exp.} \left[-.6932 \left(y/\delta_{m_{c_w}} \right)^2 \right] \qquad (3.3.2.2.1)$$

where $(\delta_{m_{c_w}})$ is defined as usual

$= y$ at $K = \frac{1}{2} K_w$ measured from the wall.

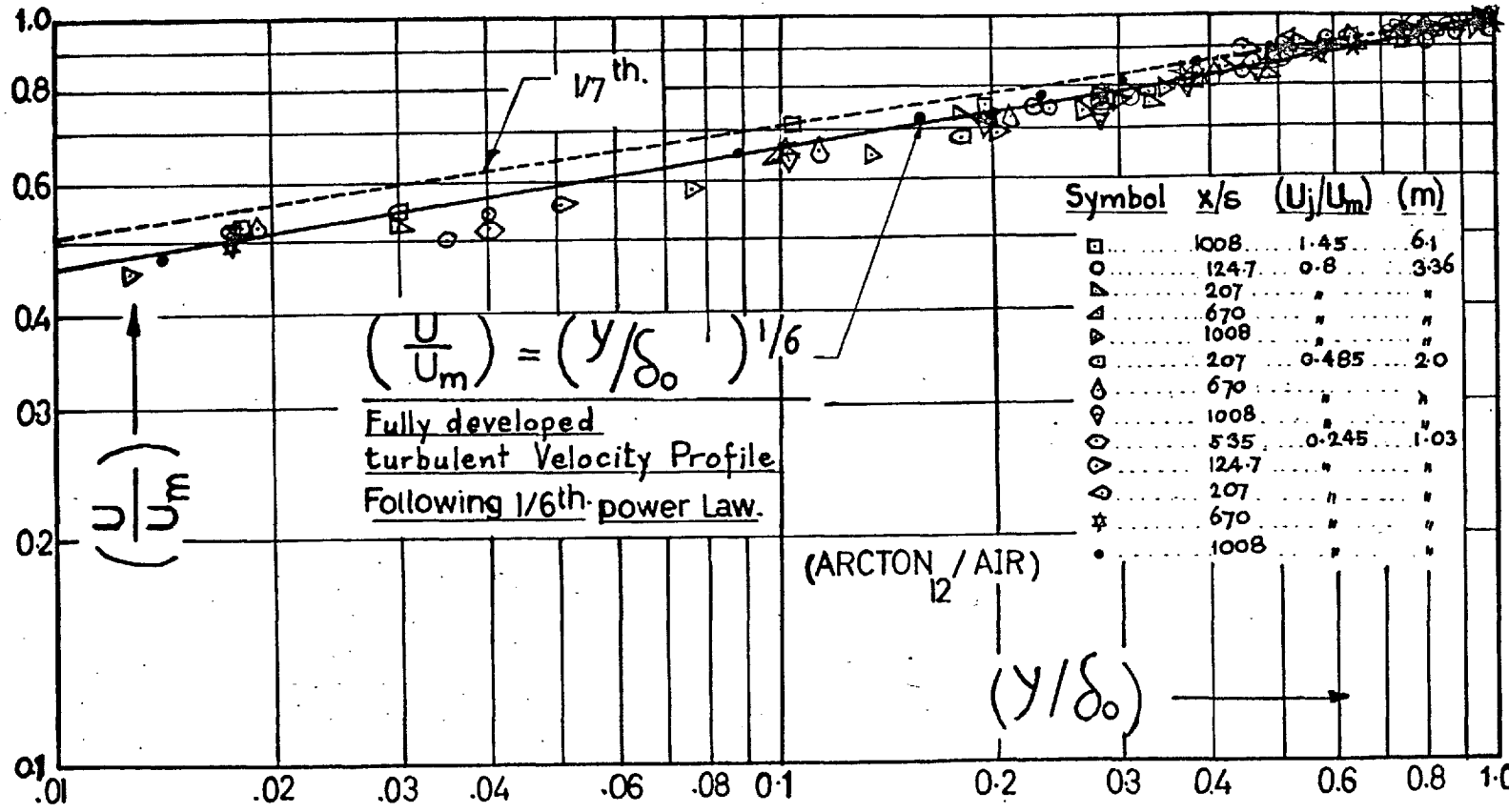

FIG.(9-a) Correlation of normalized velocity Profiles in the fully developed turbulent boundary layer region

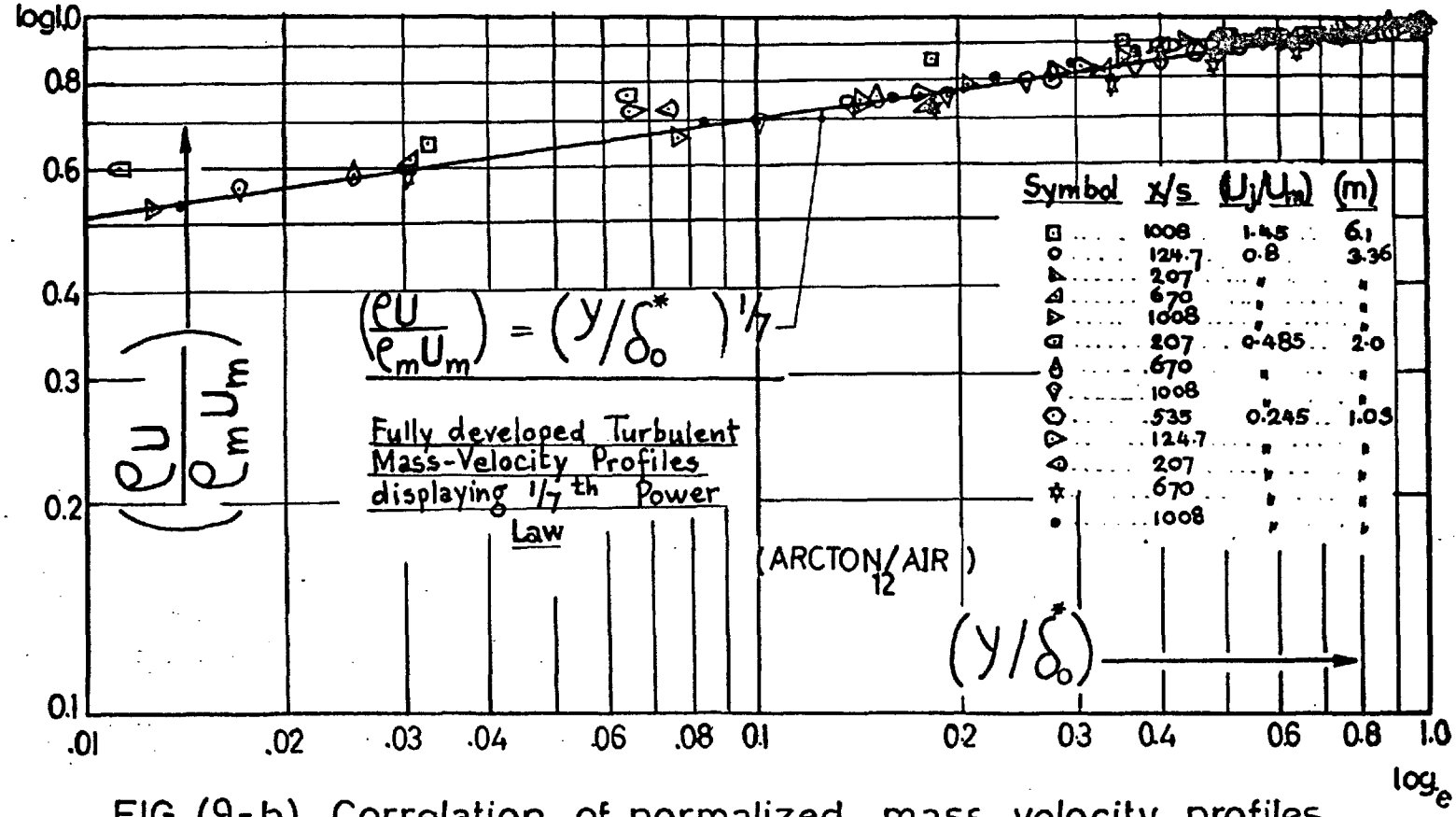

FIG. (9-b) Correlation of normalized mass velocity profiles in the fully developed turbulent boundary layer region

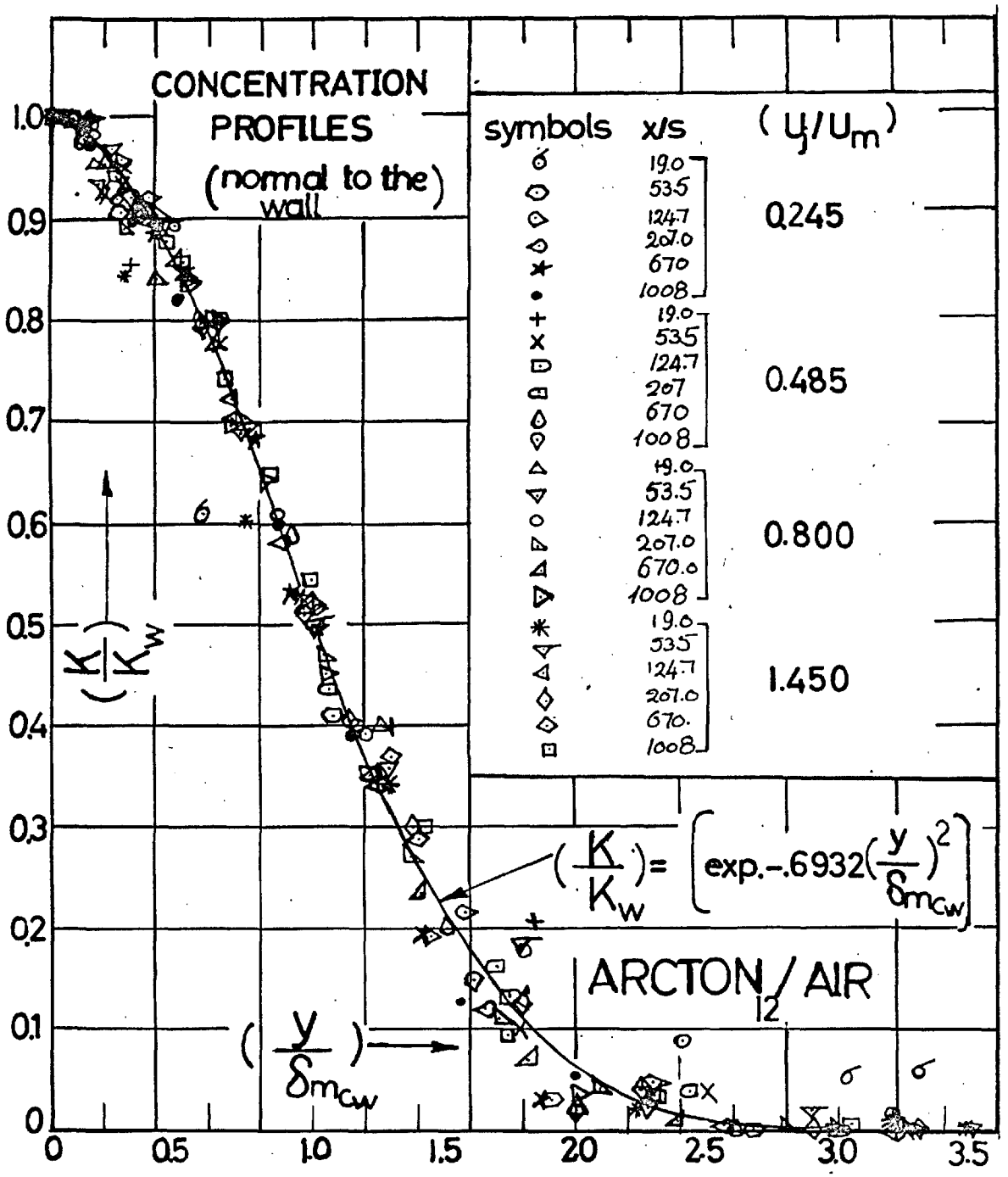

FIG.(10) Correlation of normalized concentration profiles across the boundary layer with $Arcton_{12}$ injection

4. Theory of turbulent mixing for free jet and wake flows.

4.1. Uniform density streams.

4.1.1 Introduction

The first pioneering study of the problem of free turbulent mixing of incompressible fluids was carried out by Tollmien [16] using Prandtl's mixing length theory. He solved the problem of mixing of a parallel stream with an adjacent fluid at rest (plane mixing layer) and the mixing of two-dimensional jet issuing from a very narrow slot with a medium at rest. Tollmien's first problem was extended by Kuethe[35] for two plane parallel streams and the second problem was extended by Abramovich[4] to the case of a two dimensional jet issuing into a moving stream. Each one of them used a different assumption concerning the mixing length hypothesis. In 1929-1930 Schlichting extended Prandtl's theory of free turbulence to the case of wake flow behind a body. The work of Tollmien[16], Kuethe[35] and Schlichting included experimental investigations of the velocity distribution in the flow. By using only one experimental constant they were able to establish agreement between these theories

and the experimental results. This agreement supported Prandtl's theory of free turbulence. A full account and a detailed study can be found in Abramovich[1] Schlichting[2], Pai [36] and Townsend.[4]

4.1.2 Theories of turbulence.

The discussion of these theories is limited to the eddy viscosity theories which assume that

$$\tau = -\rho\overline{vu} = \rho\epsilon\frac{\partial U}{\partial y} \qquad (4.1.2.1)$$

and which all make different assumptions for the eddy kinematic viscosity coefficient (ϵ).

(i) Prandtl's mixing length theory;

the main assumption is $\epsilon = l_o^2 \left| \frac{\partial U}{\partial y} \right|$

where l_o is the lixing length, and consequently the shearing stress from equation (4.1.2.1) can be written as

$$-\rho\overline{vu} = \tau = l_o^2 \left(\frac{\partial U}{\partial y}\right) \left| \frac{\partial U}{\partial y} \right| \qquad (4.1.2.2)$$

and hence $\sqrt{v^2} \sim l_o \left| \frac{\partial U}{\partial y} \right|$ provided that l_o is small. An additional assumption is required to determine the mixing length (l_o).

ii. The constant exchange hypothesis

This theory was also suggested by Prandtl and is sometimes called "Prandtl's new hypothesis". It is

only valid for the case of free turbulent flows. This hypothesis means essentially that the eddy kinematic viscosity (ϵ) is constant across each section of the turbulent mixing region.

Prandtl's new assumption is:-

$$\epsilon = K\delta \ (\bar{U}_{max} - \bar{U}_{min})$$

where δ is the width of the mixing region $(\bar{U}_{max} - \bar{U}_{min})$ is the maximum difference in the time mean flow velocity and (K) is a dimensionless number to be determined from the experiment. ($\frac{1}{K}$) is sometimes called the eddy Reynolds number (e.g. Townsend)[4]. Consequently the shearing stress equation (4.1.2.1) can be written as

$$\tau = \rho K \delta \ (\bar{U}_{max} - \bar{U}_{min}) \left(\frac{\partial U}{\partial y}\right) \qquad (4.1.2.3)$$

iii) G.I. Taylor's vorticity transfer theory.
The fundamental assumption is that the vorticity is constant throughout the process of turbulent mixing and hence

$$\epsilon = l_\omega^2 \left(\frac{\partial U}{\partial y}\right)$$

where $l_\omega = \frac{1}{\sqrt{2}} \ l_o$

And consequently the shearing stress equation will be

$$\tau = \tfrac{1}{2} \rho \ l_\omega^{\,2} \left(\frac{\partial U}{\partial y}\right) \left| \frac{\partial U}{\partial y} \right| \qquad (4.1.2.4)$$

Thus gives an expression that is similar to Prandtl's mixing length theory except that Taylor's mixing length(l_ω) is $\sqrt{2}$ times greater than Prandtl's(l_0).

(iv) Von Karman's similarity hypothesis.

This hypothesis can be regarded as a special case of Prandtl's theory in which

$$l_0 = k_0 \left| \frac{\partial U}{\partial y} \Big/ \frac{\partial^2 U}{\partial y^2} \right|$$

where k_0 is universal empirical constant.

Hence it assumes that $\epsilon = k_0^2 \left| \frac{\partial U}{\partial y} \Big/ \frac{\partial^2 U}{\partial y^2} \right|^2 \left(\frac{\partial U}{\partial y}\right)$

$$= k_0^2 \left(\frac{\partial U}{\partial y}\right)^3 \Big/ \left(\frac{\partial^2 U}{\partial y^2}\right)^2$$

Consequently the shearing stress equation is:-

$$\tau = \rho k_0^2 \frac{(\partial U/\partial y)^4}{(\partial^2 U/\partial y^2)^2} \qquad (4.1.2.5)$$

4.1.3 Gross development of jets and wakes

Since the relation between the turbulent and the mean motion is approximated by the above theories the next step is to consider their application to self-preserving plane jet and wake flows. Since theories (i) and (ii) have been used more extensively theories (iii) and (iv) will be disregarded in this discussion. In the regions of the flow where the pressure is constant, then for steady mean flow, the equation of

motion and continuity are respectively

$$U\frac{\partial U}{\partial x} + V\frac{\partial U}{\partial y} = \frac{1}{\rho}\left(\frac{\partial \tau}{\partial y}\right) \qquad (4.1.3.1)$$

$$\frac{\partial U}{\partial x} + \frac{\partial V}{\partial y} = 0 \qquad (4.1.3.2)$$

Assuming the shear stress relation to be

$$\tau = \rho\epsilon\left(\frac{\partial U}{\partial y}\right) \quad , \quad \text{with}$$

$$\epsilon = K\delta\ (U_{max} - U_{min}) \quad \text{(Prandtl's new hypothesis)}$$

(δ) is the width of the wake or jet and (U_{max}) and (U_{min}) are the maximum and minimum velocities in the wake or jet. Thus for a wake (U_{max}) is (U_m), the free stream velocity, whilst for a jet (U_{min}) is U_m (or = 0) and (U_{max}) is the centre line velocity. If one assumes that $\left(U_{max} \cdot \frac{d\delta}{dx}\right) \sim \sqrt{\overline{v^2}}$

(Duncan, Thom and Young*)

where $\sqrt{\overline{v^2}}$ is the root mean square of the v component of the turbulance and since, according to mixing length theories

$$\sqrt{\overline{v^2}} = \text{const.}\ l_0\frac{\partial U}{\partial y}$$

then

$$\frac{d\delta}{dx} = \left[\frac{\text{const.}\ \delta\,(\partial U/\partial y)}{(U_{max})}\right]$$

But $\epsilon = \text{const.}\ \delta\,(U_{max} - U_{min}) = \delta^2\left(\frac{\partial U}{\partial y}\right)$

i.e. $\delta\left(\frac{\partial U}{\partial y}\right) = \text{const.}\ (U_{max} - U_{min})$

---

* The Mechanics of fluid (1960).

hence finally we have

$$\frac{d\delta}{dx} = \text{const.} \left(1 - \frac{U_{min}}{U_{max}} \right) \quad (4.1.3.3)$$

Thus, in the case of a jet issuing into still air or $U_m \ll U_{max}$, $\frac{d\delta}{dx} = \text{const.}$ or $\delta \sim x$.

Correspondingly, using the momentum conservation equation together with a similarity solution in the form

$$\left(\frac{U}{U_{max}} \right) = f \left(y/\delta \right) \quad \text{we get} \quad U_{max} \sim x^{-\frac{1}{2}}$$

In the case of a wake (U_{min} will represent the velocity at the centre line $U_{\mathfrak{L}}$, whilst U_{max} will represent the freestream velocity) then from (4.1.3.3)

$$\frac{d\delta}{dx} = \text{const.} \left(1 - \frac{U_{\mathfrak{L}}}{U_m} \right)$$

From the momentum conservation equation, provided that the integral is taken far enough downstream for $(U_{\mathfrak{L}} - U_m) \ll U_m$ together with the similarity solution in the form

$$\left(\frac{U - U_m}{U_{\mathfrak{L}} - U_m} \right) = f \left(y/\delta \right) \text{ , we get}$$

$$\delta \frac{d\delta}{dx} = \text{const.} \left(C_D \right) \text{ where } C_D \text{ is the drag coefficient from which we obtain}$$

$$\delta \sim x^{\frac{1}{2}} \quad \text{and} \quad (U_{\mathfrak{L}} - U_m) \sim x^{-\frac{1}{2}}$$

We discuss later how this must also be the asymptatic solution of a jet. The laws of spreading and the decay for jets and wake are summarized below.

Type of flow	condition	law of spread	Law of centre-line decay (U_ℓ or U_{max})
plane jet	$U_m=0$ or $U_{max} \gg U_m$	x	$x^{-\frac{1}{2}}$
plane wake	$U_\ell - U_m \ll U_m$	$x^{+\frac{1}{2}}$	$x^{-\frac{1}{2}}$

4.1.4 "Exact" solutions for plane jet and wake flows.

A. The plane jet

$U_m = 0$

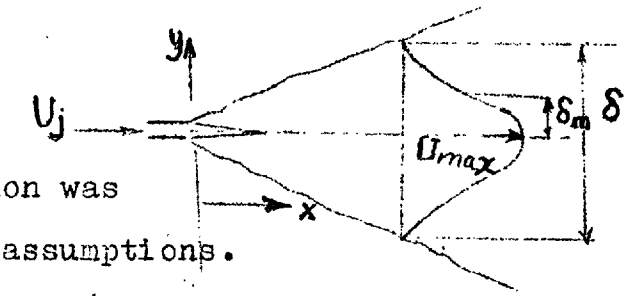

Tollmien's exact solution was based on the following assumptions.

1) $U = U_{max}\, f(\eta)$, $\eta = (y/\delta)$

2) $\tau = \rho l_0^2 \left(\frac{\partial U}{\partial y}\right)\left|\frac{\partial U}{\partial y}\right|$ from Prandtl's mixing length hypothesis with $l_0/\delta = c$ = constant

He used the equation of motion and the continuity equation as given by (4.1.3.1) and (4.1.3.2.) The solution was numerical i.e. f is not expressed directly

in term of (η). The tabulated (f) can be found in Tollmien's paper. A simple solution was obtained by Gortler (in refe. 2) which was based upon Prandtl's new hypothesis. He assumed that

δ = const. x, hence $\left(\frac{U}{U_{max}}\right)$ = f ($\sigma\xi$) where $\xi = (y/x)$

and σ denotes a free constant, & $\tau = \epsilon\left(\frac{\partial U}{\partial y}\right)$ with $\epsilon = K\delta U_{max}$. The exact solution of the equation of motion was in this form

$$f(\xi) = (1 - \tanh^2 \sigma\xi) \quad (4.1.4.1)$$

In terms of (η) rather than (ξ), the solution is

$$f(\eta) = (\operatorname{sech}^2 .8814\,\eta) \quad (4.1.4.2), \quad \& \left[\eta = \left(\frac{y}{\delta_m}\right)\right]$$

Tollmien's and Gortler's solution were compared with the experimental results due to Reichardt and Forthmann [26] (e.g. Schlichting [2]). Gortler's solution showed a slightly superior agreement with the measurements near the jet centre-line.

4.1.5 Some deduction from Tollmien's 'exact' solution

(i) (The Jet Spread) 'δ'

From Tollmien numerican solution, we obtain

$$\frac{1}{c^2}\left(\frac{\delta}{U_{max}}\right)\frac{dU_{max}}{dx} = 14$$

since $U_{max} \sim x^{-\frac{1}{2}}$

$$\therefore (\delta/x) = 28\, c^2 \qquad (4.1.5.1)$$

(ii) The centre-line velocity

The momentum conservation equation gives

$$J = \int_{-\infty}^{\infty} \rho U^2 dy = \text{constant} = 2\rho U_{max}^2 \cdot \delta \int_0^{\infty} f^2(\eta)\, d\eta$$

from (4.1.5.1) we get,

$$U_{max} = \text{const.} \left[\frac{1}{\sqrt{x}} \cdot \sqrt{J/\rho} \right] \quad (4.1.5.2)$$

According to Forthmann [26] measurements, the constant is 2.4 giving a value of $\epsilon = 0.1045$

4.1.6 The plane wake

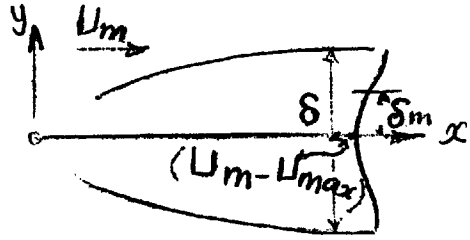

Schlichting 'exact' solution.

N.B. We shall use (U_{max}) to represent the velocity at the centre-line (so that it may not be confused with the list of symbols)

Schlichting main assumptions were:

At far downstream the velocity profiles can be expressed as $U - U_m = (U_{max} - U_m)\, f(\eta)$ where $\eta = (y/\delta)$

$$\tau = \rho l_0^2 \left(\frac{\partial U}{\partial y}\right) \left|\frac{\partial U}{\partial y}\right| \text{ from Prandtl's mixing length}$$

theory. Adopting Tollmien's assumption i.e. $l_0/\delta = c =$ const. The exact solution to the equation of motion was in this form: $f(\eta) = (1 - \eta^{3/2})^2 \quad (4.1.6.1)$

Solution based on Pradtl's new hypothesis is also available. Using $\tau = \epsilon \left(\frac{\partial U}{\partial y}\right)$ where ϵ assumed to be constant throughout the flow field $= \epsilon_0$, then the exact solution in terms of (η) can be

written as:

$$f(\eta) = \exp.\left[(-\text{const.}\,\eta^2)\right] \quad (4.1.6.2)$$

where $\eta = (y/\delta)$

These two solutions were found to be in a good agreement with Schlichting's and Reichardt's measurement for a wake behind a cylender (see Schlichting [2]) at for downstream.

4.1.7 Some deduction from Schlichting 'exact' solution for a plane wake.

(i) The wake spread "δ"

From Schlichting[2] exact solution we obtain

$$U_m \frac{\delta}{(U_{max} - U_m)} \frac{d \log (U_{max} - U_m)}{d x} = 9c^2$$

Since $(U_{max} - U_m) \sim x^{-\frac{1}{2}}$

then $\frac{1}{2}\left(\frac{\delta}{x}\right)\left(\frac{U_m}{U_{max} - U_m}\right) = 9c^2 \quad (4.1.7.1)$

This equation contains two unknowns (δ) and (U_{max}) solving it requires a further relation between them.

An additional relation can be obtained by direct appeal to the momentum conservation equation,

At far downstream the momentum conservation can be written as,

$$D = -2\rho_m U_m (U_{max} - U_m)\delta \int_0^1 f(\eta)\, d\eta \quad (4.1.7.2)$$

Where D is the drag force acting on the body, and according to the profile given by equation (4.1.6.1)

$$\therefore \int_0^1 f(\eta)\, d\eta = \text{const.} = 0.47$$

Equation (4.1.7.2) can be rearranged to give:

$$\left(\frac{\delta}{x}\right)\left(\frac{U_{max} - U_m}{U_m}\right) = -\frac{1}{(2 \times 0.47)} \left[\frac{D}{\rho_m U_m^2 x}\right] \quad (4.1.7.3)$$

From (4.1.7.1) and (4.1.7.3) we get

$$\left(\frac{U_{max} - U_m}{U_m}\right) = -\frac{.248}{c}\left(\frac{D}{\rho_m U_m^2 x}\right)^{\frac{1}{2}} \quad (4.1.7.4)$$

$$(\delta/x) = 4.46\, c \left(\frac{D}{\rho_m U_m^2 x}\right)^{\frac{1}{2}} \quad (4.1.7.5)$$

From the experimental measurements by Schlichting [2]

$c = 0.178$

It may be worth noting that the half width of the jet or the wake (δ_m) can be obtained from the above deductions using the relation ($\delta_m = 0.441\delta$).

4.1.8 The turbulent plane jet in a moving stream

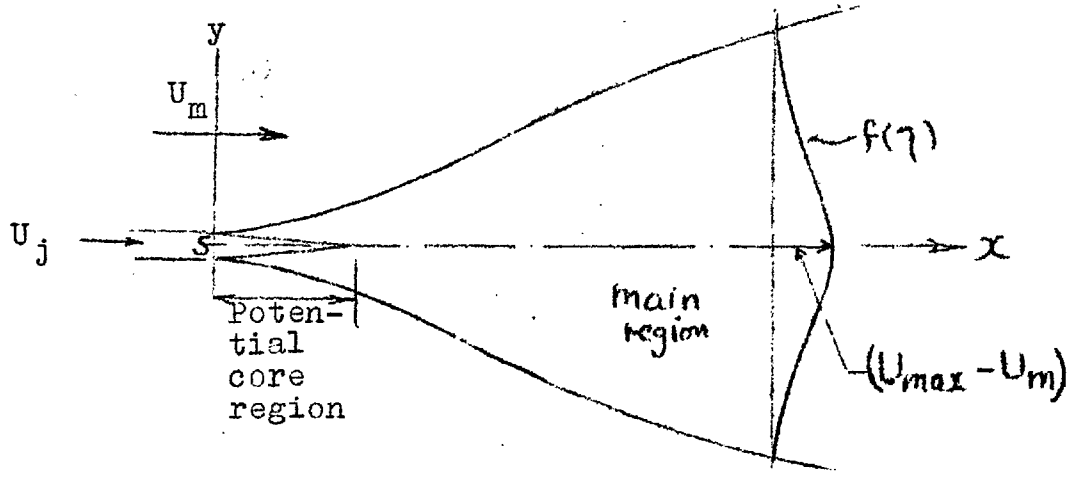

Since this flow is the main interest in the present work, it is appropriate to spend a little time in defining terms. The above figure shows the flow of a plane jet emerging from a slot of width(s) into a moving air stream of constant velocity (U_m). The jet velocity (U_j) is assumed to be uniform at the slot exit. In the immediate vicinity of the slot a region is developed in which the centre-line velocity remains constant and equal to(U_j). In this region plane mixing layers develop. These shear layers are similar to those studied by Kuethe.[35] Eventually these layers coalesce and the jet becomes fully turbulent i.e. the 'potential core' disappears and the main region of the jet is developed. A particular case of this flow is given in sections (4.1.4 and 4.1.5), the pure plane jet, where this fully turbulent region of the jet develops into a strictly self-preserving one, i.e. $U_{max} \sim x^{-\frac{1}{2}}$ and $\delta \sim x$. However for $U_m \neq 0$ Spalding[37] following Abramovich, has suggested that this fully turbulent region develops into a self preserving one far downstream from the slot, in which

$(U_{max} - U_m) \sim x^{-\frac{1}{2}}$ and $(\delta \sim x^{\frac{1}{2}})$

According to section (4.1.3), this assumption implies

that the flow in the jet would be similar to that in the wake far downstream from the slot. Spalding [37] adopted Prandtl's mixing length hypothesis, he wrote the following asymptotic expressions for the jet:-

$$f = (1 - \eta^{3/2})^2 \qquad 4.1.8.1.$$

$$\left(\frac{U_{max} - U_m}{U_m}\right) = \frac{0.248}{c} \left[\frac{U_j}{U_m}\left(\frac{U_j}{U_m} - 1\right)\frac{s}{x}\right]^{\frac{1}{2}} \qquad (4.1.8.2)$$

and

$$(\delta/x) = 4.46\, c \left[\frac{U_j}{U_m}\left(\frac{U_j}{U_m} - 1\right)\frac{s}{x}\right]^{\frac{1}{2}} \qquad (4.1.8.3)$$

Equation (4.1.8.2) was in agreement with Weinstein's [3] measurements for (U_{max}) (e.g. Spalding [38]) though these measurements were not far downstream from the slot $(x/s \leq 60)$. Equation (4.1.8.3) did not (and indeed should not) correlate Weinstein's [3] results for the jet spread (δ). Following Townsend,[4] Bradbury [39] assumed that the self-preservation in the flow will be developed from an apparent origin which is different from the actual origin of the flow at the slot exit, and that the nozzle is a source of excess momentum flux (J) (e.g. Townsend [4]). Using dimensional analysis he wrote:

$$\left(\frac{U_{max} - U_m}{U_m}\right) = f_1\left[\left(\frac{J}{\rho_m U_m^2 (x - x_o)}\right)\right] \qquad (4.1.8.4)$$

and $\left[\delta / (J/\rho U_m^2)\right] = f_2\left[\left(\frac{J}{\rho U_m^2 (x-x_o)}\right)\right]$ (4.1.8.5)

where (x_o) is the apparent shift in the origin of the flow, (J) was taken to be $\int_{-\infty}^{+\infty} \rho U(U - U_m)\, dy$,

then $\frac{(U_{max} - U_m)}{\sqrt{J/\rho}} \sqrt{x-x_o} = \text{const.}$ (4.1.8.6)

as $x \longrightarrow x_o$, $\delta \sim (x - x_o)$

In other words, equation (4.1.8.4) will be similar to that obtained for a jet issuing into still air (§ 4.1.4). These arguments, in fact, seem to indicate that self-preservation in a jet into a moving stream is not possible throughout the entire flow field (e.g. Townsend[4]), however, two types of self-preserving flow can exist in limited regions of the flow. Near the slot exit where $(U_{max} \gg U_m)$ a self-preserving flow in which $U_{max} \sim x^{-\frac{1}{2}}$ and $\delta \sim x$ (e.g. Bradbury.[39]), whereas far downstream where $(U_{max} - U_m) \ll U_m$ there will be possibility for self-preservation in which $(U_{max} - U_m) \sim x^{-\frac{1}{2}}$ and $\delta \sim x^{\frac{1}{2}}$ (e.g. Spalding[32]).

4.1.9. The turbulent axi-symmetric jet

The present investigation is not directly concerned with the axi-symmetric jet, however, some of the results on this self-preserving flow are of particular interest. Theoretical analyses for a round jet exhausting into a moving stream have been made by

many workers for example, Squire [40], Szablewski [41], Abramovich[1] and Kuchemann[42]. Detailed accounts of these analyses and others can be found in Abramovich[1] and Schlichting[2]. Perhaps the most interesting analytical treatment was by Squire [40] who extended the plane jet solution of Kuethe [35] to cover the case of an axi-symmetric jet. The flow in the core region and that of the main mixing region of the jet were investigated separately. These two solutions were matched together at the section where the potential core disappears. The solution was simplified by adopting a cosine profile and assuming Prandtl's mixing length hypothesis. Squire [40] prediction was compared with Landis's[43] data; the agreement was not altogether satisfactory. The following table summarises the theoretical profiles which have been obtained for round jets and circular wakes on the basis of different hypotheses for the mechanism of turbulent mixing.

Shear stress assumption.	Type of flow	Profile derived
Prandtl's mixing length theory	1) Round jet $U_m = 0$ Circular wake	Tollmien[16] exact solution (tabulated) $f(\eta) = (1 - \frac{3}{2}\eta)^2$ (e.g. Swain, in refer. 2)
Constant exchange hypothesis. (Prandtl's new hypothesis)	1) Round jet $U_m = 0$, $\delta \sim x$	$f = \frac{1}{(1+\frac{1}{4}\bar{\xi}^2)^2}$ $\bar{\xi} = (\sigma y/x)$ (e.g. Schlichting[2])
	2) $U_m \neq 0$	$f = \frac{1}{(1+\text{const.}\eta^2)^2}$ (e.g. Szablewski[44])
	Round jet $U_m \neq 0$	Squire[40] assumed $f(\eta) = \frac{1}{2}(1+\cos \pi y/\delta)$

4.2 Non uniform density streams

All the jet mixing problems considered so far, in the previous section (4.1), are jets of one fluid only i.e. the fluid in the jet is the same as the receiving medium. The more complex problem, however, arises when the jet fluid is of different density to that of the surrounding medium. A density gradient can be imposed on the flow field, either by using different temperature streams of the same fluid or by using different fluids at the same temperature (or both). If the molecular weight of the fluid in the jet differs considerably from that in the surrounding medium then the diffusion equation must also be satisfied. Density differences are, therefore, expected to be of some importance, though one may tentatively suggest that the density difference diminishes rapidly with distance, and the jet soon behaves much like the constant density one.

4.2.1 The governing equations for compressible, turbulent jet mixing at constant pressure.

The governing equations for steady two-dimensional flow are:

$$\rho U \frac{\partial U}{\partial x} + \rho V \frac{\partial U}{\partial y} = \frac{\partial}{\partial y}\left[(\mu_t \frac{\partial U}{\partial y})\right] \quad \text{Momentum (4.2.1.1)}$$

$$\frac{\partial \rho U}{\partial x} + \frac{\partial \rho V}{\partial y} = 0 \quad \text{Continuity (4.2.1.2)}$$

$$\rho U \frac{\partial h^o}{\partial x} + \rho V \frac{\partial h^o}{\partial y} = \frac{\partial}{\partial y}\left[(P_r^{-1} \mu_t \frac{\partial h^o}{\partial y})\right] \quad \text{Energy (4.2.1.3)}$$

$$\rho U \frac{\partial C}{\partial x} + \rho V \frac{\partial C}{\partial y} = \frac{\partial}{\partial y}\left[(S_c^{-1} \mu_t \frac{\partial C}{\partial y})\right] \quad \text{Diffusion (4.2.1.4)}$$

where the dissipation function is neglected,

(μ_t) is the turbulent coeeficient of viscosity

$= (\rho \epsilon)$,

S_c is the turbulent Schmidt number

$= (\epsilon / D_{12})$

and

P_r is the turbulent Prandtl number

$= (c_p \frac{\mu_t}{\mathcal{K}})$

The analytical solution of these equations is greatly impeded by the present limited knowledge of the fundamentals of turbulent transport (momentum, energy and diffusion) and the theoretical results are always empirical in the sense that the variation of the transport property along and across the flow must be obtained from experiment. The usual technique in solving these equations is, therefore, by introducing some sort of transformation (in which are normally included the transport coefficients (μ_t), (μ_t / S_c) and

(μ_t / P_r) to render them into a set of linear differential equations of well known form. The scaling of the flow properties, for example the total enthalpy (h^o) or the concentration (C) distribution from the transform plane to the real plane will be entirely dependent on the variation of these transport coefficients. All the analytical treatments have assumed that S_c and Pr are constants along and across the layer, and hence, they concentrated on the variation of the kinematic eddy viscosity (ϵ). A very short account of some of the analytical treatments to this problem, which have been reported by a number of authors (e.g. Crane and Pack[44], Libby [17] and Schetz [45]) is given below.

Crane and Pack[44] have adopted the constant exchange hypothesis in an attempt to obtain an analytical solution for an isothermal plane gas jet exhausting into still air. They used the momentum and the diffusion equations (4.2.1.1 and 4.2.1.4). They assumed incompressible flow of the gas and the eddy kinematic viscosity $\epsilon = (\frac{\mu_t}{\rho})$ to be constant across the jet and dependent on (x) only far downstream from the slot. They used the following transformation:

$$Z = \int_0^y (\rho / \rho_m)\, dy \quad , \quad \mathcal{Y} = \int_0^x \frac{\epsilon(x)}{\epsilon_o}\, dx,$$

where ϵ_0 is constant (Richardt's constant exchange coefficient) and the stream function was

$$\rho U = \frac{\partial \psi}{\partial y} \quad , \quad \rho V = - \frac{\partial \psi}{\partial x}$$

For a first approximation ($\frac{\rho}{\rho_m} = 1$), the momentum equation was reduced to that obtained by Bickley [46] for a laminar jet. Crane & Pak [44] considered Bickley's stream function (ψ) as starting point for the solution of the compressible flow. The second approximation was obtained by expanding Bickley's stream function in a Rayleigh-Janzen series in powers of a parameter related to the concentration. Their result for the velocity, has indicated that if the injected gas is heavier than the surrounding atmosphere, the velocity on the axis (U_{max}) will be less than it would be if both fluids have the same density. This result was in disagreement with the physics of the problem and with the experimental results of Keagy and Weller[8], who found that the increased density caused the velocity to fall less rapidly than for the constant density case. Crane's approximate expression for the momentum flux profile (ρU^2) was found to be insensitive to the changes of the density at far downstream from the slot which is in agreement with Corrsin and Uberoi's[7] total head measurements as would be expected

from the small density ratio ($\rho_m/\rho_j = 2$) of Corrsin's experiment.

Libby [17] has treated the problem of a compressible axi-symmetric gas jet moving into an external stream. The momentum and the diffusion equations were transformed from $(x-y)$ plane to $(x-\psi)$ plane using the Von Mises transformation. He assumed that the dynamic viscosity coefficient ($\rho\epsilon$) to be constant across the jet and dependent on x only. Therefore, additional transformations, namely

$$X_u \sim \int_o^x (\rho\epsilon)\ dx \quad , \quad X_c \sim \int_o^x S_c^{-1}\ (\rho\epsilon)\ dx,$$

were used for the momentum and the diffusion equations respectively to render them into the form of the one-dimensional heat conduction equation whose solution is known. To complete the transformation of the solution back to the real plane, however, Libby has postulated an expression for ($\rho\epsilon$) which was based on Prandtl's new hypothesis, he wrote

$$(\rho\epsilon) = \text{const.}\ \rho_m U_m\ \delta_m\ \left(1 - \frac{\rho_{max}}{\rho_m}\ \frac{U_{max}}{U_m}\right)$$

This expression correlated Ferri's [13] result with limited amount of success, and was in disagreement with Zakkay's [18] and Alpinieri's [15] results for both supersonic and high subsonic flows. An attempt

has been made by Schetz [45] to solve the two-dimensional compressible jet following Libby[17]. The momentum equation was written, using the Von Mises transformation, in this form

$$\frac{\partial U}{\partial x} = \frac{\partial}{\partial \psi}\left(\frac{\rho^2 \epsilon}{\rho_m^2 U_m^2} U \frac{\partial U}{\partial \psi} \right) \quad (4.2.1.5)$$

where $\frac{\partial \psi}{\partial y} = (\rho U / \rho_m U_m)$

He assumed, following Ting and Libby[47], that

$$(\rho^2 \epsilon) = f(x) = \rho_{max}^2 \bar{\epsilon}_{(x)}$$

where $\bar{\epsilon}(x)$ is the incompressible eddy kinematic viscosity and, following Libby [17], he wrote

$$(\rho^2 \epsilon) = \text{const.} \quad \delta_m \rho_{max} \left[(\rho U)_{max} - (\rho U)_{min.} \right]$$

Schetz,[45] also assumed that the dimensionless velocity $\left(U(x, \psi) / U_m\right)$ within the braket on the right hand side of equation (4.2.1.5) can be written as $\left\{ \frac{1 + \frac{U_{max}}{U_m}}{2} \right\}$. His justification for this later assumption was to obtain an approximate solution. His transform coordinate, therefore, was assumed to be

$$X \sim \frac{1}{2} \int_0^x (\rho^2 \epsilon) \left(1 + \frac{U_{max}}{U_m}\right) dx$$

and correspondingly the momentum equation was reduced to this form

$$\frac{\partial \tilde{U}}{\partial X} = \psi_j \frac{\partial^2 \tilde{U}}{\partial \psi^2} \qquad 4.2.1.6$$

where ψ_j defined as $(\rho_j U_j s / \rho_m U_m)$, and $\tilde{U}$ is the dimensionless velocity. Equation (4.2.1.6) is similar to that obtained by Pai [36] for a laminar compressible jet, and whose solution is well known i.e.

$$\frac{U - U_m}{U_j - U_m} = \frac{1}{2}\left[\text{erf.}\ \frac{1-\psi}{2\sqrt{X}} + \text{erf.}\ \frac{1+\psi}{2\sqrt{X}}\right] \qquad (4.2.1.7)$$

where $\text{erf}(t) = \frac{2}{\sqrt{\pi}} \int_0^{t_1} e^{-t^2}\, dt_1$

The stgnation enthalpy (h^o) and the concentration (C) fields were obtained from the velocity solution using the generalized Corocco relation, assuming that Pr.= Sc.= 1. According to Schetz [45], the transformation back to the physical plane has required that

$$\left(\frac{y}{s}\right) = m \int_0^{\tilde{\psi}} \left[\frac{\rho_m U_m}{\rho u}\right] d\tilde{\psi}'$$

$$\left(\frac{x}{s}\right) = \text{const.}\ m^2 \int_0^{\tilde{X}} \frac{(\rho_m/\rho_{max})^2\, d\tilde{X}'}{\left(\frac{\delta_m}{s}\right)\left|\left(\frac{\rho_m}{\rho_{max}} - \frac{U_{max}}{U_m}\right)\right|\left(1 + \frac{U_{max}}{U_m}\right)}$$

However, according to a brief note recently reported by Schetz *, these complex relations were approximated by power laws of the form ,

$$\left(y/s\right) = m^{0.75}\ F(\tilde{\psi})$$

$$\left(x/s\right) = \text{const.}\ m^{1.44}\ G(\tilde{X})$$

*Journal of Applied Mechs. Vol.32 No.1. 1965 (198-200).

where(F)and(G)are integral functions dependent on the stream function(ψ), the eddy kinematic viscosity(ϵ), the density and the velocity at the jet axis respectively. No experimental measurements have been made to check these formulae.

It appears from the above analysis (e.g. Crane, Libby and Schetz) that there are at least three formulae that have been suggested or used for the kinematic eddy viscosity (ϵ) which, in general, may be written as,

$$\epsilon = \left[\left(\frac{\rho_{max}}{\rho}\right)\right]^{N'} \bar{\epsilon}$$

[$\bar{\epsilon}$ is the eddy kinematic viscosity for incompressible flow] with $N' = 0, 1, 2$

$N' = 0$ means that (ϵ) is constant across the layer and has been used by Crane [44].

$N' = 1$ corresponds to a constant dynamic viscosity coefficient ($\rho\epsilon$) and has been suggested by Libby [17].

$N' = 2$ Permits the transformation from the compressible boundary-layer to an incompressible form, has been suggested by Ting and Libby [47] and used by Schetz.[45] Profile measurements in the mixing layer of supersonic air stream ($M^* = 2.76$) with adjacent fluid at rest were compared with the theoretical profiles calculated with $N' = 0, 1, 2$ by Hill[48]. The profile

with $N' = 2$ was not in agreement with the experimental results, while the profiles with $N' = 0, 1$ were in fair agreement with the data.

4.2.2 Reynolds Analogy.

If $Pr = S_c = 1.0$, the governing equations (4.2.1.1), (4.2.1.3) and (4.2.1.4) can be written according to Von Mises transformation as

$$\frac{\partial U}{\partial x} = \frac{\partial}{\partial \psi}\left[(\rho^2 \epsilon U \frac{\partial U}{\partial \psi}\right] \text{ Momentum (4.2.2.1)}$$

$$\frac{\partial h^o}{\partial x} = \frac{\partial}{\partial \psi}\left[(\rho^2 \epsilon U \frac{\partial h^o}{\partial \psi}\right] \text{ Energy (4.2.2.2)}$$

$$\frac{\partial C}{\partial x} = \frac{\partial}{\partial \psi}\left[(\rho^2 \epsilon U \frac{\partial C}{\partial \psi}\right] \text{ Diffusion (4.2.2.3)}$$

From (4.2.2.1) and (4.2.2.2) a possible solution is

$$h^o = A' U + B' \quad (4.2.2.4)$$

and from (4.2.2.1) and (4.2.2.3) a possible solution is

$$C = E' U + F' \quad (4.2.2.5)$$

where A', B', E', and F' are constants.

Hence from (4.2.2.4) we obtain

$$\left[\frac{T - T_m}{T_j - T_m}\right] = \left[\frac{U - U_m}{U_j - U_m}\right] \quad (4.2.2.6)$$

and from (4.2.2.5) we get

$$\left[\frac{C - C_m}{C_j - C_m}\right] = \left[\frac{U - U_m}{U_j - U_m}\right] \qquad (4.2.2.7)$$

Therefore,

$$\left[\frac{C - C_m}{C_j - C_m}\right] = \left[\frac{T - T_m}{T_j - T_m}\right] = \left[\frac{U - U_m}{U_j - U_m}\right] \qquad (4.2.2.8)$$

Equation (4.2.28) is the well known Reynolds analogy for a unit Lewis number, which is usually applied to many engineering problems connected with heat or mass transfer since it simplifies the mathematical treatment considerably.

5. The development of a simple theory for a two dimensional jet of gas into a moving air stream (ρ is non-Uniform)

5.1 Introduction

In this section the general problem of a plane jet of foreign gas issuing into a moving stream is discussed. Particular cases of this general development are compared with the existing asymptatic theories.

Dimensional analysis.

The application of the dimensional analysis gives for the mean velocity in the jet,

$$\frac{U}{U_m} = \Phi_1 \left(\frac{U_j}{U_m}, \frac{\rho_j}{\rho_m}, x/s, y/s, Rej \right) \quad (5.1.1)$$

and for the centre line quantities,

$$\left(\frac{U_{max} - U_m}{U_m}\right) = \left(\frac{U_o}{U_m}\right) = \Phi_2 \left(\frac{U_j}{U_m}, \frac{\rho_j}{\rho_m}, x/s, Rej \right) \quad (5.1.2)$$

$$C_{max} = \Phi_3 \left(\frac{U_j}{U_m}, \frac{\rho_j}{\rho_m}, x/s, Rej, Sc. \right) \quad (5.1.3)$$

$$\left(\frac{\delta_m}{s}\right) = \Phi_4 \left(\frac{U_j}{U_m}, \frac{\rho_j}{\rho_m}, x/s, Rej, S_c \right) \quad (5.1.4)$$

In any experiment the slot geometry and the model will affect the flow in the region close to the

slot because of the initial boundary-layer thickness at the slot. Both the present experimental results and others show that one can assume, provided that the jet velocity is 3 times or more than free stream velocity, that downstream of the potential core region these effects will have become negligibly small. However, in the case where the jet velocity is lower than the free stream velocity, the initial momentum deficit due to the boundary-layer thickness cannot be ignored even far downstream (see sec.7). Therefore it is important to calculate the local excess momentum flux ($\int_{-\infty}^{+\infty} \varrho U(U - U_m)\, dy$) rather than assuming this to be equal to $\left[\varrho_j U_j (U_j - U_m)s\right]$ The connection between these two quantities and the compensation for the drag over the aerofoil is given in sec.(5.5).

5.2. <u>The flow similarity solution</u>.

Since the analytical treatment to be developed makes use of the momentum equation, some assumptions must be made concerning profile similarity for both jet and wake flows. On the assumption that the velocity and concentration distributions across the jet of a foreign gas issuing into a moving air stream are of exponential form (e.g. Craven[49]),

it will be assumed that the mass flux and the momentum flux profiles can be written in the form

$$\Delta(\rho U) = \Delta(\rho U)_{max} \exp.\left(-a\eta^2\right) \quad (5.2.1)$$

$$\Delta(\rho U^2) = \Delta(\rho U^2)_{max} \exp.\left(-b\eta^2\right) \quad (5.2.2)$$

where $\Delta(\rho U) = \rho U - \rho_m U_m$

$\Delta(\rho U^2) = \rho U^2 - \rho_m U_m^2$

, a, b are constants with $a/b \simeq 1.0$

and $\eta = (y/\delta_m(x))$, $\delta_m(x)$ is defined in the usual way, i.e. the half way width of the individual profile. These assumptions are justified, except for some of the helium data, by the present experimental results (see figures 4. g, h, i and j)

The conservation of momentum gives

$$\int_{-\infty}^{+\infty} (\rho U)\ (U - U_m)\, dy = \left[\rho_j U_j\ (U_j - U_m)S\right] - D = J$$
$$= \text{const.} \quad (5.2.3)$$

Substituting eqns. (52.1.) and (5.2.2) into (5.2.3) gives

$$\delta_{m(x)} \int_{-\infty}^{+\infty} \left[\rho_m U_m^2 + \Delta(\rho U^2)_{max}\, e^{-b\eta^2} - U_m\left(\rho_m U_m + \Delta(\rho U)\, e^{-a\eta^2}\right)\right] d\eta$$
$$= J \quad (5.2.4)$$

From $\int_{-\infty}^{+\infty} e^{-At^2}\, dt = \sqrt{\frac{\pi}{A}}$ a direct integration yields,

$$\delta_m(x)\left[\sqrt{\frac{\pi}{b}}\,\Delta(\rho U^2)_{max} - \sqrt{\frac{\pi}{a}}\,U_m\,\Delta(\rho U)_{max}\right] = J \quad (5.2.5)$$

dividing by $\rho_j U_j^2\ \delta_m(x) \cdot \sqrt{\frac{\pi}{b}}$ gives

$$\therefore \left(\frac{\Delta (\rho u^2)_{max}}{\rho_j U_j^2}\right) - \left(\sqrt{\frac{b}{a}}\,\frac{\Delta (\rho u)_{max}}{\rho_j U_j}\right)\cdot\left(\frac{U_m}{U_j}\right) = \sqrt{\frac{b}{\pi}}\left(\frac{J}{\rho_j U_j^2 \delta_m(x)}\right) \qquad (5.2.6)$$

Equation (5.2.6) is the general form of the momentum conservation equation which includes 3 unknowns, ($U_{max}(x)$, $\rho_{max}(x)$ and $\delta_m(x)$)

Exact solution of this equation therefore requires two additional relations between (U_{max}), (ρ_{max}) and ($\delta_m(x)$)

Some Special cases from equation (5.2.6)

1) $\rho_j = \rho_m = \text{const.}$ $\quad U_m = 0$

Equation (5.2.6) reduces to

$$\left[\frac{(U_{max})}{U_j}\right]^2 = \left(\sqrt{\frac{b}{\pi}}\,\frac{J}{\rho_j U_j^2 \delta_m(x)}\right)$$

which $\delta_m \sim (x)$ (Tollmien[16]) self-preserving plane jet.

$$\therefore \frac{U_{max}}{U_j} = \text{const.}\ )\ (s/x)^{\frac{1}{2}} \qquad (5.2.7)$$

2) $\rho_j \neq \rho_m$ $\quad Um = 0$

Equation (5.2.6) reduces to (following Craven [49] and Keagy and Weller[8] where $\delta_m(x) \sim x$)

$$\left(\frac{\rho u^2}{\rho_j U_j^2}\right)_{max} = \text{Const.}\ (s/x) \qquad (5.2.8)$$

The asymptatic solution for the centre-line velocity (x/s is large)

$$\frac{U_{max}}{U_j} = \text{const.} \quad \left(\frac{\rho_j}{\rho_m}\right)^{\frac{1}{2}} s/x \qquad (5.2.9)$$

N.B. The corresponding expression to (5.2.8) and (5.2.9) for the axi-symmetric jet are

$$\left(\frac{(\rho U^2)_{max}}{\rho_j U_j^2} \right)^{\frac{1}{2}} = \text{Const.} \ (s/x) \qquad (5.2.10)$$

$$\frac{U_{max}}{U_j} = \text{const.} \ \left(\rho_j/\rho_m \right)^{\frac{1}{2}} \ (s/x) \qquad (5.2.11)$$

Equation (5.2.10) was empirically obtained by Valis[10], and equation (5.2.11) has been found to be in a good agreement with Keagy and Weller's[8] data for around jets of helium, CO_2 and N_2 in still air for all (x/s).

3) $\rho_j = \rho_m = \text{const.}$ and $U_m \neq 0$

Consider the plane jet expanding into a moving stream of the same fluid. Equation (5.2.6) can be rearranged to read

$$\frac{\Delta(\rho U^2)_{max}}{\rho_m U_m^2} = \sqrt{\frac{b}{a}} \quad \frac{\Delta(\rho U)_{max}}{\rho_m U_m} = \sqrt{\frac{b}{\pi}} \left(\frac{J}{\rho_m U_m^2 \delta_m(x)} \right) \qquad (5.2.12)$$

If $a = b$, $\psi(\rho)$ is const. this equation reduces to

$$\left(\frac{U_o}{U_m} \right)^2 - \left(\frac{U_o}{U_m} \right) = \sqrt{b/\pi} \left[\frac{H}{\delta_m(x)} \right] \qquad (5.2.13)$$

where $U_o = U_{max} - U_m$, $= \Delta (U)_{max}$

and $H = (J/\rho_m U_m^2)$

Equation (5.2.13) is a quadratic equation with two unknown quantities (U_o) and $\delta_m(x)$.

Equation (5.2.13) can be written as

$$\frac{\delta_m(x)}{H} = \left[\frac{\text{const}}{\left(\frac{U_o}{U_m}\right)^2 \pm \left(\frac{U_o}{U_m}\right)} \right] \qquad (5.2.14)$$

where the signs (+) or (-) are introduced to take the account of (U_o) in positive or negative (wake). One can, however, make use of the two known particular solutions, namely:

i) $U_j \gg U_m$ or $(U_o \gg U_m)$
gives $\frac{U_o}{U_m} \sim (H/x)^{\frac{1}{2}}$ (e.g. Tollmien[16])

ii) $U_j < U_m$ or $(U_o \ll U_m)$
gives $\left(\frac{U_o}{U_m}\right. \sim -(H/x)^{\frac{1}{2}}$ (e.g. Schlichting[2])

After some algebra (5.2.14) becomes:

$$\left(\frac{\delta_m(x)}{H}\right) = \left[\frac{\text{const.}\ (x/|H|)}{1 + \text{Const.}\ (x/|H|)^{\frac{1}{2}}} \right] \qquad (5.2.15)$$

Hence equation (5.2.12) can be written as:

$$\left(\frac{U_o}{U_m}\right)^2 - \left(\frac{U_o}{U_m}\right) = \text{const.}\left[\frac{(1+\text{const.}(x/H)^{\frac{1}{2}}}{x/H}\right] \qquad (5.2.16)$$

which yields to:

(i) For H is large (strong jet),

$$\left(\frac{U_o}{U_m}\right) = C_1 (x/H)^{-\frac{1}{2}} \qquad (5.2.17)$$

$$\left(\frac{\delta_m(x)}{H}\right) = \text{const.}\ (x/H) \qquad (5.2.18)$$

(ii) For H is small (wake and weake jet)

$$\left(\frac{U_o}{U_m}\right) = -C_2 (x/|H|)^{-\frac{1}{2}} \qquad (5.2.19)$$

and $$\left(\frac{\delta_m(x)}{|H|}\right) = \text{const.}\ (x/|H|)^{\frac{1}{2}} \qquad (5.2.20)$$

Because (5.2.15) has the correct asymptatic behaviour of the spread parameter ($\delta_m(x)/H$) for both the wake, weak jet and strong jet cases it is assumed reasonable for all (U_j/U_m).

4. Plane jet into a general stream of different density ($\rho_j \neq \rho_m$), $U_m \neq 0$)

From equation (5.2.12), the solutions for the velocity decay and the spread parameter require some specification for the density distribution since (ρ_{max}) is implicit in the equation. However, as a first approximation one uses (5.2.16) ($\rho \cong$const) which is

reasonable for (x/s) large.

Writing $\frac{U_o}{U_m} = \left(\frac{U_{max} - U_m}{U_j - U_m}\right)\left(\frac{U_j}{U_m} - 1\right)$

then the first approximation to the velocity field is (from (5.2.17))

$$\left(\frac{U_{max} - U_m}{U_j - U_m}\right)\left(\frac{U_j}{U_m} - 1\right) = C_1 (H/x)^{\frac{1}{2}} \qquad (5.2.21)$$

for $U_j \gg U_m$, and

$$\left(\frac{U_{max} - U_m}{U_j - U_m}\right)\left(\frac{U_j}{U_m} - 1\right) = - C_2 (|H|/x)^{\frac{1}{2}} \qquad (5.2.22)$$

from (5.2.19) for $(U_j/U_m < 1)$

For the spread parameter, equation (5.2.15) is used.

5.3. The centre-line concentration.

As a first approximation, the centre-line concentration can be obtained by applying "Reynolds analogy" (§ 4.2.2) namely:

$$\left[\frac{U_{max} - U_m}{U_j - U_m}\right] = \left[\frac{C_{max} - C_m}{C_j - C_m}\right]$$

Hence, after some algebra, the centre-line concentration is

$$\left[\frac{\left(\frac{U_j}{U_m} - 1\right)}{1 + \left(\frac{1 - K_{max}}{K_{max}}\right) / (1 + \beta)}\right] = C_1 (H/x)^{\frac{1}{2}} \qquad (5.3.1)$$

for the strong jet and

$$\frac{\left(\frac{U_j}{U_m} - 1\right)}{1 + \left(\frac{1 - K_{max}}{K_{max}}\right) / (1+\beta)} = - C_2 \quad (. |H|/x)^{\frac{1}{2}} \quad (5.3.2)$$

for the wake or weake jet

5.4. Further approximation for (U_{max} and C_{max})

A second approximation to the velocity field can be obtained using the first approximation to the concentration field. Consider equation (5.2.12), dividing by $\left(\frac{\rho_{max}}{\rho_m}\right)$, keeping in mind that

$$\left(\frac{\rho_{max}}{\rho_m}\right) = (K_{max} \cdot \beta + 1)$$

Hence, for a strong jet the solution is (compare 5.2.8)

$$\left(\frac{U_{max} - U_m}{U_j - U_m}\right)\left(\frac{U_j - 1}{U_m}\right) = C_1 \left[\frac{H}{x\,(K_{max}\,\beta + 1)}\right]^{\frac{1}{2}} \quad (5.4.1)$$

From equation (5.3.1) equation (5.4.1) (after some algebra) yields:

$$\left(\frac{U_{max} - U_m}{U_j - U_m}\right)\left(\frac{U_j}{U_m} - 1\right) = C_1 \left[\frac{H}{x\left[\frac{\beta}{(\beta+1)\left[\left(\frac{H}{m s}/C_1\left(\frac{H}{x}\right)^{\frac{1}{2}}\right) - \frac{\beta}{\beta+1}\right]} + 1\right]}\right]^{\frac{1}{2}} \quad (5.4.2)$$

where m is the mass flux ratio = $(\rho_j U_j / \rho_m U_m)$

A similar expression, can be written for the concentration decay as:

$$\left[\frac{\left(\frac{U_j}{U_m} - 1\right)}{1 + \left(\frac{1-K_{max}}{K_{max}}\right)/(1+\beta)}\right] = C_1 \left[\frac{H}{x\left[\frac{\beta}{(\beta+1)\left[\left(\frac{H}{ms}/C_1\frac{H}{x}\right)^{\frac{1}{2}} - \left(\frac{\beta}{\beta+1}\right)\right]} + 1\right]}\right]^{\frac{1}{2}} \qquad (5.4.3)$$

Equations (5.4.2) and (5.4.3) can be considered as a better approximation for both velocity and concentration distribution along the axis of the jet. It can be shown that equation (5.4.2) will reduce to that obtained for ρ uniform (5.2.17) simply by putting

$\beta = 0$ or at $x \longrightarrow \infty$

5.5. <u>The effect of the initial boundary-layer thickness</u>

The effect of the initial boundary layer thickness is to reduce the effective jet thrust. The correct expression for the momentum conservation equation is (see equation (5.2.3))

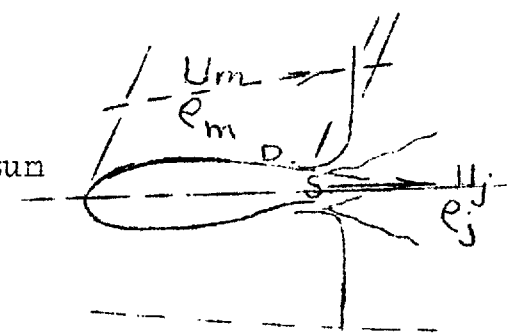

$$\int_{-\infty}^{+\infty} \rho U (U - U_m)\, dy = m_j (U_j - U_m) - D \qquad (5.5.1)$$

D is the drag force acting on the aerofoil and m_j is the mass flow rate coming out from the slot = $(\rho_j U_j s)$. Equation (5.5.1) can be written in dimensionless form as

$$\frac{1}{\rho_m U_m^2} \int_{-\infty}^{+\infty} \rho U (U-U_m)\, d(y/s) = \frac{U_j}{U_m}\left[\frac{U_j}{U_m} - 1\right] - \left(\frac{D}{\rho_m U_m^2 s}\right) \qquad (5.5.2)$$

$$\text{or} \quad \frac{H}{s} = \frac{\theta_j}{s} - C_{D_s} \qquad (5.5.3)$$

where θ_j is the jet momentum thickness at exit

C_{D_s} is a drag coefficient based on the slot width.

For a strong jet θ_j is large ($U_j \gg U_m$), then

$$\frac{H}{s} \simeq \frac{\theta_j}{s} \qquad (5.5.4)$$

For a weak jet (U_j slightly exceeds U_m)

$$\frac{H}{s} = \left(\frac{\theta_j}{s} - C_{D_s}\right) \qquad (5.5.5)$$

For a small deficit wake ($U_j < U_m$), θ_j is (-ive)

$$\therefore \frac{H}{s} = -\left[\left(\frac{\theta_j}{s} + C_{D_s}\right)\right] \qquad (5.5.6)$$

5.6. <u>The jet entrainment rate</u>

The interesting result that can be obtained directly from the previous analysis is the inflow rate. For a jet issues into a still air, the integral $\int_{-\infty}^{+\infty} \rho u\, dy$

has a finit value and represents the total mass flow rate hence the rate of mass entrained by the jet is

$$\frac{1}{(\rho U_{max})}\frac{d}{dx}\int_{-\infty}^{+\infty}\rho U\, dy = \left(\rho \frac{1}{U_{max}}\right)\cdot \frac{d\dot{m}}{dx} = \text{const.}$$

When the surrounding atmosphere is moving i.e.(U_m) is finite, the integral$\left(\int_{-\infty}^{+\infty}(\rho U)\, dy\right)$is infinite and thus cannot serve as a measure for the amount of fluid which has been significantly influenced by the jet. It would be possible to define the entrainment rate as

$$(\rho U)_m \frac{dm_e}{dx} = \frac{d}{dx}\int_{-\infty}^{+\infty}\rho\,(U - U_m)\, dy$$

However, this definition would be inappropriate because for very small relative velocity the expression tends to zero but the zone of influence of the jet increases by turbulent diffusion at a rate which is not equal to zero (e.g. Spalding [38]). However, as a first approximation, the general equation which governs the entrainment rate can be written as,

$$\left(\frac{1}{\int_{-\infty}^{+\infty} f(\eta)\, d\eta}\right)\frac{d\left(\frac{m_e}{H}\right)}{dx} = \left(\frac{U_o}{U_m}\right)\cdot\frac{d}{dx}\left(\delta_M^{(x)}/H\right) + \left(\frac{\delta_m^{(x)}}{H}\right)\cdot\frac{d}{dx}\left(U_o/U_m\right) \qquad (5.6.1)$$

---

where $m_e = \dot{m}/\rho_M U_m$, $\dot{m}$ mass flow rate

and $f(\eta) = e^{-a(y/\delta_M^{(x)})^2}$

case (i) strong jet ($U_j >> U_m$)

from equations (5.2.16) and (5.2.17) ($\rho \cong$ const)

The entrainment rate, as a first approximation, will be

$$\frac{d m_e}{dx} = \text{const.} \ (H/x)^{\frac{1}{2}} \qquad (5.6.2)$$

case (ii) for the wake ($U_j < U_m$)

from equations (5.2.18) and (5..2.19) the entrainment rate is

$$\frac{d m_e}{dx} = \text{const} \ \left(\frac{H}{x}\right) \qquad (5.6.3)$$

These particular cases, suggest a general form of the entrainment rate namely:

$$\frac{dme}{dx} = \text{const.} \ \left(\frac{H}{x}\right) \left[\frac{1}{1 + \text{const} \left(\frac{|H|}{x}\right)^{\frac{1}{2}}}\right] \qquad (5.6.4)$$

6. Flow past a wall. (The wall-jet and the wall wake flows.)

6.1 Introduction

This section is concerned with the mixing of a plane jet when it is injected tangentially to a wall underneath a free stream of constant velocity. The injection velocity is higher or lower than the external stream velocity and the slot fluid is similar or dissimilar to that of the external stream.

When a jet is injected between the wall surface and a gas stream three separate regions can be recognized; a potential core region in which the jet quantities at the centre-line remain constant and equal their values at exit. The slot fluid is then mixed with the external stream forming a turbulent mixing region started at the point where the potential core disappeared. In this region, however, if $U_j \gg U_m$ a flow which is similar to that in a self-preserving turbulent wall jet is found. If $U_j < U_m$ this mixing region is very short and a region is soon developed which is similar to that in a fully developed turbulent boundary-layer.

6.2. The turbulent wall jet ($U_j > U_m$)

The turbulent wall jet has been studied experimentally and theoretically by many workers over the past years for example, Zerbe[50], Jakob[51],

Sigalla[52], Glauert [9], Bakk [28] and Schwarz[34] who considered a self-preserving plane wall-jet and Seban[53], george[32], Bradshow [30], Verhoff, [29] Eichelbrenner [54], Mathieu [55], Patel [33], Kraka [31], Gortshore [56], Spalding[57] and Harris [58] who considered a turbulent wall jet in a moving stream. These investigators were mainly interested in the hydrodynamic behaviour of the problem though some, notably Zerbe[50], Jakob [51], Seban [53] and Spalding [57] were concerned with both velocity and temperature fields. Most of these workers have adopted an approximate similarity solution, flowing Glauert [19], in which the velocity profiles were assumed to be relatively invariant with the downstream distance (x). The essential feature of this near similarity solution was the splitting the flow into inner and outer regions at the position of maximum velocity. The flow in the outer region was assumed to be similar to that in a self-preserving plane free jet, i.e.

$$U_{max} \sim x^{-\frac{1}{2}} \quad , \quad \delta_m \sim x$$

and, in the inner layer, the velocity profiles were assumed to be either, semi-logarithmic profile in the form

$$\left(\frac{U}{U_\tau}\right) = \text{Const. } \log. \left(y \rho \frac{\sqrt{\tau_w/\rho}}{\mu}\right) + \text{Const.}$$

or power low profile in the form

$$\left(\frac{U}{U_{max}}\right) = \left(y/\delta_i\right)^{\frac{1}{n}}$$

The comparison between previous experimental results and Glauert's [19] Theory was satisfactory provided that $U_j \gg U_m$ (strong jet). However its application to a weake wall jet in which U_j is slightly exceed U_m is not satisfactory (see sec.3 figure (6.a)).

6.2.1 The existance of a finite shear stress at $y = \delta_i$

In the case of a plane free jet, by symmetry, the shear stress vanishes at the point of maximum velocity. Beyond the edge of the boundary-layer the flow is invicid and the shear stress is zero. For the turbulent wall-jet it would appear, from Prandtl's mixing length theory in which $\tau = -\rho l_o^2 \left(\frac{\partial U}{\partial y}\right) \left|\frac{\partial U}{\partial y}\right|$ that the shear stress would again vanish at the point of maximum velocity. This assumption, in fact, has been used by a number of investigators, e.g. Glauert [19], Patel [33] and Mayers [59] in their analytical treatment. However, this assumption was found experimentally to be incorrect, for instance, the hot wire measurements for the plane wall-jet by Bradshow [30] have shown that

$$-\tau_w = \tau_{max}$$

The recent analytical treatments for turbulent wall-jet in a moving stream were carried out by Gortshore,[56] Spalding [57] and Harris[58]. The solutions of Gortshore and Harris are very similar and are mainly based on a computer solution of the momentum integral equation. Gortshore [56] assumed the mean velocity profiles in the outer and inner layers to be:

$$\left(\frac{U - U_m}{U_{max} - U_m}\right) = \exp.\ \left[-.6932\ (y/\delta_m)^2\right] \quad \text{for } y \gtrless 0$$

and

$$\left(\frac{U}{U_{max}}\right) = \left(\frac{y + \delta_i}{\delta_i}\right)^{\frac{1}{n}} \qquad -\delta_i < y < 0$$

in the $(x - y)$ plane as given below

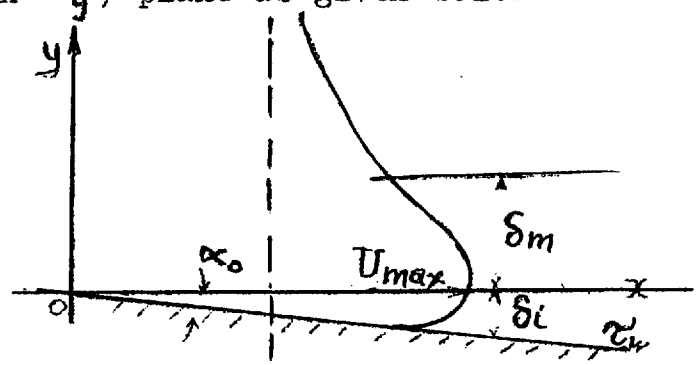

The momentum integral equation, therefore, was written in this form

$$\frac{d}{dx}\int_{-\delta_i}^{y} U\,(U - U_m)\,dy + (U_m - U)\,\frac{d}{dx}\int_{-\delta_i}^{y} U\,dy = \frac{\tau}{\rho} - \frac{\tau_w \cos\alpha_o}{\rho}$$

with α_o, assumed to be very small.

Following Patel[33] the shear stress assumptions were in this form

$$\left(\frac{\tau}{\rho}\right) = -\left(\frac{\delta_m}{R_T}\right)(U_{max} - U_m)\left(\frac{\partial U}{\partial y}\right)_{\delta_m}, \quad \text{and}$$

$$\left(\frac{\tau_w}{\rho U_m^2}\right) = .0129\left(\frac{U_{max}\,\delta_i}{\nu}\right)^{-\frac{1}{6}}$$

where R_T is a constant number in Townsend's equilibrium hypothesis for large eddies. The momentum integral equation was solved numerically first with upper limit $y \longrightarrow \infty$, $\tau = 0$ and $U = U_m$, and second with upper limit $y = \delta_m$, $U = \frac{1}{2}(U_{max} + U_m)$ and

$$\left(\frac{\tau(\delta_m)}{\rho}\right) = -\frac{.6932}{R_T}\left[(U_{max} - U_m)^2\right]$$

Harris[58] assumed the velocity profiles in the outer and the inner layers to be

$$\left(\frac{U - U_m}{U_{max} - U_m}\right) = \exp.\left[-.6932\left(\frac{y - \delta_i}{\delta_m - \delta_i}\right)^2\right]$$

$$\left(\frac{U}{U_{max}}\right) = \left(y/\delta_i\right)^{\frac{1}{n}}, \quad n = 10$$

The shear stress assumptions were, following Bradshow[30] in this form

$$\left(\tau_{max}/\rho\right) = -\tau_w/\rho \cdot \left(\frac{U_{max} - U_m}{U_{max}}\right)^2$$

$$\left(\tau_w/\rho U_m^2\right) = .01575\left(\frac{U_{max}\,\delta_i}{\nu}\right)^{-\frac{1}{55}}$$

The momentum and the energy integral equation were then solved numerically. Despite the differences in the subsequent analytical treatment and the differences in the phenomenological assumptions concerning the shear stress distribution; both Gortshore's [56] and Harris's[58] solutionswere in good agreement. (e.g. Harris [58]) Following Coles[60], Spalding's [57] 'unified theory' (1964) postulates a velocity profile across the whole boundary-layer, just outside the viscous sub-layer, as a linear sum of a wall-shear stress dependant component and a free turbulent wake component i.e.:

$$U = \left[U_\tau \quad g\left(y \frac{U_\tau}{\nu} \right) + U_m \, (1-Z_E) \quad f\,(y/\delta) \right]$$

where Z_E is a measure of the relative contribution of the wall component to the total velocity. At $Z_E = 1$ the wake component will vanish and the velocity profile reduces to a conventional turbulent boundary-layer profile. At $Z_E = 0$, $U_\tau = 0$ the velocity profile is simply a wake profile. The function g was chosen by Spalding [57] to be a semi-logarithmic profile, while the function f (Coles's [60] wake component) was approximated as a cosine profile. The form of the "log-plus-cos" velocity profile adopted in Spalding's Unified theory was in this form

$$\frac{U}{U_m} = \frac{1}{k_2} \frac{U_\tau}{U_m} \log \left(E_1 \, y \frac{U_\tau}{\nu} \right) + \tfrac{1}{2} \, (1-Z_E) \quad (1- \cos \pi (y/\delta)$$

where E_1 is the profile constant $\cong 6.5$

and k_2 is a mixing length constant $\cong 0.4$

The shear stress assumption adopted by Spalding [57] was based on Prandtl's mixing length theory, assuming that the mixing length (l_o) distribution across the whole boundary-layer to be, as given by the figure below

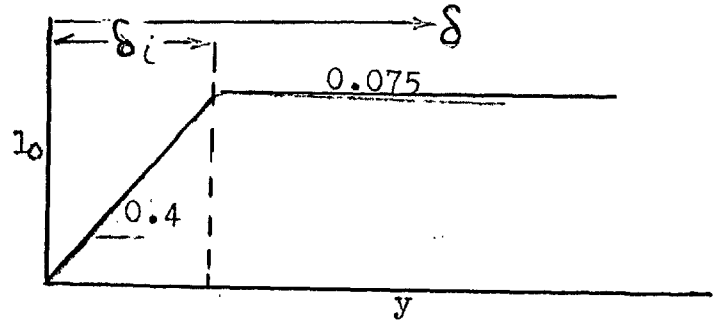

i.e. near the wall $l_o \cong k_2 y \quad (0 \leq y \leq \delta i)$

and $- l_o = \text{const.}\,\delta -$ further outwards.

The governing equations used by Spalding [57] were the integral momentum equation and the integral-kinetic energy equation. Solution of these equations together with the "log-plus-cos" profile was obtained numerically. According to a recent note by Spalding* the profile has been abandoned as it did not fit the experimental data for wall jets well in respect of the position of the velocity maximum, and it has been suggested that the theory needs to be developed.

---

* Note on the present form and status of the "unified theory" Imperial College, Mech. Eng. Dept. July 1965.

6.3 The wall Wake ($U_j < U_m$)
(Film cooling flow)

This flow field has been the subject of considerable analytical and experimental study over the past few years. Most of the theories that have been developed were based on the assumption that the mixing region is non-existent and at far downstream ($x/s \gg 1$) the flow resembles that in the boundary-layer (e.g. ref. 21). Thus for (x/s) large, the temperature profiles are similar gives

$$T = T_m + (T_w - T_m) f\ (y/\delta_m)$$

and the mass velocity are also similar in the form

$$\frac{\rho U}{\rho_m U_m} = (\ y/\delta\ )^{\frac{1}{n}}$$

The agreement between the theoretical model and the various experimental results for film cooling an adiabatic wall were fairly satisfactory. The accuracy of the model improved as x/s increased.

6.4 Development of the simple theory of a turbulent boundary-layer with fluid injection

6.4.1 The turbulent wall jet ($U_j \gg U_m$), (ρ uniform)

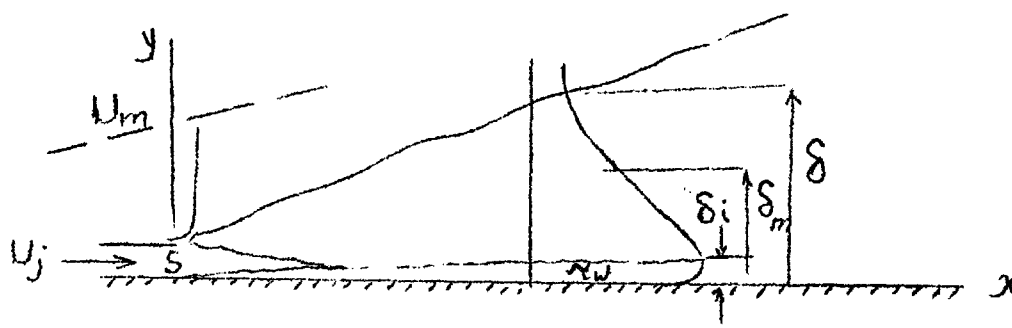

Assumption:

1. To a good degree of accuracy the velocity profile in the outer layer of the wall jet can be written in the form

$$U - U_m = (U_{max} - U_m) \exp. \left[-.6932 \left(\frac{y - \delta_i}{\delta_m - \delta_i} \right)^2 \right] \qquad (6.4.1.1)$$

2. The wall boundary-layer represents only a small portion of the flow, ($\delta_i << \delta$), provided that the jet momentum flux is very much greater than the wall friction ($\rho_j U_j^2 >> \tau_w$)./ From assumption 2), except for the small loss of momentum due to the wall friction, the flow would be of a constant momentum so that, at least, the overall characteristics of the jet would depend on this momentum. The boundary-layer equations are:

$$U \frac{\partial u}{\partial x} + V \frac{\partial U}{\partial y} = \frac{1}{\rho} \frac{\partial \tau}{\partial y} \qquad (6.4.1.2) \text{ momentum}$$

$$\frac{\partial (\rho U)}{\partial x} = - \frac{\partial}{\partial y} (\rho V) \qquad (6.5.1.3) \text{ continuity}$$

B.C's $y = 0 \quad U = V = 0 \quad \tau = \tau_w$

$y = \infty \quad U = U_m \quad \tau = 0$

The integration of the momentum equation (6.4.1.2) with ρ = constant and no mass transfer through the wall gives

$$\frac{d}{dx} \int_0^\infty \rho U (U - U_m) \, dy + \tau_w = 0 \qquad (6.4.1.4)$$

The profile as given by equation (6.4.1.1) and assumption 2 one gets (from the free jet results section 5)

$$\left(\frac{U_{max} - U_m}{U_m}\right) = \text{const.} \left(\frac{H}{x}\right)^{\frac{1}{2}} \qquad (6.4.1.5)$$

$$\left(\delta_m / H\right) = \text{const.} \left(x / H\right) \left[\frac{1}{1 + \text{Const.} \left(x / H\right)^{\frac{1}{2}}}\right] \qquad (6.4.1.6)$$

This means that the peak velocity decay, the spread parameter and the entrainment action of the wall jet would be similar, at least, qualitatively to those of the free turbulent jet provided that $U_j >> U_m$. For a weake wall jet, however, this analysis would not be expected to hold since (δ_i) is relatively large (see figure 5-c).

6.4.2 The Wall "wake" ($U_j < U_m$) (ρ is not uniform)

(The boundary -layer solution for the conserved property at the wall)

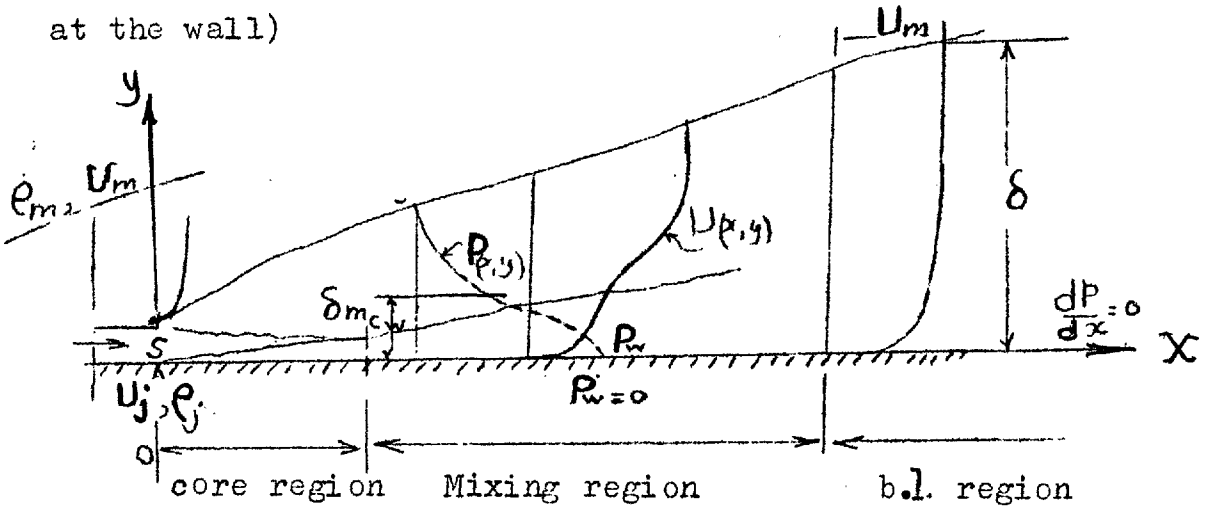

Film cooling model

Assumptions:

1. The flow is boundary-layer and

$$\delta/x = \text{const.} / (R_{ex})^{1/5} = B_1 R_{ex}^{-1/5}$$

2. The pressure is constant throughout the flow field with no heat or mass transfer through the wall.

3. The velocity, temperature and the diffusion boundary-layers have the same thickness.

4. At large (x/s) the mass velocity profiles are similar and can be written in power law form

$$\left(\frac{\rho U}{\rho_m U_m}\right) = \left(y/\delta\right)^{\frac{1}{n}} \qquad n = 7$$

5. From the diffusion, energy and momentum equations (§ 4) with $S_c = P_r = 1$ it follows that

$$\left(\frac{T - T_m}{T_w^{(x)} - T_m}\right) = \left(\frac{C - C_m}{C_w^{(x)} - C_m}\right) = f\left(y / \delta_{T \text{ or } C}^{(x)}\right)$$

and $$\delta_{T \text{ or } C}^{(x)} = \int_0^\infty \left(\frac{P_{(x,y)} - P_m}{P_w^{(x)} - P_m}\right) dy$$

where P = C or = T

It is possible to show, using the continuity, the equation for the conserved property $P_{(x,y)}$ i.e.

$$\frac{\partial(\rho u)}{\partial x} + \frac{\partial(\rho v)}{\partial y} = 0$$

$$\rho u \frac{\partial P}{\partial x} + \rho v \frac{\partial P}{\partial y} = \epsilon_0 \frac{\partial^2 P}{\partial y^2}$$

and introducing assumptions (4) and (5) together with the boundary conditions:

$$y = 0 \quad P = P_w \quad , \quad \frac{\partial P}{\partial y} = 0$$
$$y = \infty \quad P = P_m$$

that

$$\frac{P - P_m}{P_w - P_m} = \exp. \left[- E_2 \left(y / \delta_{C \text{ or } T} \right)^{\frac{1+2n}{n}} \right]$$

where $E_2 = \left[\Gamma \frac{1 + 3n}{1 + 2n} \right]^{\frac{(1+2n)}{n}}$

$$\simeq \exp \left[-.6932 \left(y/\delta_{m_{C \text{ or } T}} \right)^2 \right]$$

where $\delta_m = y$ at $P - P_m = \frac{1}{2} (P_w - P_m)$

$n \neq 1/7$

It may be worth noting that (P_w') is zero then if (P) stand for enthalpy (or temperature) this implies an adiabatic wall, if (P) stands for mass fraction concentration it then implies an impervious wall.

Analysis:

The integral (P) conservation equation over the whole boundary-layer, with $(P_w') = 0$ is

$$\frac{d}{dx} \int_0^{\delta} \rho U \quad (P - P_m) \, dy = 0 \quad ..(6.4.2.1)$$

This equation can be written as:

$$\frac{d}{dR_{ex}} \left[(P_w - P_m) \right] \quad R_{em} \quad I.(U, P) = 0 \quad ..(6.4.2.2)$$

where

$$R_{ex} = \int_0^x \frac{\rho_m U_m}{\mu_m} dx \qquad (6.4.2.3)$$

$$R_{em} = \int_0^\delta \frac{\rho_m U_m}{\mu_m} dy \qquad (6.4.2.4)$$

$$I_{(U,P)} = \int_0^1 \left(\frac{\rho U}{\rho_m U_m}\right) \left(\frac{P - P_m}{P_w - P_m}\right) d\eta \qquad (6.4.2.5)$$

$$\eta = (y/\delta)$$

From equation (6.4.2.2)

$$(P_w - P_m)\ R_{em}\ (I_{(U,P)}) = \underline{\text{const.}}^{*} \qquad (6.4.2.6)$$

If the fluid emerges from the slot of width s velocity (U_j) and density (ρ_j) then equation (6.4.2.6) becomes $(P_w - P_m)\ \rho_m U_m \delta I_{(U,P)} = \rho_j U_j (P_j - P_m)\ s$ (6.4.2.7)

$$\text{or } \left(\frac{P_w - P_m}{P_j - P_m}\right) = \left[\frac{1}{(I_{(U,P)})}\right] \left(\frac{\rho_j U_j}{\rho_m U_m}\right) \left(\frac{s}{\delta}\right) \qquad (6.4.2.8)$$

From assumption (1) $(\delta = B_1 \times R_{ex}^{-.2})$ after some algebra equation (6. .2.9) reads

$$\left(\frac{P - P_m}{P_j - P_m}\right) = \left[\frac{1}{B_1\ (I_{(U,P)})}\right] \left(\frac{x}{m\ s}\right)^{-0.8} (Re_j)^{0.2} \left(\frac{\mu_j}{\mu_m}\right)^{0.2} \qquad (6.4.2.9)$$

According to assumptions (4) and (5) the profiles

---

* The constant has the significant of flow of (P) in the boundary-layer.

similarity) then

$$\left[\frac{1}{B_1 I\ (U, P)}\right] = \text{const.} = A_1$$

If P is the mass fraction concentration then the 'impervious' wall concentration distribution for a binary gas mixture reads

$$\left[\frac{1}{1 + \left(\frac{K_j - K_w}{K_w - K_m}\right)\frac{M_m}{M_j}}\right] = A_1 \left(\frac{x}{ms}\right)^{-0.8} \left(Rej \frac{\mu_j}{\mu_m}\right)^{0.2} \qquad (6.4.2.10)$$

If P stands for the total enthalpy h^o then equation (6.4.2.9) gives

$$\left(\frac{h^o_w - h^o_m}{h^o_j - h^o_m}\right) = A_1' \left(\frac{x}{ms}\right)^{-0.8} \left(Rej \frac{\mu_j}{\mu_m}\right)^{0.2} \qquad (6.4.2.11)$$

A_1' may be different than A_1, and this depends on S_c/P_r ratio. In terms of temperature rather than total enthalpy, for a nearly uniform density streams equation (6.4.2.11) yields

$$\left(\frac{T^o_w - T^o_m}{T^o_j - T^o_m}\right) = A_1' \left(\frac{x}{ms}\right)^{-0.8} (Rej)^{0.2} \qquad (6.4.2.12)$$

and for non-uniform density streams (e.g. refe. 21)

$$\left[\frac{1}{1+\left[\frac{T_j^o - T_w^o}{T_w^o - T^o{}_m}\right]\frac{C_{p_j}}{C_{p_m}}}\right] = A_1' \left(\frac{x}{ms}\right)^{-0.8} \left(Re_j \frac{\mu_j}{\mu_m}\right)^{0.2} \qquad (6.4.2.13)$$

The constant A_1' was taken to be (3.09) in ref. (21) which is based on the assumption that n = 1/7 and $B_1 = 0.37$ which are the typical values for flat plate turbulent boundary-layer, i.e.

$$\left[\frac{1}{B_1, I(U,P)}\right] = \left(\frac{1}{0.37} \times 8/7\right) = 3.09 \text{ for } (\eta)$$

small. However, the constants A_1 and A_1' are mainly influenced by:-

1) The power index of the mass velocity profiles (n)
2) The concentration or the temperature distribution.
3) The boundary-layer growth assumption.

Other factors may be introduced due to the experimental set up, wall roughness ... etc.

7. Correlation with the present experimental results and general discussion.

7.1 The free turbulent flows.

7.1.1 Centre-line velocity.

The data obtained for the decay of the centre-line velocity (U_{max}) are shown in figures (11) and (12) for helium, $Arcton_{12}$ and air jets. They are plotted using the parameters suggested by equation (5.2.21) and (5.2.22) for the free jet and free wake flows respectively. The figures show that the data are following one of two lines depending on whether (U_j/U_m) (the velocity ratio) is less than or greater than one. Despite the large difference in density between the two gas streams the data of ($U_j/U_m < 1$) are correlated, disregarding the flow in the potential core, reasonably well by the free wake model (fig. 12). The correlation of the data of $U_j/U_m > 1$, using the jet model, in general, is less satisfactory. In particular these data of velocity ratios $\frac{U_j}{U_m} \leq 2.76$ for both helium and air as shown in figure (11). As for comparison the two particular expressions following Forthmann's [26] measurements for plan jet ($U_m = 0$) and Schlichting's[2] measurements for plane wake are shown in figures (11)

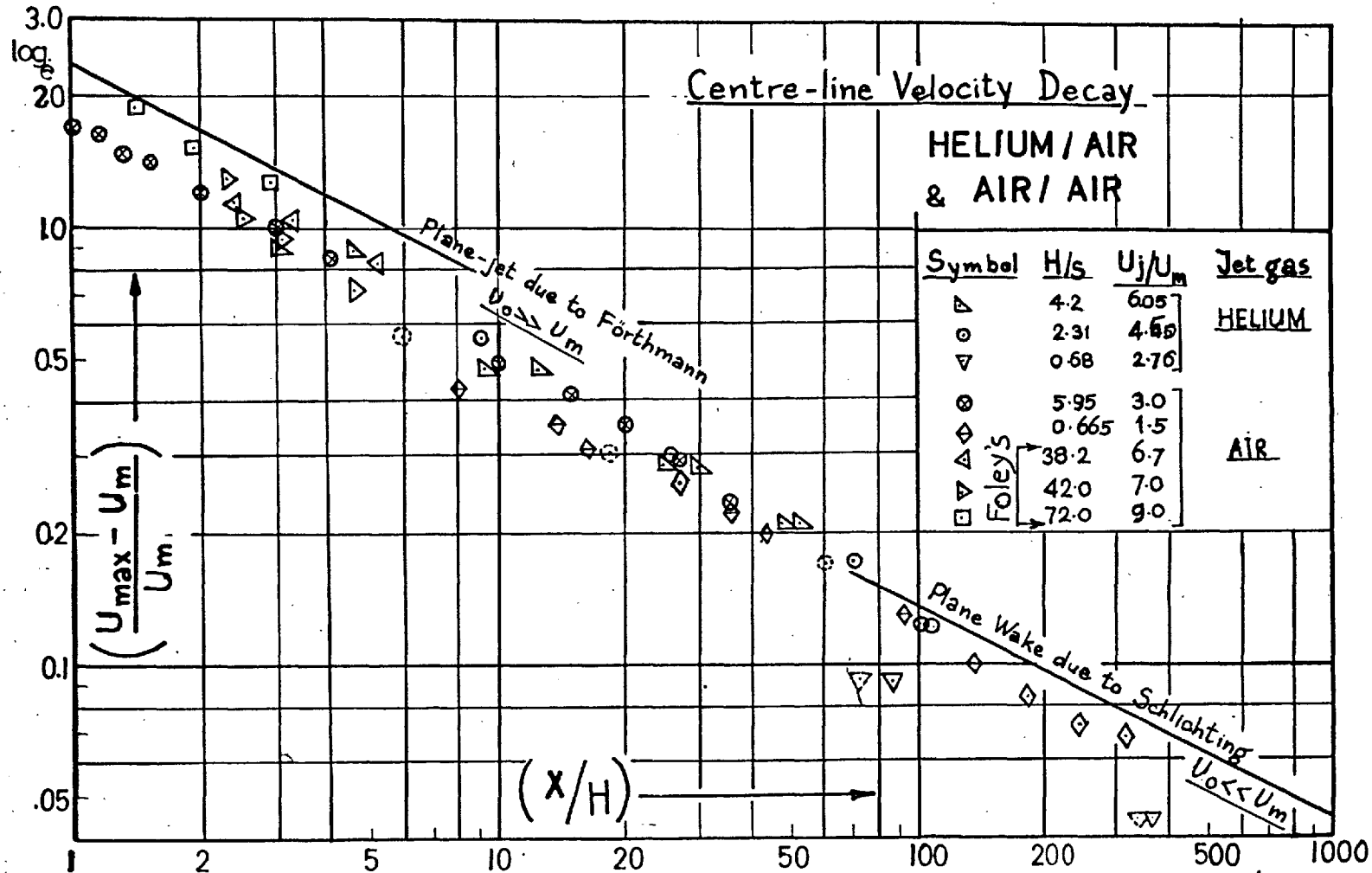

FIG. 11 plane jets of air & helium into a moving stream $(Uj/U_m > 1)^{\log_e}$ correlation of data and comparison with the assymptotic theories.

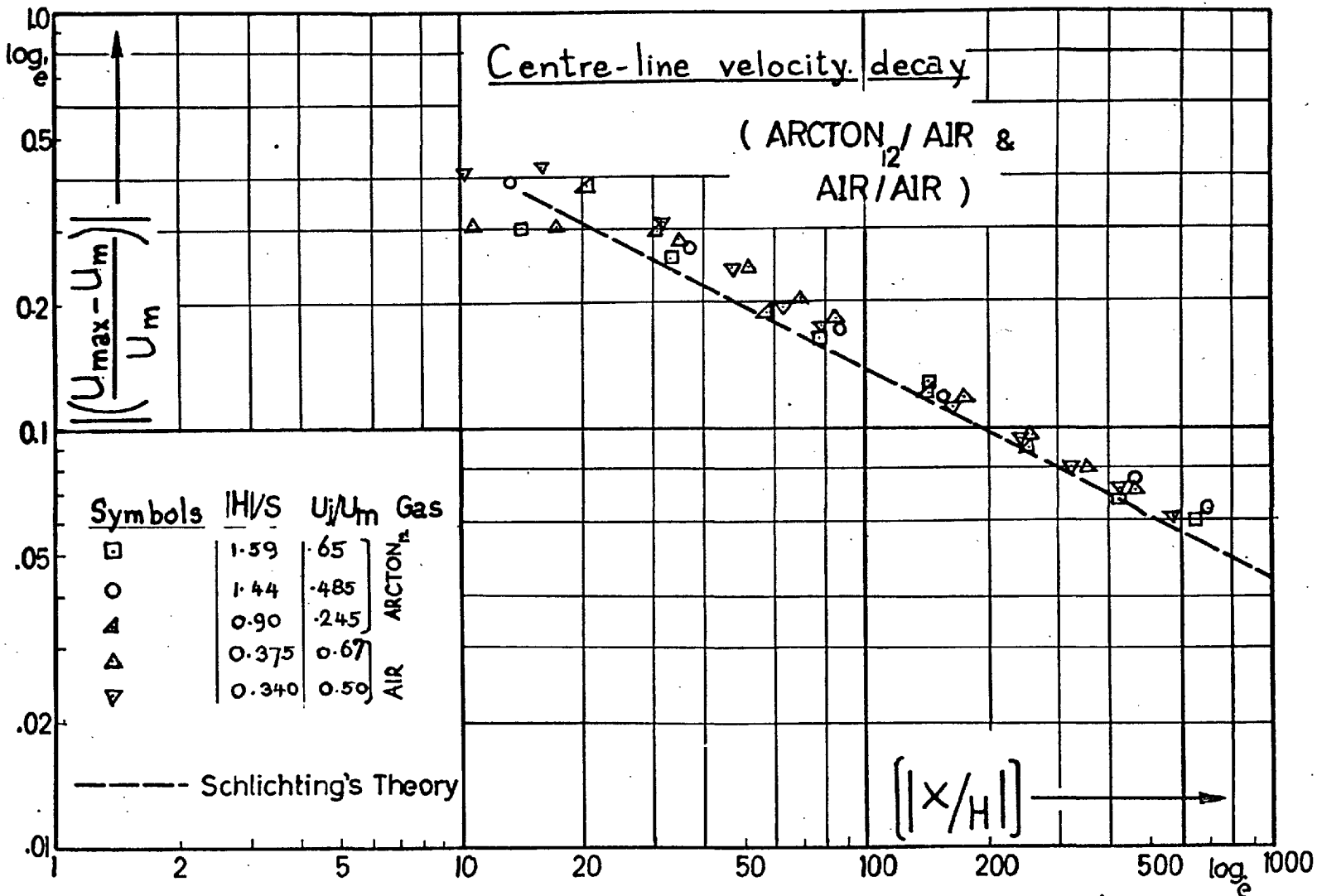

FIG. 12 plane wake of air & Arcton$_{12}$ into a moving stream ($U_j/U_m < 1$) correlation of data and comparison with theory.

and (12) respectively. Some other data obtained from the results of Foley [61] for strong air jets ($U_j \gg U_m$) are also shown in figure (11). The correlations as shown in both figures indicate that the agreements between the experimental data and the two asymptotic theories are possible for:-

(i) The strong jets in which $U_j \gg U_m$ (e.g. some of Foley's[61] results $U_j/U_m = 9$) where the plane jet model is valuable.

(ii) The weak jets (U_j slightly exceeds U_m) and the wake $U_j < U_m$) where the plane wake model is relevant.

For jets which are neither strong nor weak i.e. (between (i) and (ii)) the data for air/air and helium/air are almost approaching those of the wake, and it would appear, however, from the intermediate region of figure (11) that the slope of the corresponding rate of decay of (U_{max}) is not strictly following ($x^{-\frac{1}{2}}$) but, (U_{max}) ~ $x^{-.60}$ approximately. This is expected since the flow is not strictly self-preserving (e.g. Townsend,[4] Bradbury [39] and Wygnanski[62]). The shift from the plane jet to the plane wake, however, is more clearly demonstrated later on in figures (15) and (16). An attempt is made to obtain a better correlation by platting the helium results according to

equation(5.4.2.) We felt that the second approximation would bring, for a given value of (H/s), the helium/Air data more closer to the air/air data. However, for the present limited range of flow parameters investigated, the correlation as shown in figure (11) by the dotted symbols is slightly improved. It is probably worth noting that the values of (H/s) which are used in the correlation of the results are the average values of the dimensionless local excess momentum flux at the various downstream locations for each individual run. Examples of calculation are given in tables (4), (5), (6) and (7).

Table - 4 -

$\frac{U_j}{U_m} = 1.5$	air/air		$(\theta_j/s) = 0.75$
(x/s)	(δ_m/s)	(U_o/U_m)	(H/s)
18	1.0	.265	0.675
24	0.2	.226	0.695
29	1.4	0.189	0.685
60.5	2.2.	0.125	0.655
90	2.8	0.10	0.650
120	3.1	0.089	0.655
160	3.5	0.081	0.651
210	3.85	0.066	0.648
	average	H/s	0.664

Table - 5 -

$\frac{U_j}{U_m}$ = 0.5	Air/Air		θ_j/s =-0.25
x/s	δ_m/s	$-(U_o/U_m)$	-(H/s)
24	0.94	-.205	0;398
29	1.0	0.186	0.356
60.5	1.5	0.120	0.324
90	2.04	0.089	0.301
120	2.12	0.082	0.374
160	2.25	0.0725	0.322
210	2.64	0.064	0.312
	average	-H/s	0.34

Table - 6 -

$\frac{U_j}{U_m}$ = 4.5	Helium /air		θ_j/s = 2.19
x/s	δ_m/s)	(U_o/U_m)	(H/s)
19	2.3	0.57	2.16
53.5	4.6	0.300	2.3
124.7	8.2	0.160	2.32
227.17	10.5	0.120	2.3
	average	H/s	2.27

Table - 7 -

$\frac{U_j}{U_m}$ = 0.65	Arcton$_{12}$/air		θ_j/s = -.955
x/s	(δ_m/s)	$-U_o/U_m$	-(H/s)
19	2.35	0.300	1.59
53.5	3.4	0.250	1.62
124.7	5.05	0.165	1.62
227.17	6.5	0.130	1.60
670	12.	0.07	1.57
1008	16.5	0.060	1.58
	average H/s		-1.59

From the above tables, it is seen that the constancy of the momentum flux is fairly satisfactory (within the experimental and the numerical integration accuracy) throughout the flow field. The interesting result which can also be noticed from these tables, is the effect of the initial boundary-layer thickness at the slot i.e. the effect of (C_{D_s}) as given by equation (5.5.3). For $(U_j/U_m) > 1$ table (6) shows that C_{D_s} is negligible and $\frac{H}{s} \simeq \frac{\theta_j}{s}$. From table (4) for a weak jet, the value of C_{D_s} becomes slightly pronounced and $\frac{H}{s} = (\frac{\theta_j}{s} - C_{D_s}) < \frac{\theta_j}{s}$

(C_{D_s} is about 10% Of Θ_j. At $(U_j/U_m < 1)$ and correspondingly $(\frac{H}{s})$ is negative then from tables 5 and 7

$$\left|\frac{H}{s}\right| = -\left(\frac{\theta_j}{s} + C_{D_s}\right) \quad > \quad \left|\frac{\theta_j}{s}\right|$$

(C_{D_s} is about 35% of θ_j. Therefore, the momentum deficit due to this boundary-layer thickness at $(U_j/U_m < 1)$ is significant and cannot be ignored. Tables (4, 5 and 7) in fact, demonstrate the importance of using $(\frac{H}{s})$ rather than (θ_j/s).

7.1.2 <u>The centre-line concentration</u>.

The centre-line concentration (C_{max}) data are plotted using the parameters of equations (5.3.1 and 5.3.2) as shown in figure (13). Again, except for some helium results where $(U_j/U_m \cong 2.76$ – weake jet), the correlation is satisfactory following one of the two lines depending on whether (U_j/U_m) is greater or is less than one. For the weak jet, it appears that the data are approaching those of the wake . For $\frac{H}{s} \cong 0$, however, the prediction of the centre-line concentration is not possible by either equation (5.3.1) or (5.3.2). An alternative way in which the concentration results (C_{max}) can be made independent of the precise slot condition is shown in figure (14). In

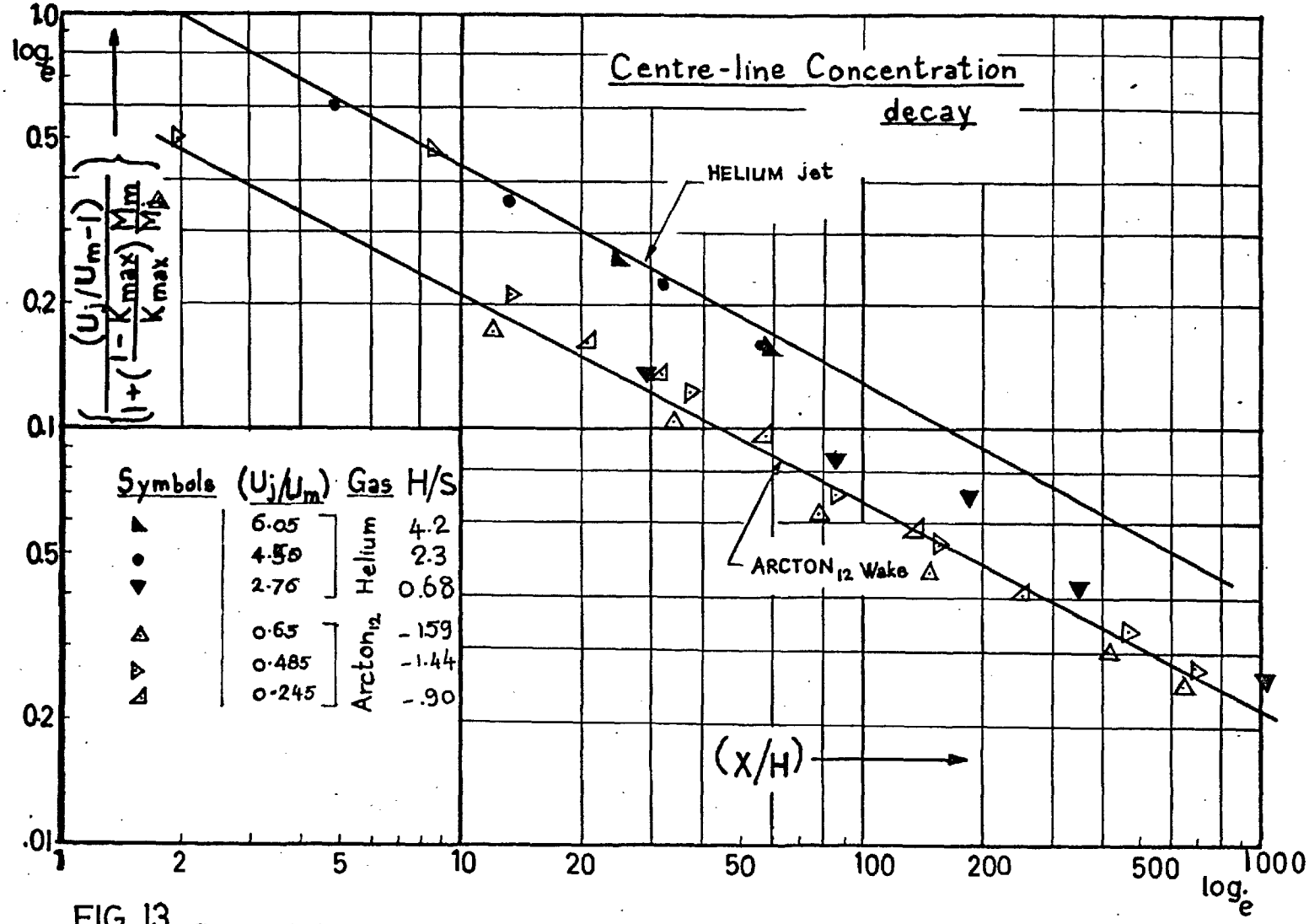

FIG. 13 Correlation of the helium (jet) & the Arcton$_{12}$ (wake) data ($C_{max.}$) according to the parameter (H/s) ($1 < U_j/U_m < 1$)

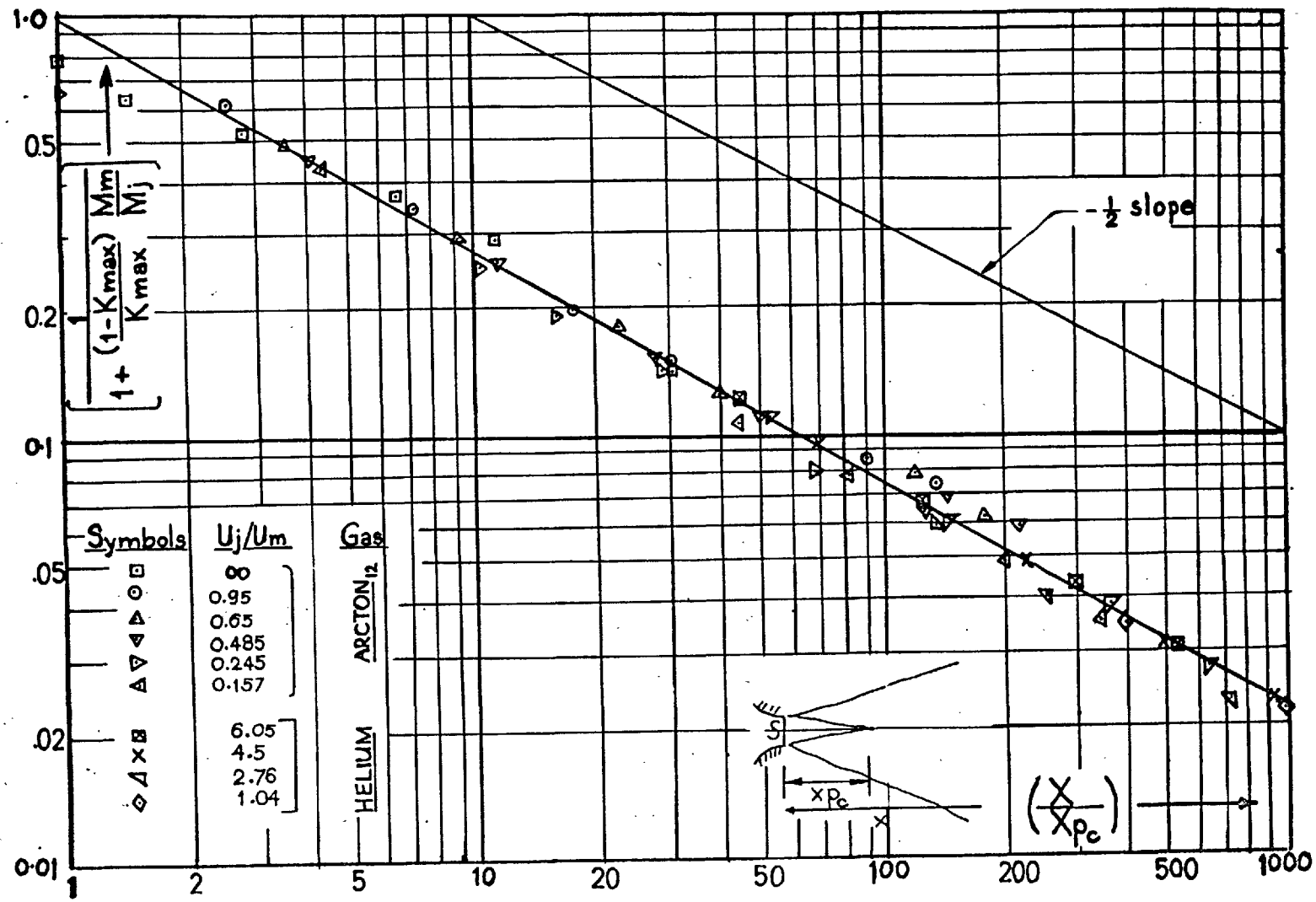

FIG. 14 Correlation of the centre-line concentration ($C_{max.}$) according to the distance parameter (X_{p_c}/s).

this figure (C_{max}) is plotted as a function of $x/(xp_c)_D$, where $(xp_c)_D$ is the positive distance measured from the slot location to the point where (C_{max}) started to change (see sec.8.3). A reasonable smooth curve is obtained for both gas combinations showing a better correlation of the data and indicating that the parameter $(x/xp_c)_D$ is a similarity parameter for the mixing in this region for the whole range of the velocity and density ratios examined.

7.1.3 The jet spread parameter

From the analysis given in section (5) the general form of the jet spread parameter can be written as:

$$(\frac{\delta_m}{H}) = \text{function of } (x/H)$$

The data obtained for (δ_m) for air, helium and Arcton 12 are plotted as suggested by this expression as shown in figures (15) and (16) respectively. The asymptotic forms of (δ_m/H) for the pure jet and plane wake following Forthmann's [26] and Schlichting's [2] measurements are present for comparison. As it is expected the data for (δ_m) showed an agreement with the respective asymptotic theories in a similar manner as those results for (U_{max}) given by figures (11) and (12) i.e. despite the large difference in density the measured δ_m at ($U_j/U_m < 1$) are in a quite reasonable agreement

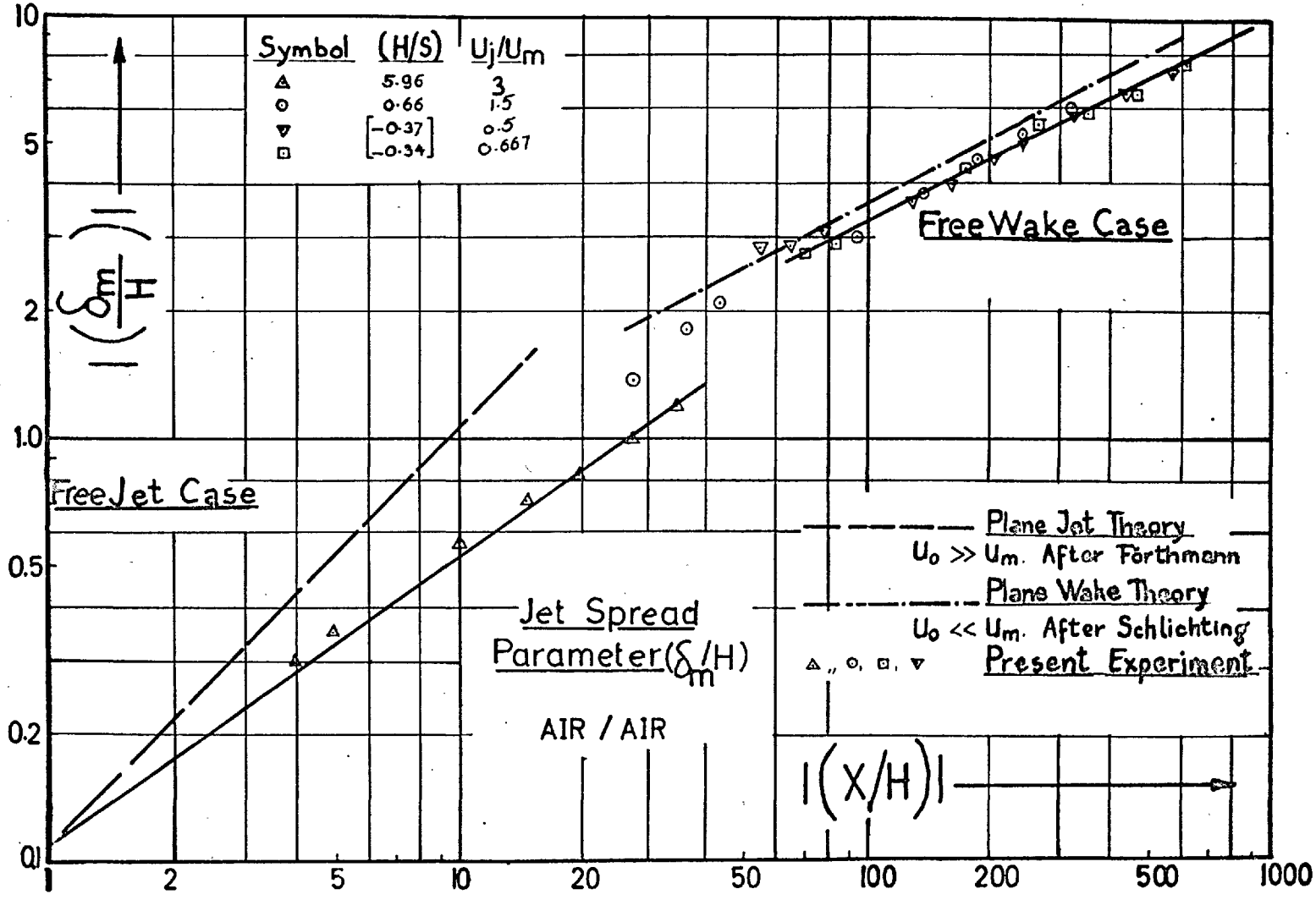

FIG. 15 Correlation of the spread parameter (δ_m/H) and comparison with the assymptotic theories ($1 < U_j/U_m < 1$).

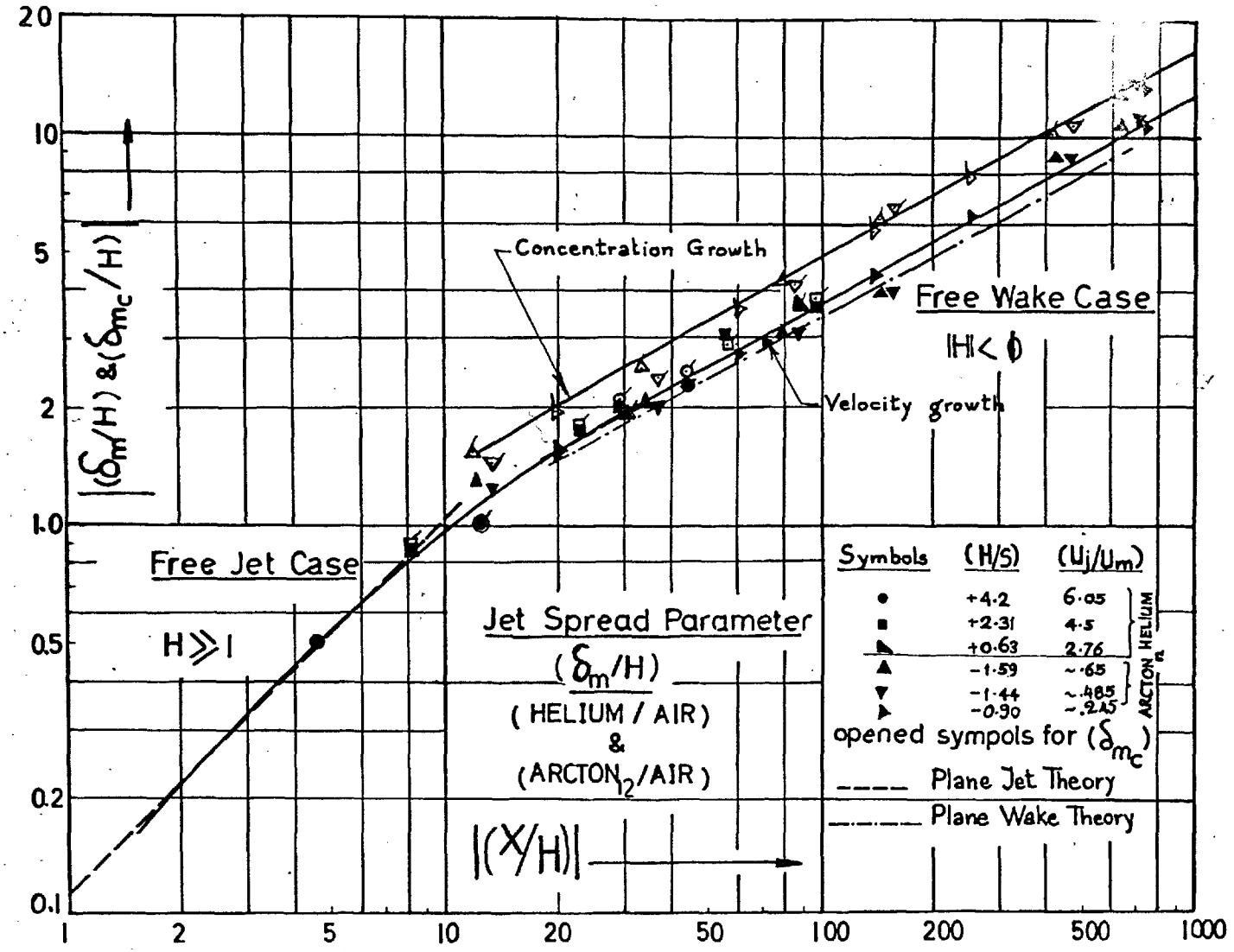

FIG. 16 Correlation of the, velocity & concentration, spread parameters and comparison with the assymptotic theories, ($1 < Uj/Um < 1$)

with the wake model, while those data of ($\frac{U_j}{U_m} > 1$) the agreement is less satisfactory with the corresponding assymptotic model. Similarly the measured (δ_m), for a weak jet, begin to deviate from the jet prediction towards the wake prediction ($\delta_m \sim x^{\frac{1}{2}}$). This shift in the flow behaviour, perhaps is not very clear from figure (11) since (U_{max}) has the same power law ($x^{-\frac{1}{2}}$) though, the proportionality constants (C_1 and C_2) are quite different. According to figures (15) and (16) except for some results of the helium/air data, it would appear that, to within 20% accuracy, the general form of the spread parameter (δ_m/H), following equation (5.2.15) can be written as

$$(\delta_m/H) = 0.1 \left[\frac{x/|H|}{1 + 0.22\,(x/|H|)^{\frac{1}{2}}} \right] \qquad 7.1.3.1$$

Though, within $\pm$ 5% accuracy, Schlichting formula namely,

$$(\delta_m/|H|) = 0.37 \quad (x/|H|)^{\frac{1}{2}} \qquad 7.1.3.2$$

could predicted, the weak jet and the wake data as shown in figures (15) and (16). It would have been possible to adopt an effective origin (x_o), (for example, Bradbury [39]) in order to obtain a best fit curve for the data of ($U_j/U_m > 1$). However, the concept of an effective origin, in fact, is not a

particular definite procedure and a considerable latitude is available in its choice.

7.1.4 Verification of Reynolds analogy

From figures (11), (12), (13) and (16), it looks as though the Reynolds analogy is not wholly justified. By comparing the data giving (U_{max}), (C_{max}), (δ_m) and (δ_{m_c}) in these figures, the assumption seems to be adequate for the helium results (i.e. $S_c = 1.0$ for H_e) while for the $Arcton_{12}$ (C_{max}) decay much faster than (U_{max}) (figures 12 and 13) and (δ_{m_c}) spreads faster than (δ_m) (figure 16). It can be shown, from the analysis given in section (4.2.2) and those analysis of Eckert [63], that if S_c is constant throughout the flow field and is less than one the mass will spread more and decays less than the velocity. This relative inefficiency in the transport mechanism has been found by many workers who measured the mass and the momentum transport in jet flow e.g. Keagy and Weller[8], Forstall,[9] Landis,[42] Alpinieri [15] and Eckert [63] using different gases. The average values of S_c which have been reported by these workers, were between (0.75 - 0.5). For the $Arcton_{12}$ data, however, three various ways are adopted in measuring the Schmidt number and three different values are obtained.

1) The profiles measurements i.e.

$$\left(\frac{U - U_m}{U_{max} - U_m}\right) \sim \left(\frac{C - C_m}{C_{max} - C_m}\right) \text{ gives } S_c = 0.85$$

2) The spread rate measurements i.e.

$$\delta_m \sim \delta_{m_c} \qquad \text{gives } S_c = 0.75$$

3) The centre-line decay measurements

$$\text{i.e.} \left(\frac{U_{max} - U_m}{U_j - U_m}\right) \sim \left(\frac{C_{max} - C_m}{C_j - C_m}\right) \text{ gives } S_c = 0.5$$

7.2 <u>The turbulent wall jet data</u>

<u>Prediction of the Peak velocity (U_{max}) and the wall jet growth (δm).</u> (ρ is uniform)

The simplified theory (§ 6.2) showed that (U_{max}) and (δ_m) are expressed (provided that $\rho_j U_j^2 >> \tau_w$) as; $\left(\frac{U_{max} - U_m}{U_m}\right) = \text{const.}\ (H/x)^{\frac{1}{2}}$

and,

$$(\delta_m/H) = \text{function}\ (x/H)$$

The virtual origin is assumed to be located at the slot as before in connection with the free turbulent flow. The velocity distributions will be assumed to be quite close to rectangular profiles at the jet exit plane (boundary-layer thickness is very small at the slot edge). Since $C_{D_s} << \frac{H}{s}$

$\therefore$ from equation (5.5.3) $\frac{H}{s} = \frac{\sigma_j}{s} = \frac{U_j}{U_m}\left(\frac{U_j}{U_m} - 1\right)$

Therefore the peak velocity expression can be written as (for ρ is uniform)

$$\left(\frac{U_{max} - U_m}{U_m}\right) = \text{const.} \left[\frac{U_j}{U_m}\left(\frac{U_j}{U_m} - 1\right) s/x\right]^{\frac{1}{2}}$$

or $$\left(\frac{U_{max} - U_m}{U_j - U_m}\right) = \text{const.} \left[(U_j/U_m)/\left(\frac{U_j}{U_m} - 1\right) s/x\right]^{\frac{1}{2}}$$

For correlation purpose, (U_{max}) and (δ_m) may be written, in general, as

$$\left(\frac{U_{max} - U_m}{U_j - U_m}\right) = \text{function of} \left[\left(\frac{U_j}{U_m} - 1\right)/\left(\frac{U_j}{U_m}\right) x/s\right]$$

$$(\delta_m/H) = \text{function of } (x/s)$$

Figures (17) and (18) show the present experimental results for (U_{max}) and (δ_m) along the walltogether with those results presented by George [32], Verhoff [29], Kraka [31], Seban and Bock [53], Gortshore [56] and Mayers[59], when they are plotted as suggested by the above expressions respectively. All the experimental results for the range of velocity ratios $2 \leq \frac{U_j}{U_m} \leq 18$ correlate reasonably well except those data for $U_j/U_m = 1.48$, did not correlate. These findings, in fact, emphasize that the assumption of approximate self-preservation leads to a reasonable correlation of (U_{max})

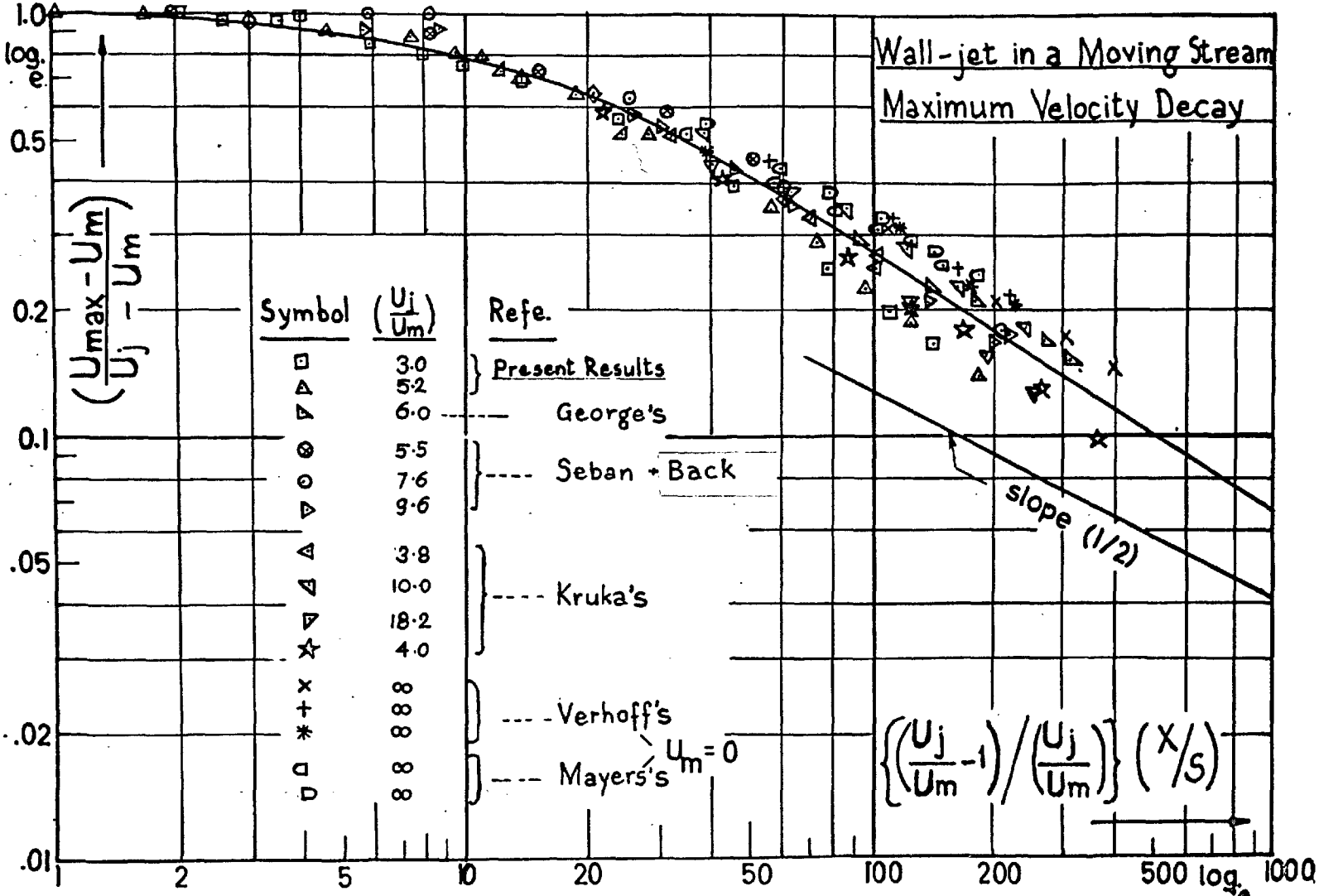

FIG. 17 The correlation of the peak velocity of the present & of the other's experimental results. ($U_j/U_m > 2$)

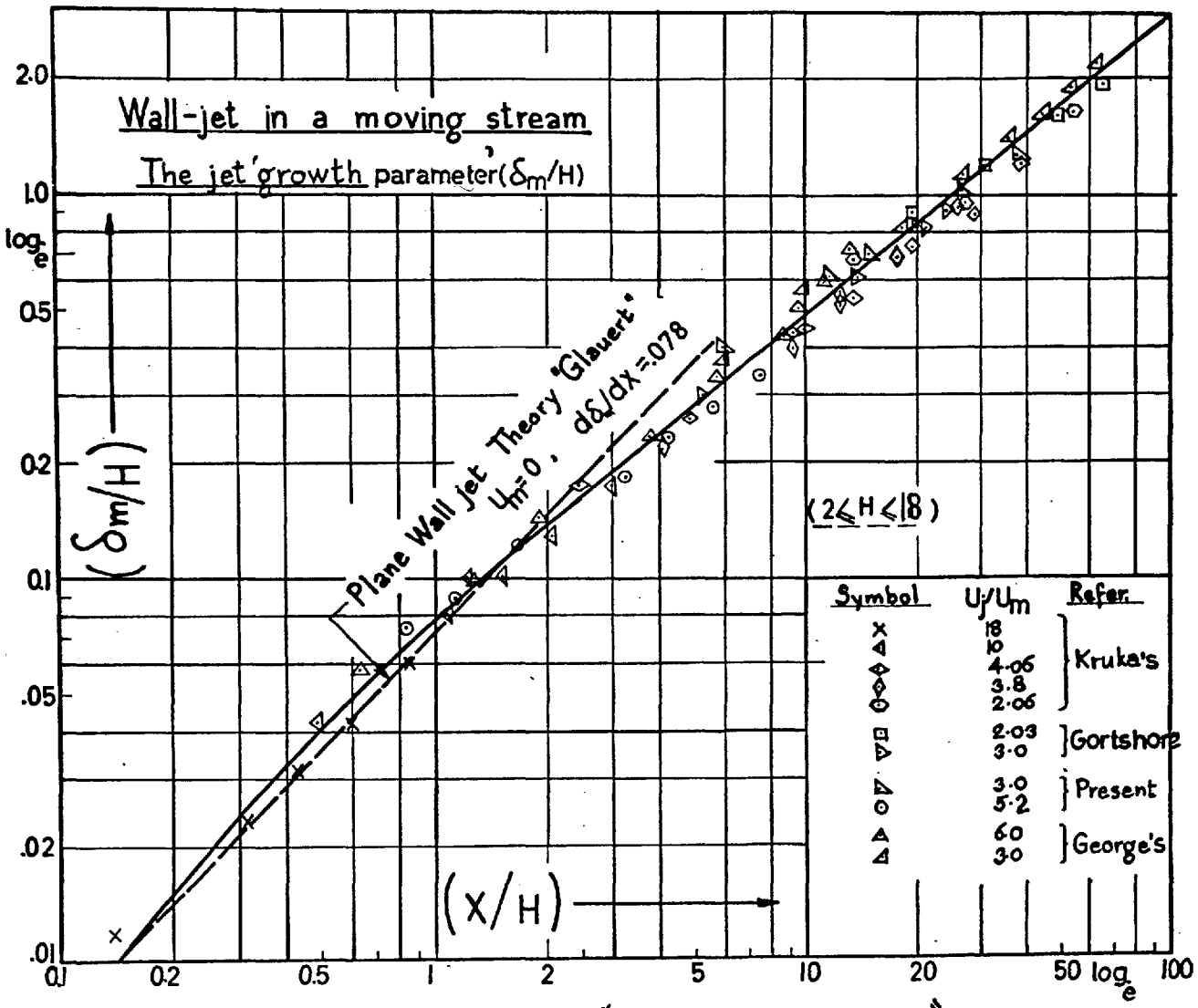

FIG 18 The correlation of the "growth parameter" of the present and of the other's experimental results & the comparison with Glauert' theory.

and (δ_m) for the general case of the plane wall jet provided that $(\frac{H}{s} \geqslant 2)$ or $(\frac{U_j}{U_m} \geqslant 2)$. The inadequacy of the simplified model for the data where $(0 < \frac{H}{S} < 2)$, however, is expected since the whole character of the flow will change from jet-like to 'boundary-layer-like' within a few slot widths of the jet exit. A more satisfactory analytical theory for the turbulent wall jets in a moving stream, however, is not available despite the extensive numerical treatment given by Verhoff[29], Gortshore [56], Spalding[57] and Harris [58]. It would appear from figures (17) and (18) that for all values of (x/H) upto 100 the peak velocity decay can be predicted to an accuracy of 15% by

$$\left(\frac{U_{max} - U_m}{U_m}\right) = 2.8\ (x/H)^{-.61} \qquad (7.2.1)$$

and the wall-jet growth can be predicted with an even higher degree of accuracy by the general expression of the spread parameter, as,

$$(\delta_m/H) = 0.078 \left(\frac{x/H}{1+0.172(x/H)^{\frac{3}{2}}} \right) \qquad (7.2.2)$$

provided that $(H/s \geqslant 2)$ with $\frac{d\delta m}{dx} = 0.078$ for $U_m=0$ as compared with plane wall jet (e.g. Verhoff [29])

7.3 Film cooling data (wall-wake)

The wall concentration distribution and the development of the velocity and the concentration boundary-layers.

The basic assumption in film cooling theory is that the flow far down stream from the slot is similar to that in the fully developed turbulent boundary-layer. From section (6.2), in the absence of heat and mass transfer, the boundary-layer solution is

$$\left[\frac{1}{1+\left(\frac{K_j - K_w}{K_w - K_m}\right)\frac{M_j}{M_m}}\right] = A_1 \left(\frac{x}{ms}\right)^{-0.8} \left(\mathrm{Rej}\,\frac{\mu_j}{\mu_m}\right)^{0.2} \qquad (7.3.1)$$

and, the characteristic thickness (δ) (§ 6.4.2 assumption 1.), after some algebra, can be written as:

$$\left(\frac{\delta}{ms}\right) = B_1 \left(\frac{x}{ms}\right)^{0.8} \left(\mathrm{Rej}\,\frac{\mu_j}{\mu_m}\right)^{-0.2} \qquad (7.3.2)$$

Hence from (7.3.1) and (7.3.2) one gets

$$\left[\frac{1}{1+\left(\frac{K_j - K_w}{K_w - K_m}\right)\frac{M_j}{M_m}}\right] \sim \left(\frac{1}{Re_m}\right) \qquad 7.3.3$$

where $R_{e_m} = \left(\frac{\rho_m U_m \delta}{\mu_m}\right)$ Reynolds number based on boundary-layer thickness.

7.3.1 The wall concentration distribution (C_w)

The data obtained for the wall concentration using Arcton_{12} are shown in figure (19) when they are plotted

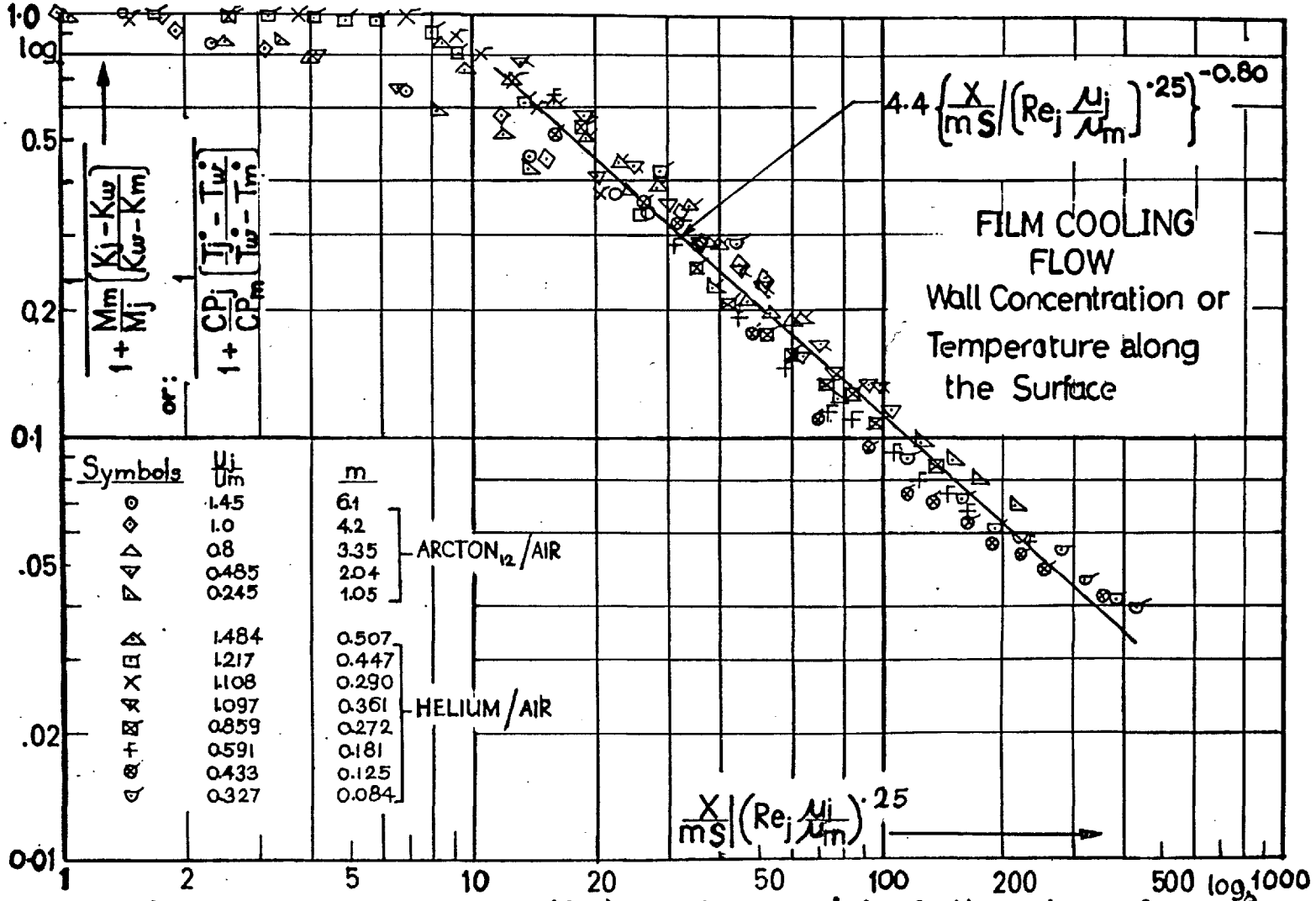

FIG.19 The present data of (C_W) for Arcton$_{12}$/air & the data of Hatch and Papell[20] of (T_W) for helium/air ($0 < U_j/U_m \leq 1.5$), are compared with the b.l. solution.

as suggested by equation (7.3.1). In the figure some data for ($\frac{U_j}{U_m} \leq 1.5$) obtained from the results of Hatch and Pappel[20] for the adiabatic wall temperature using helium as coolant are also present for comparison. The correlation as given in figure (19) is quite satisfactory, though for prediction a proportionality constant $A_1 = 4.4$ is needed rather than 3.09 as given by Stollery.[21]

7.3.2 The boundary-layers growth (δ_o & δ_{mc_w})

For the boundary layers growth (δ_o) defined as y at $U = 0.99\ U_m$) and ($\delta_{m_{c_w}}$) the present data using air and Arcton 12 together with some data for (δ_o) obtained from the results of Hartnett,[64] using air as coolant are reasonably well correlated according to equation (7.3.2) as shown in figures (20) and (21) respectively. From both figures it would appear that the concentration growth ($\delta_{m_{c_w}}$) asymptote to the 0.8 slope more rapidly than (δ_o). and at (x/s) is large ($\delta_{m_{c_w}}$) can be reasonably predicted by,

$$\left(\frac{\delta_{m_{c_w}}}{ms}\right) = 0.3 \left(\frac{x}{ms}\right)^{0.8} \cdot (Rej \frac{\mu_j}{\mu_m})^{-0.2}$$

However, from figures (19), (20) and (21), it looks as though the boundary-layer is fairly appropriate solution for a film cooled adiabatic wall using foreign gas

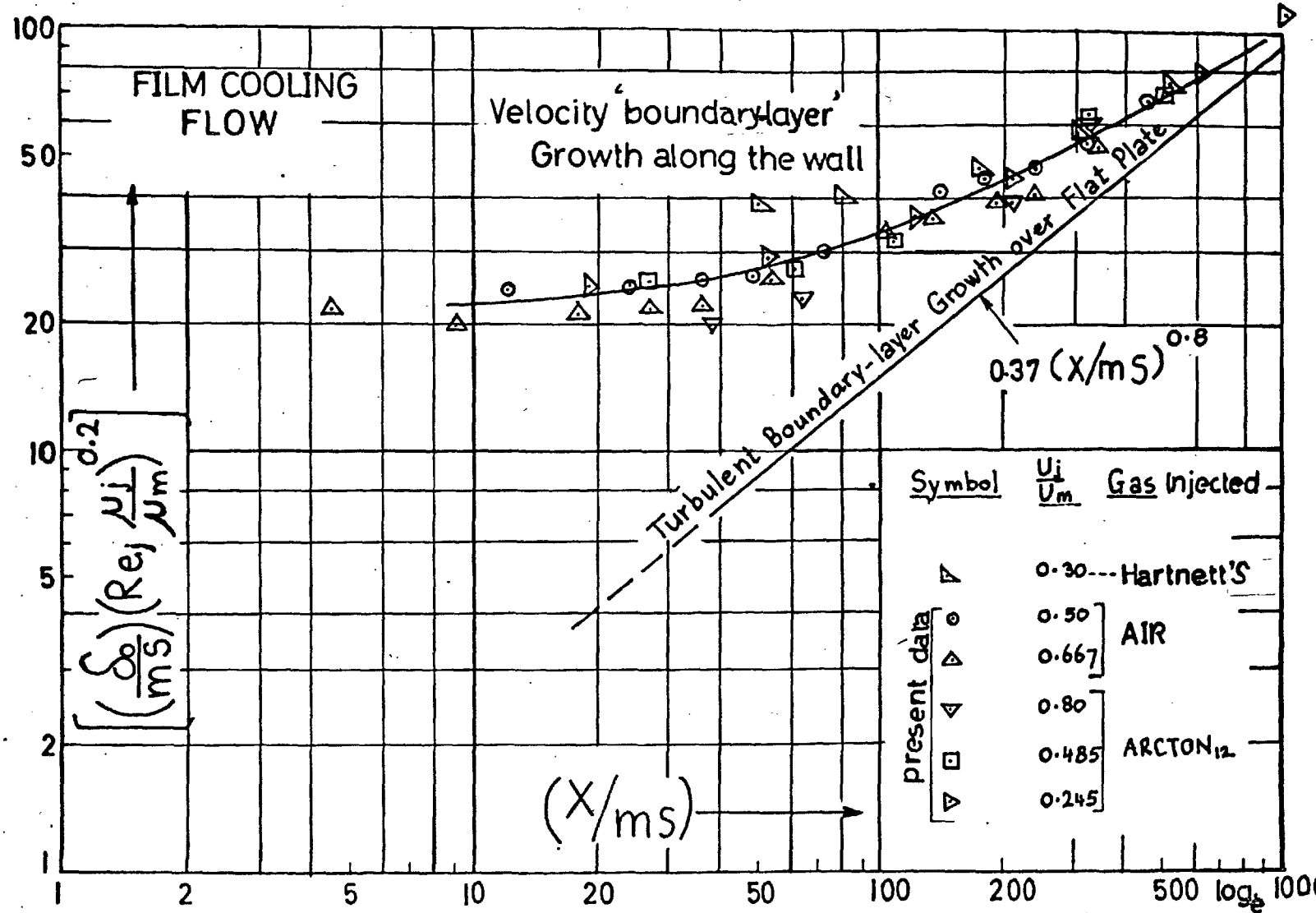

FIG. 20 The present data for air & Arcton$_{12}$ injection and the data of Hartnett[64] for air/air. ($0 < U_j/U_m < 1$)

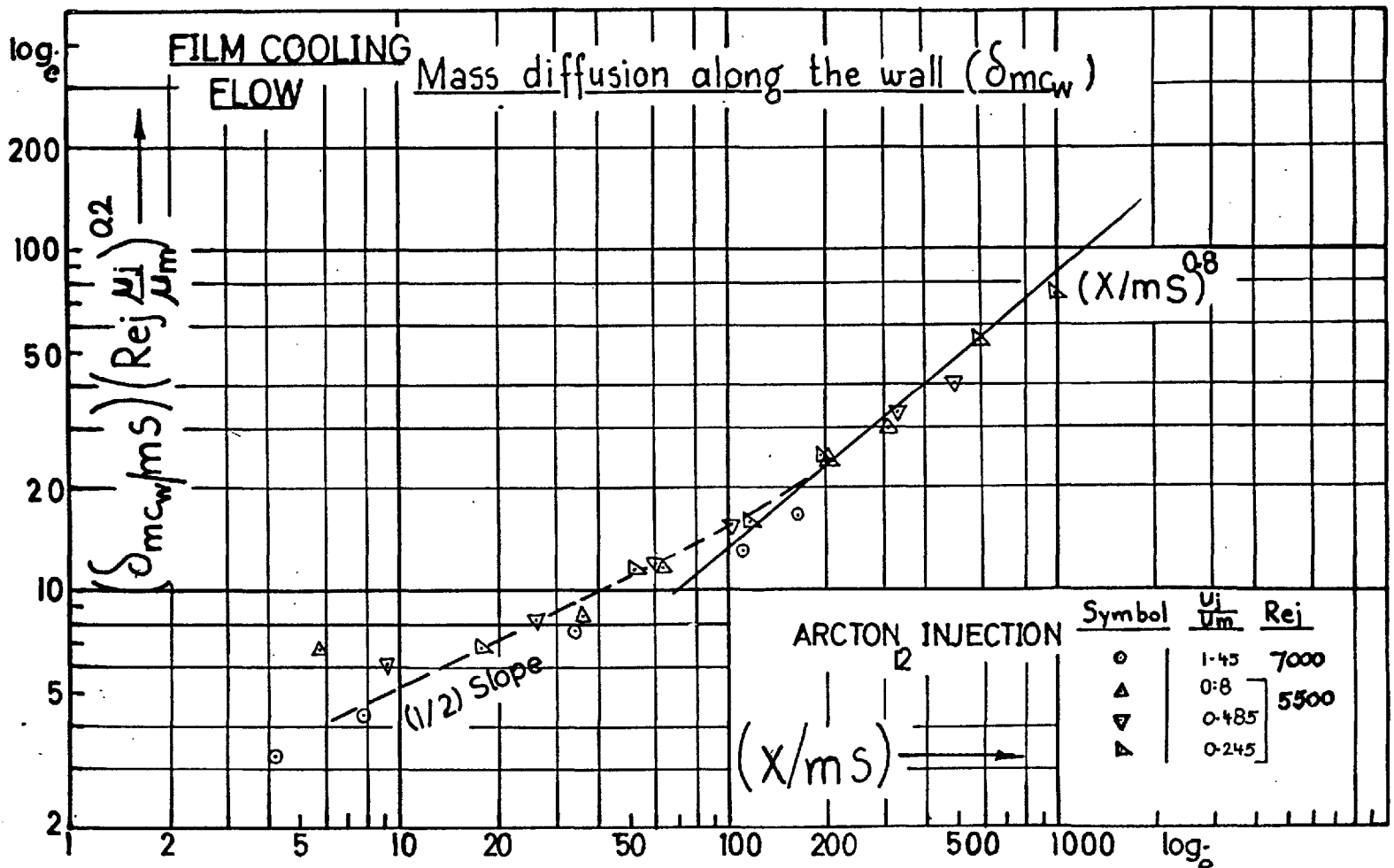

FIG. 21 The present data for Arcton$_{12}$/air giving the concentration growth ($0 < U_j/U_m \leqslant 1.5$)

injection and its accuracy increases as (x/s) increases. According to the density ratios examined herein, its validity is no longer limited to $m \leqslant 1.5$ (e.g. refer.[21]) but the data suggest that it is also useful for $m > 1.5$ provided that $\frac{U_j}{U_m} \leqslant 1.5$.

8. The initial region of the jet (The potential core)

Since this region is of interest to the present work it is, therefore, appropriate to spend some time in its discussion. No new analysis will be put forward but the existing theories will be reviewed. The central interest of the discussion is the prediction of its length (x_{p_c}). According to its definition (e.g. secs. 4.1.7 and 4.2) the experiments on free jet, wall jet and film cooling flows, in general, give information on velocity, thermal and diffusion potential core. simply by measuring the distance. from the slot location along the jet axis (free jet) or along the wall (wall jet and film cooling) up to the point where. the velocity (U_{max}), temperature (T_{max} or T_w) and the concentration (C_{max} or C_w) start to change respectively. The usual way in measuring this length is either by experiment using a probe, which needs extensive measurements in the initial region of the nozzle, or by extrapolating the rate of decay of the centre-line quantities (free jet) or the wall quantities (wall jets) expressed as,

$$\left(\frac{U_{max} - U_m}{U_j - U_m} \right) \text{ or } \left(\frac{T_{max} - T_m}{T_j - T_m} \right) \text{ or } \left(\frac{C_{max} - C_m}{C_j - C_m} \right)$$

when they are plotted vr x/s on a log-log scale,

back until they meet the lines of $\left(\frac{U_{max} - U_m}{U_j - U_m}\right)$ or $\left(\frac{T_{max} - T_m}{T_j - T_m}\right)$ or $\left(\frac{C_{max} - C_m}{C_j - C_m}\right) = 1.0$, give

$(x_{p_c})_U$, $(x_{p_c})_T$ and $(x_{p_c})_D$ respectively. This method has been considered as a good approximation for the length (x_{p_c}) by many previous workers and is used in the present study.

8.1. The hydrodynamic potential core length for uniform density streams.

For a uniform or nearly uniform density stream the available theories are as follows, The theory of Kuethe[35]. which is an extension of Tollmien's first problem to the case of two plane parallel streams of the same fluid. Kuethe used Prandtl's mixing length theory to solve the equations

$$U \frac{\partial U}{\partial x} + V \frac{\partial U}{\partial y} = \frac{1}{\rho} \cdot \frac{\partial \tau}{\partial y}$$

$$\frac{\partial U}{\partial x} + \frac{\partial V}{\partial y} = 0$$

where, $\tau_{(x,y)} = l_o^2 \left(\frac{\partial U}{\partial y}\right) \left|\frac{\partial U}{\partial y}\right|$

and (l_o), the mixing length, is given by

$$l_o = c' x$$

He assumed that the velocity profiles were similar and of the form $U = f(y/x)$

i.e. the width of the mixing region is proportional to x. For the fifth boundary condition Kuethe used

$U_m V_m = - U_j V_j$ as suggested by Von-Karman.

The free constant (c') appeared in the numerical solution of the equation of motion has been assigned the value suggested by Kuethe on the basis of measurements performed at Gottingen = .0174. The calculated values of x_{p_c} /s are

Table - 8 -

$\frac{U_j}{U_m}$	0	0.1	0.2	0.4	0.6	0.8	0.9	1.0
$\frac{x_{p_c}}{s}$	5.8	6.4	7.6	8.8	11.4	16.1	21.2	∞
$\frac{U_j}{U_m}$	1.0	1.1	1.25	1.67	2.5	5	10	∞
$\frac{x_{p_c}}{s}$	∞	22.6	18.3	14.9	13.9	13.1	12.7	12.1

Table (8) shows that the theory asymptots to the plane mixing layer solution (with adjacent fluid at rest) as $\frac{U_j}{U_m} \longrightarrow \infty$ (Tollmien[16]) and gives an infinite core length as $\frac{U_j}{U_m} \longrightarrow 1.0$. Korst [65] in the

discussion of Seban and Back's[66] paper considered the development of the flow near a wall in the potential core region as given by the figure below

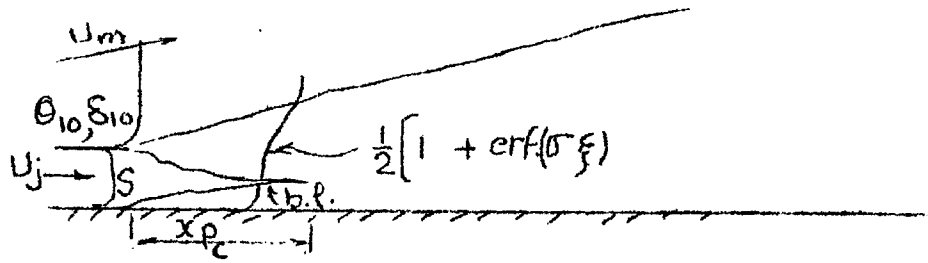

He assumed that the wake component within the boundary-layer can be represented by an error function in the form

$$\left(\frac{U - U_j}{U_m - U_j}\right) = \frac{1}{2}\left[1 + \text{erf.}\left(\sigma \frac{Y}{x}\right)\right]$$

where $\sigma = \left(M^*, \frac{T_j^o}{T_m^o}, \frac{U_j}{U_m}\right)$.

While the wall layer growth like a conventional boundary-layer over a flat plate immersed into a uniform stream of velocity (U_j). From Korst [65] definition the potential core length would be the distance downstream from the slot up to the point where the two-layers meet, as shown in the above figure. Korst [65] defined (θ_{10}), (δ_{10}) to be the momentum and the displacement thickness at the slot edge, solved the momentum integral equation assuming a laminar wall boundary-layer, and from Seban's [66] experimental condition he chose $\sigma = \left(\frac{12}{(1 - \frac{U_j}{U_m})}\right)$

The potential core length was, therefore, written in this form

$$\left(\frac{x_{p_c}}{s}\right)=\left\{\frac{1-1.45\,\frac{U_j}{U_m}\left(1-\frac{U_j}{U_m}\right)}{I_o\,(R_{e_j})^{\frac{1}{2}}}+\left[\left[\left[\frac{1.45\,\frac{U_j}{U_m}\left(1-\frac{U_j}{U_m}\right)}{I_o\,(R_{e_j})^{\frac{1}{2}}}\right]^2+\left(\frac{\theta_{10}}{s}-\frac{U_j}{U_m}\left(1-\frac{U_j}{U_m}\right)\right)\sigma\right]\right]^{\frac{1}{2}}\right\}^2 \qquad (8.1.1)$$

where (I_o) is a numerically integrated function of $(M^*, \frac{T_j^o}{T_m^o}, \frac{U_j}{U_m})$ was calculated for an error function velocity distribution with turbulent Prandtl's number = 1.0. These are the only available theories known to the author, however, it would be appropriate to show how those simple analyses which are given in sections (5) and (6) could predict the potential core length. From section 5, assuming a nearly uniform density streams, then, we have, for the free jet

$$\left(\frac{U_{max}-U_m}{U_m}\right)=C_1\left(\frac{H}{x}\right)^{\frac{1}{2}}$$

where C_1 is a constnat. From the first definition of the potential core length (x_{p_c}) i.e. at $x = x_{p_c}$

$$\left(\frac{U_{max} - U_m}{U_m}\right) = \left(\frac{U_j}{U_m} - 1\right)$$ therefore, we get

$$\left(\frac{x_{p_c}}{s}\right) = \text{const.} \left[\frac{(H/s)^{\frac{1}{2}}}{\left(\frac{U_j}{U_m} - 1\right)}\right]^2$$

Since $\frac{H}{s} = \left(\frac{\theta_j}{s} - C_{D_s}\right)$ (§ 5.5) and for $\left(\frac{\theta_j}{s}\right)$ is large

hence we obtain $\left(\frac{x_{p_c}}{s}\right) = \text{const.} \left(\frac{\frac{U_j}{U_m}}{\left(\frac{U_j}{U_m} - 1\right)}\right)$ (8.1.2)

From section (6.2.1), this equation is expected to hold for the wall jet case. Equation (8.2.1) would asymptote to a constant value at $U_m = 0$ and will be infinite at $U_j = U_m$ (Compare with Kuethe[35]). Similarly, we obtain, for the wall wake (sec. 6.2.2) from equation (6.2.2.9)

$$\left(\frac{x_{p_c}}{s}\right) = \text{const.} \quad m \, (Re_j \frac{\mu_j}{\mu_m})^{0.25} \qquad (8.1.3)$$

Fig. 22 shows the measured values of (x_{p_c}) using air injection for both free and wall jet data together with some results obtained from Weinstein [31], Forthmann,[26] Verhoff [29], George [32], Patel[33] and Seban and Back[53].

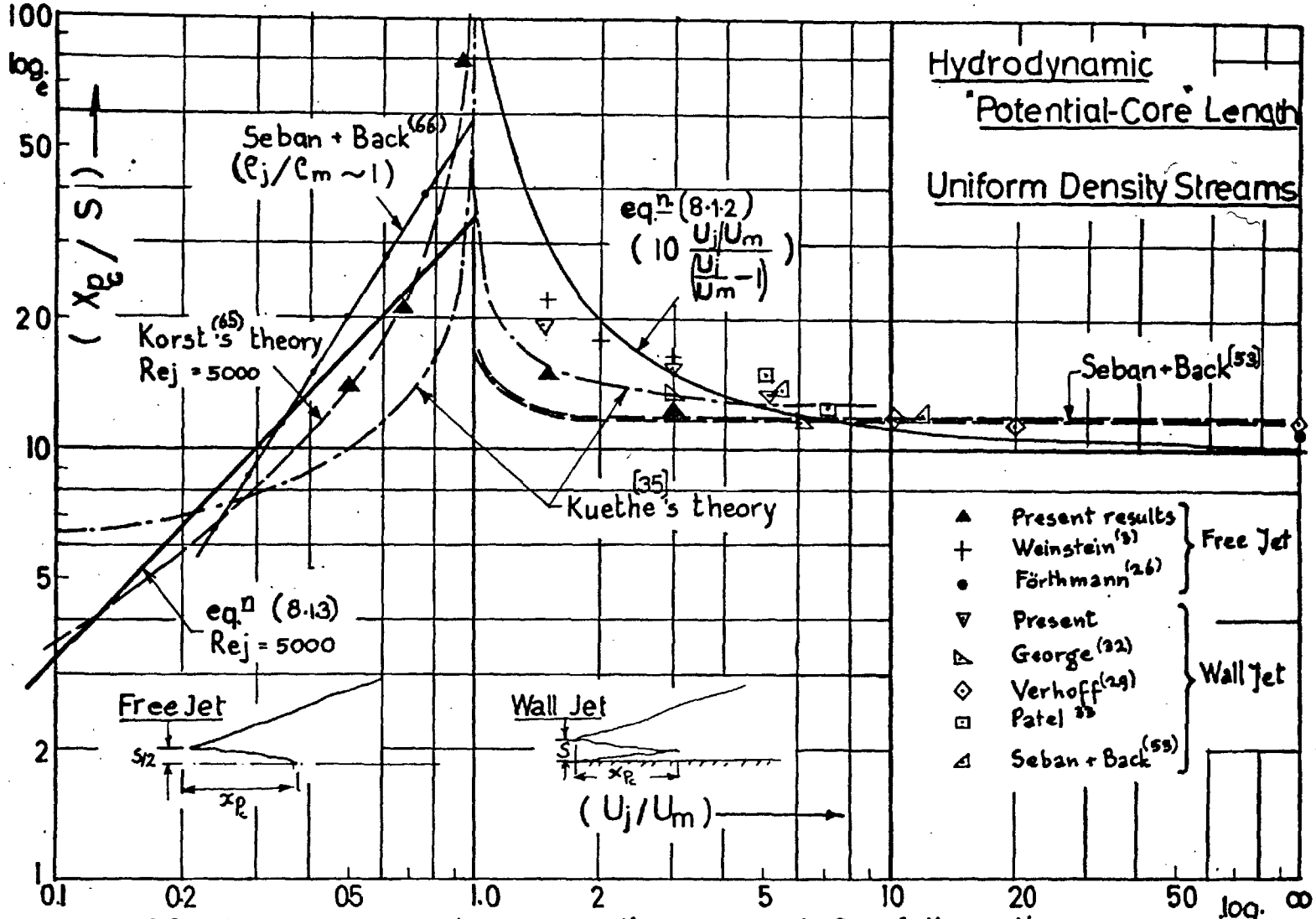

FIG. 22 Comparison between the present, & of the others experimental data, and the verious theoretical results giving (X_{p_c}/S).

The variation of (x_{p_c}/s) as given according to Kuethe's[35] theory, Korst's[65] theory, equation (8.1.2) and equation(8.13) are plotted for comparison. Some other empirical predictions obtained by Seban and Back[53, 66] expressed as

$$\left(\frac{x_{p_c}}{s}\right) = 12 \quad \text{for } U_j/U_m > 5$$

$$\left(\frac{x_{p_c}}{s}\right) = 56\ (m)^{1.5} \quad \text{for } m \leq 0.8$$

for a nearly uniform density streams are also shown in figure(22). From the figure the data seem to agree, in general, with Korst's prediction in the region where $U_j < U_m$ and with Kuethe s theory for $U_j > U_m$. It would appear, also from figure(22), that U_j/U_m is large the data are in quite reasonable agreement with equation (8.1.2) using a proportionality constant of 10, while equation (8.1.3) using a proportionality constant 4.1* (e.g. refe. 21) is less satisfactory.

8.2 The dissimilar gas streams.

If $P_r = S_c = 1.0$ then the hydrodynamic, the thermal and the diffusion potential core lengths will be similar. Therefore, any expression which can be written for one of them will be adequate for the others.

---

* $4.1 = (3.09)^{1.25}$

However, in the potential core region, the assumption of unit S_c or P_r is not strictly correct and in the most general case the actual lengths of these regions are different. In this section, however, we shall consider the diffusion potential core length $(x_{p_c})_D$.

Fig.(23) shows the measured values of $(x_{p_c}/S)_D$ as they are plotted in a similar way to figure (22) for both helium and Arcton $_{12}$ results. The relevant expression for comparison in this case, according to sec.(5.3) is

$$\left(\frac{x_{p_c}}{s}\right)_D = \text{const}\left\{\left(\frac{\rho_j}{\rho_m}\right)\left(\frac{\frac{U_j}{U_m}}{\left(\frac{U_j}{U_m}-1\right)}\right)\right\} \qquad (8.2.1)$$

for $\frac{U_j}{U_m}$ is large.

The data as given by figure (23) show that, $\left(\frac{x_{p_c}}{s}\right)_D$ increases, for bothe helium and Arcton$_{12}$ jets, as the velocity ratio increases, there is no maximum point as compared with figure (22). The comparison between the data for both gas combinations and the simple analysis, given by equation (8.2.1), is not satisfactory though it would appear that there is a slight agreement for the Arcton$_{12}$ data at $U_m = 0$. An attempt was made to correlate $(x_{p_c})_D$ on the basis of the parameter (m) following Ferri [5] and Seban[66] the correlation was not satisfactory. From figures (22) and

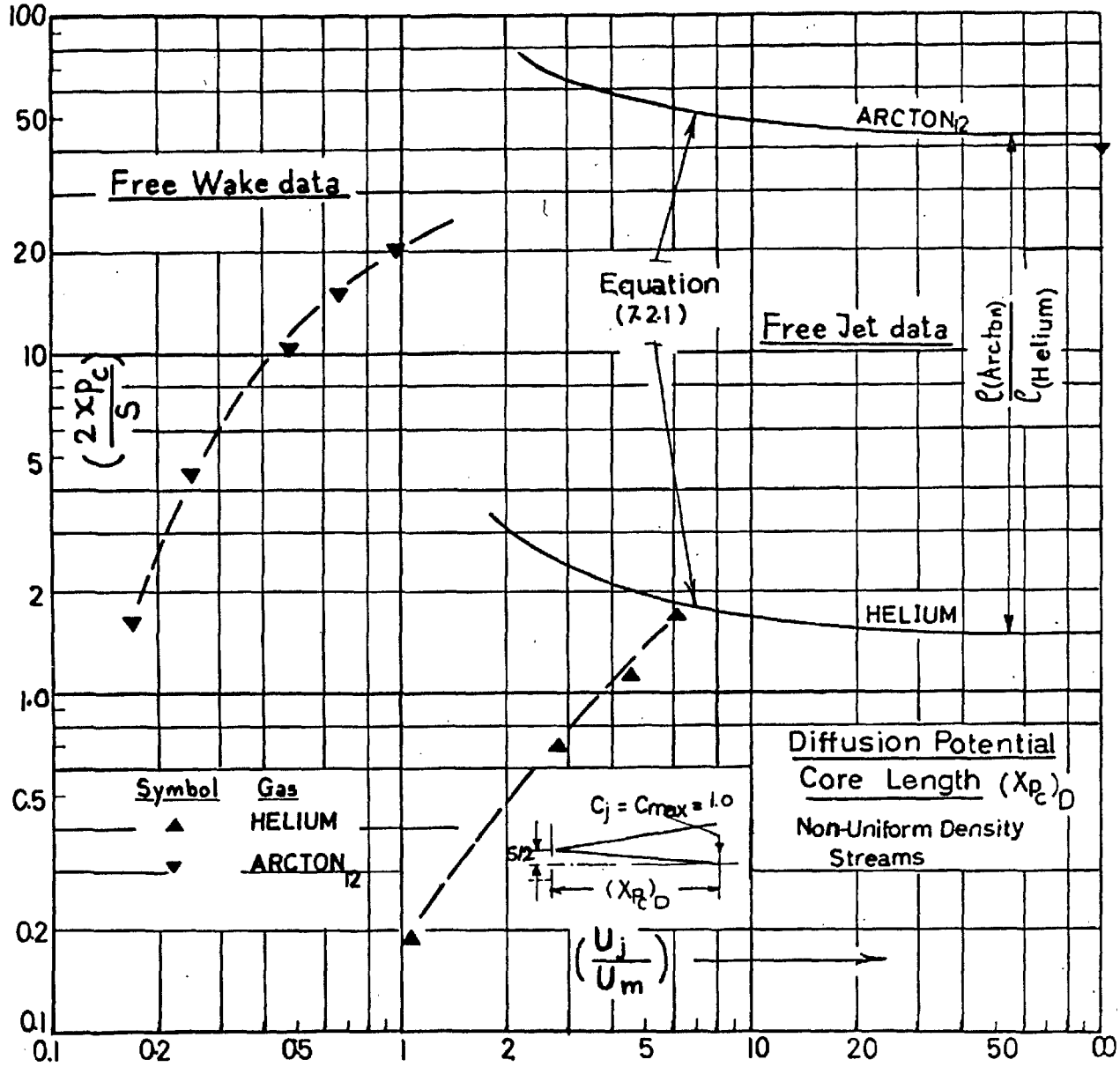

FIG. 23 The present data giving $(Xp_c/S)_D$ for helium, free, jet and for Arcton$_{12}$ free wake

(23) it looks as though a satisfactory theory on the development of the initial region of the jet, in general, is not available, in particular, for the dissimilar gas streams (foreign gas injection) where a more careful and controlled analysis is required. However, for correlation purpose the dimensional analysis, in general, would require

$$\left(\frac{x_{p_c}}{s}\right) = f\left[\left(\rho_j/\rho_m\right)^{n_1} \left(\frac{U_j}{U_m}\right)^{n_2} (Rej)^{n_3} \left(\frac{\mu_j}{\mu_m}\right)^{n_4} S_c^{n_5} \quad P_r^{n_6} \right] \qquad (8.2.2)$$

Assuming that $P_r = S_c = 1.0$,

$n_3 = n_4$ for simplicity and from the experimental result ($n_1 = n_2$).

From figure (24), it appears that the diffusion potential core length can be reasonably predicted for both helium and Arcton $_{12}$ jets as

$$\left(\frac{x_{p_c}}{s}\right)_D = 0.16 \left[m(Rej \frac{\mu_j}{\mu_m})^{0.25} \right]^{1.25} \qquad (8.2.3)$$

compare with Ferri[5] who wrote $\left(\frac{x_{p_c}}{s}\right)_D = 11.0 \ (m^{\frac{1}{2}})$

Equation (8.2.3) is purely empirical and the main idea is to express $\left(\frac{x_{p_c}}{s}\right)_D$ so that equation (8.2.3) together with figure (14) see sec.7) would describe the centre-line concentration distribution for the design purpose of combustion chamber.

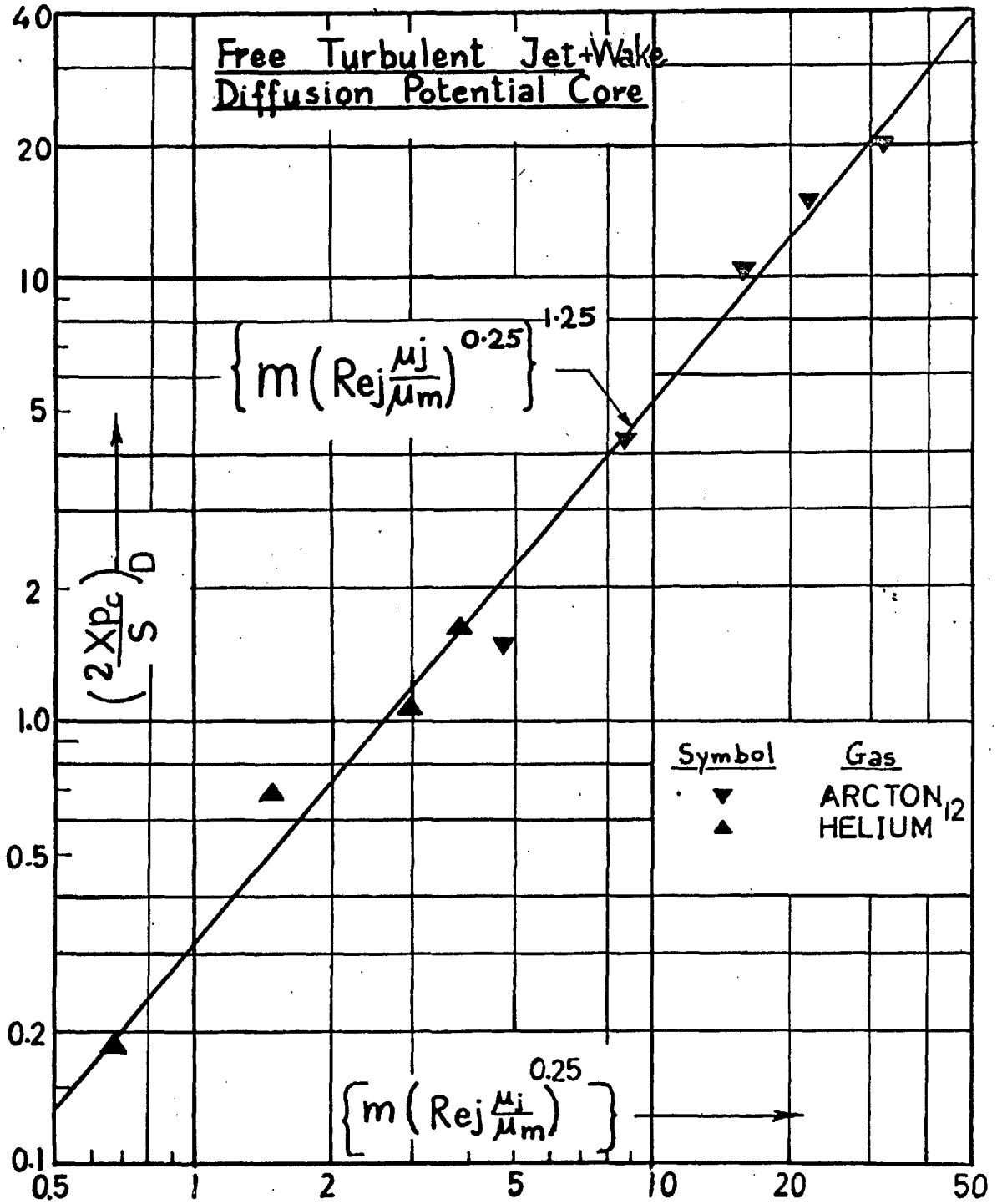

FIG. 24 Correlation of the data giving (X_{p_c}/S) for helium and Arcton$_{12}$ on the basis of the mass-velocity & the slot Reynold's number.

9. The mixing parameters

9.1 Uniform density streams

According to the analysis given in section (4) no matter whether it is based on Prandtl's mixing length theory or the constant exchange hypothesis, both are in a good agreement with the idea that the most important flow parameter that controls the mixing process between two moving streams is the velocity ratio $(\frac{U_j}{U_m})$ i.e. the mixing process is mainly due to the shear stress and the condition of segregation between the streams at $\gamma = 0$ is predicted. Therefore, from Prandtl's mixing length theory we have

$$l_o \sim \delta_m \rightarrow 0 \ , \quad n_e \rightarrow 0 \text{ and } H \rightarrow 0$$

or $U_j = U_m$.

From the constant exchange hypothesis, we have

$$\epsilon \rightarrow 0, \quad (U_j - U_m) \longrightarrow 0 \quad \text{or} \quad U_j = U_m \quad .$$

The application of these phenomena to the experimental results are shown, in some way, in figure (22) (section 8). There it is seen that the nearer the velocity ratio $(\frac{U_j}{U_m})$ is to one the longer is the potential core length and hence the tendency towards segregation between the streams. The data as given by figure (22) therefore, are in good agreement, at least, qualitatively with these hypotheses.

9.2 The dissimilar gas streams.

In this complex problem, however, according to some recent papers e.g. Vulis,[11] Libby [17], Zakkay[18], Regsdal[12] and Alpinieri[15], it seems that there are conflicting statements concerning the corresponding mixing parameter between the dissimilar gas streams and, hence, the condition of segregation between them. Vulis[11], for instance, conducted an experiment using hot air jets exhausting into a cold airstream, he specified the ratio $\left(\frac{T_{max} - T_m}{T_j - T_m}\right)$ as measure of the intensity of the transfer of energy in the flow, in the sense, that conditions of segregation or minimum mixing would correspond to higher values of this ratio. From his own experimental results he showed that the maximum value of this ratio coincided with $\rho_j U_j^2 = \rho_m U_m^2$. The momentum flux ratio was then considered as the most important flow parameter and the condition of segregation at $\frac{\rho_j U_j^2}{\rho_m U_m^2} = 1.0$ was predicted.
The form of the turbulent coefficient of viscosity proposed by Libby [17] (See section 4.2) as given by

$$(\rho\epsilon) \sim \delta_m \left| (\rho U)_{min} - (\rho U)_{max} \right|$$

consisted of attributing the mixing to be solely dependent on the mass velocity ratio (n) and therefor, the condition of segregation, at $\frac{\rho_j U_j}{\rho_m U_m} = 1.0$

would be predicted.

Regsdal[12] has postulated an alternate form for the eddy kinematic viscosity(ϵ^*) such that the laminar analysis can be extended to include the turbulent flow, by substituting the turbulent transport coefficient for the corresponding laminar ones. Therefore,ϵ^* was introduced as follows:-

$$\mu_t = \mu \left[1 + \epsilon^*\right] \quad , \quad D_t = D_{12} \left(1 + \frac{\epsilon^*}{D_{12}}\right)$$

where(μ_t) and(D_t) are the turbulent coefficients of viscosity and diffusion respectively while(μ) and(D_{12}) are the corresponding laminar ones. According to Regsdal[12] definition, ϵ^* would be the ratio of the turbulent to the laminar coefficient of viscosity

i.e. $\epsilon^* = \left(\frac{\rho \epsilon}{\mu}\right)$, assumed to be constant over the whole flow region. Following Prandtl's new hypothesis, ϵ^* was expressed in this form

$$\epsilon^* = f_1 \left(\frac{U_m}{U_j} - 1\right) f_2 \ (Rej)$$

From his own experimental results, using B_r/air, he showed that:

$$\epsilon^* = .0172 \left|\frac{U_m}{U_j} - 1\right|^{\frac{1}{2}} (Rej - 250)$$

For $255 \leqslant Rej \leqslant 3850$, $\quad .83 \leqslant \frac{U_m}{U_j} \leqslant 0.97$

$$1.25 \leqslant \frac{U_m}{U_j} \leqslant 49$$

According to the above expression, for $Rej > 250$, a vanishing turbulent component would be predicted at $U_j = U_m$ and, hence, the optimum penetration (segregation between the streams) would take place since the mixing would be mainly due to laminar diffusion for $Rej \leqslant 4000$. Alpinieri[15] used coaxial gas jets of H_2/air and CO_2/air has examined the mixing process, in particular, at $\frac{U_j}{U_m} = 1.0$ and $\frac{\rho_j U_j}{\rho_m U_m} = 1.0$. His results showed that the condition of minimum mixing was neither $\frac{U_j}{U_m} = 1$ nor $\frac{\rho_j U_j}{\rho_m U_m} = 1.0$ nor even

$$\frac{\rho_j U_j^2}{\rho_m U_m^2} = 1.0 \ *$$

9.2.1 The contribution of the present results to the mixing parameter.

Following Vulis[11] the centre-line concentration (C_{max}) is chosen as the basic quantity which characterises the intensity of the turbulent transfer (e.g. of mass) in the mixing process. There are other quantities which can be used, for instance, the centre-line velocity or the potential core length.

---

* This condition was given in a footnote in his paper, though his own results did not cover this condition.

However, the concentration is preferable to the velocity since the former can be measured more accurately. The higher values of (C_{max}) mean less mixing and obviously the lower values mean severe mixing. (C_{max}) is plotted against the parameters $\left(\frac{U_j}{U_m}\right)$, $\left(\frac{\rho_j U_j}{\rho_m U_m}\right)$ and $\left(\frac{\rho_j U_j^2}{\rho_m U_m^2}\right)$ in a way as suggested by Vulis[11] as shown in figure (25). For a matter of convenience figure (25) is split into two parts one for each gas used. There it is seen the condition of minimum mixing is neither $\frac{U_j}{U_m} = 1.0$ nor $\frac{\rho_j U_j}{\rho_m U_m} = 1.0$, nor even $\frac{\rho_j U_j^2}{\rho_m U_m^2} = 1.0$ and this conclusion is in agreement with Alpinieri[15]. The mixing decreases as $(\frac{U_j}{U_m})$ increases and it increases as $(\frac{U_j}{U_m})$ decreases and it looks as though there are no simple combinations of jet and external stream flow properties that would give a condition of minimum mixing. It appears, however, from figure (25), that an increase of the jet velocity and correspondingly the mass flow rate would simply delay the rate of decay of the centre-line quantities as well as increase the length of the potential core (e.g. figure 23). These findings, in fact, emphasize that the mixing process between

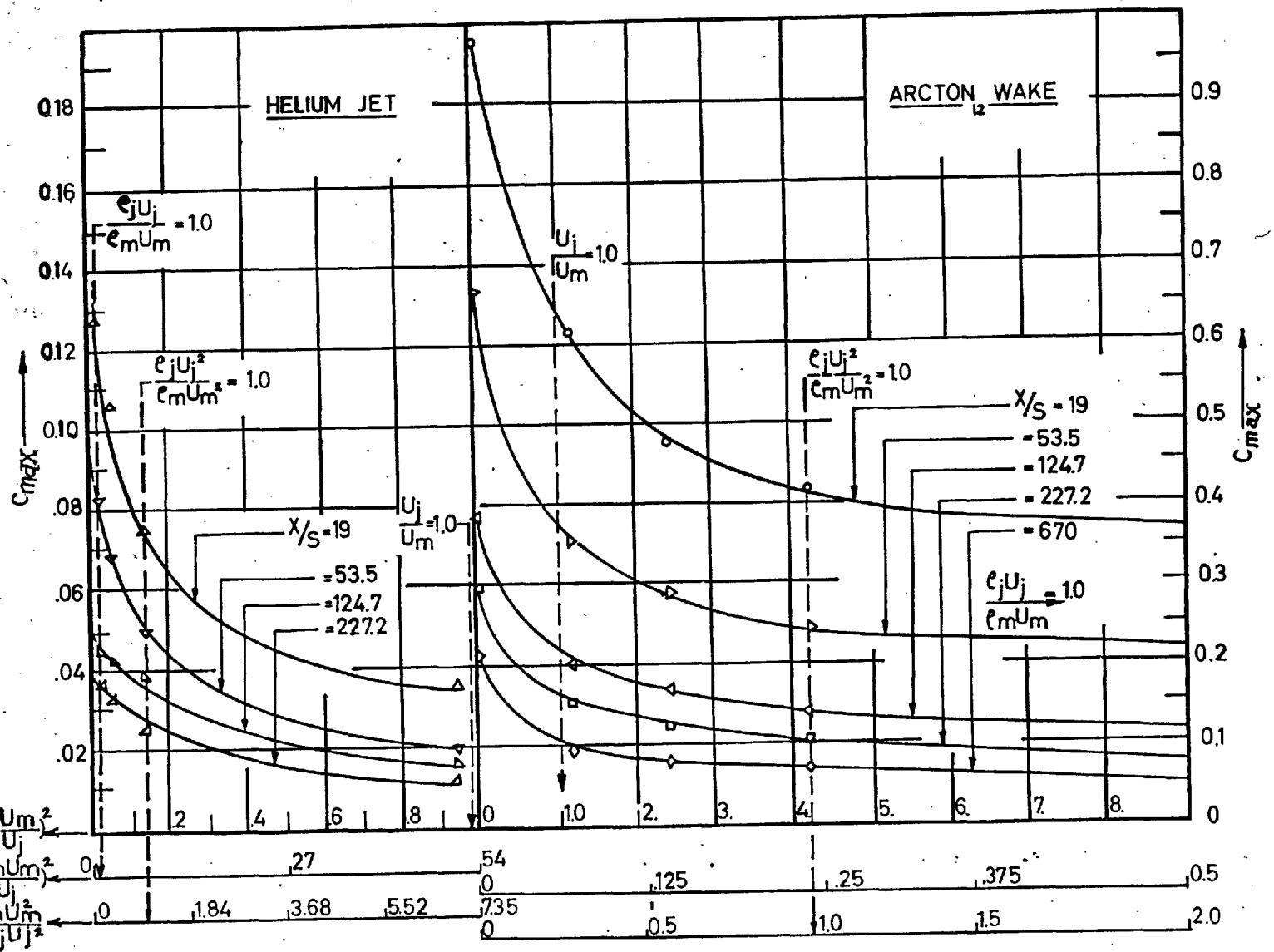

FIG. 25 Variation of C_{max} with the flow parameters.

dissimilar gas streams is not due mainly to shear but to turbulent diffusion; and correspondingly one would expect a mixing parameter to include both diffusion and shear terms. It may appear from figure (25) that the condition of minimum mixing occurs at $U_m = 0$ and this might be attributed to the following:-

a. The free stream turbulence level will be a minimum when the stream is at rest.

b. The effect of the ihitial boundary-layer thickness which exists at the slot edge is zero.

Recommendation for the practical application purpose.

It appears then, from figure (25), that for minimum mixing a fast jet of heavy gas is needed, and for minimum penetration (e.g. for combustion) a slow jet of light gas should be used. This simple statement implies that, for combustion applications, a large slot size, for a given quantity of fuel, is needed and a correspondingly large combustion chamber would be required.

Conclusions

1. Except for some of the helium velocity profiles, the Gaussian distribution function can well represent the profiles (velocity, concentration, mass flux and momentum flux) for both jet and wake flows downstream of the potential core ($x/s \gtrsim 30$).

2. Despite the large difference in density the parameter (H/s) correlates the data for, jets, weak jets and wakes fairly satisfactory.

3. Only when (x/s) is large does the flow in the jet become similar to that of the wake and the wake model become relevant.

4. The correlation of the data for the wall jet on the basis of the parameter (H/s) is fairly satisfactory considering the crude, simplifying assumptions, provided that ($\frac{U_j}{U_m} \gtrsim 2$). The disagreement of the results for weak wall jets ($\frac{U_j}{U_m} < 2$) is expected since the flow becomes similar to that in a boundary-layer at (x/s) large.

5. The correlation of the data for the weak wall jet and the 'wall:wake' (film cooling) flows, on the basis of the parameter (n) is satisfactory - provided that $\frac{U_j}{U_m} \lesssim 1.5$ - over the range of (x/s) currently of interest. The accuracy of the boundary-layer model

increases as (x/s) increases.

6. Conclusions 2, 4 and 5 indicate that (x/H) is the similarity parameter for the free jet, free weak jet free wake and strong wall-jet flows, while $(\frac{x}{ms})$ is the similarity parameter for the weak wall jet and film cooling flows.(wall wake).

7. Minimum mixing does not occur when the velocity ratio, mass velocity ratio, momentum flux ratio and the excess of the momentum flux ratio is made equal to unity for the gas combinations tested.

Scope of future work

A. Free turbulent flows.

1. A more accurate theory together with an extensive experimental measurement for the potential core of the jets using dissimilar gas streams are required in order to eliminate the need for empirical correlation functions used both in the present investigation and by others.

2. Extensive measurements of the turbulent structure and the density flacutation in the main region of the plane jets, issuing into a moving stream of different density, are essential to obtain information concerning the eddy diffusivity and, therefore,

provide a better knowledge concerning the mixing mechanism between two turbulent gas streams.

B. Wall-jet flows

1. Experimental data on mixing of wall jets of different density fluids with an external air stream are still needed (e.g. using helium and hydrogen) in order that the utility and the limitation of the theoretical models can be finally established.

REFERENCES.

1) Abramovich G.N. "The Theory of Turbulent jets". The MIT Press (1964)

2) Schlichting "Boundary Layer Theory". 4th edition McGRAW HILL (1960)

3) WeinsteinA.S., Osterle J.Forstall W., and Pittsburgh "Momentum diffusion from slot jet into a moving secondary". ASME (55-A-60).

4) Townsend A.A. "The Structure of Turbulent Shear Flow". CAMBRIDGE UNIVERSITY PRESS (1956).

5) Ferri A. "Review of Problems in application of supersonic combustion". R.A.S. JOURNAL (Sept.1964)

6) Rundun P. "Turbulente Ausbreitungevorgange in Freistrahl". DIE NATURWISS 21 HFFT 21/23 375-378 (1933).

7) Corrsin S. and Uberoi M.S. "Further experiments on the flow and heat transfer in a Heated Air Jet.." NACA T.N 1865 (1949).

8) Keagy W.R. and Weller A.E. "A study of Freely Expanding Inhomogeneous jets". HEAT TRANSFER AND FLUID MECH. INST. BERKELEY, CALIFORNIA (1949).

9) Forstall W and Shapiro A.H. "Momentum and Mass Transfer in Coaxial gas jet." JOURNAL OF APPLIED MECH. 17, 4,399 (1950).

10) Vulis L.A. and Terekhina N.N. "Propagation of a Turbulent Gas Jet in a Medium with a different density". JOURNAL OF TECH. PHYS. VOL. I (1956).

11) Vulis L.A. "The process of Transfer in a free Turbulent flow". THE INST. OF MECH. OF THE U.S.S.R. HEAT TRANSFER CONFERENCE, MINSK (1961).

12) Ragsdale R.G., Weinstein H. and Lanzo C.D. "Correlation of a Turbulent Air Bromine Co-axial-flow experiment." NASA TN D2121 (1964).

13) Ferri, A. "PIBAL report No.787 (1963)

14) Zakkay V and Krause E. "Mixing Problem with Chemical Reaction", 21st MEETING IN COMBUSTION AND PROPULSION CONFERENCE (1963) PERGAMAN PRESS, NEW YORK (1964).

15) Alpinieri L.J. "Turbulent mixing of a Co-axial jet". JOURNAL OF AIAA. Vol.2, No.9 (1964).

16) Tollmien W. "Berechnung der Turbulenten Ausfreitungsvorgange," ZAMM Bd IV (1926). (Translated as NACA TM 1085. 1945.

17) Libby P.A. "Theoretical Analysis of Turbulent Mixing of Reactive Gases with Application to Supersonic Combustion of Hydrogen" ARS. J. 32 (1962)

18) Zakkay V., Krause E and Woo S. "Turbulent Transport properties for Axisymmetric Hetrogeneous Mixing." JOURNAL AIAA Vol. No.11 (1964)

19) Glauert M.B. "Wall jet" JOURNAL OF FLUID MECH. Vol.1 (1956).

20) Hatch J.E. and Pappell S.S. "Use of a Theoretical flow model to correlate Data for Film Cooling or Heating an Adiabatic Wall by Tangential, Injection of gases of different Fluid Properties". NASA TN D-130 (1959).

21) Stollery J.L. and El-Ehwany A.A.M. Journal of Heat and Mass Transfer (Enclosed in the report).

22) Powell R.W. "Modern Refrigeration" (Dec. 1956)

23) Lock R.C. "The Interference of a Wind Tunnel on a Symmetrical Body". R & M. 1275 (1929)

24) Jeans J. "An Introduction to the Kinetics Theory of Gases". CAMBRIDGE UNIVERSITY PRESS. (1948)

25) Eskinazi S. "Mixing of Wakes in a Turbulent Shear Flow". NASA D- 83 (1959).

26) Forthmann E. "Ingeniem Archis BD. V, (1936) 42.

27) Maczynski J. "A round jet in an ambient Co-axial stream." JOURNAL OF FLUID MECH Vol.13 (1962)

28) Bakk P. "An experimental Investigation of a wall-jet". JOURNAL OF FLUID MECH. Vol.2 (1957).

29) Verhoff A. "The Two-dimensional turbulent wall-jet with and without an external stream". PRINCETON UNIV. Dept. of Aero. report No. 626 (1963).

30) Bradshow P. and Gee M.T. "Turbulent Wall jets with and without an external stream". ARC. R. and M. No.3252 (1962)

31) Kruka V. and Eskinazi S. "The wall jet in a moving stream." JOURNAL OF FLUID MECH. Vol.20 (1964).

32) George A.R. "An Investigation of a wall jet in a Free Stream". PRINCETON UNIV. Aero Dept. Report No.479 (1959)

33) Patel R and Newman B. "Self-preserving two dimensional jets and wall jets in a moving stream." McGILL UNIV. Report Ae.5-(1961)

34) Schwarz W.H. and Cosart W.P. "The Two-Dimensional Turbulent Wall jet " JOURNAL OF FLUID MECH. Vol. 10 (1961)

35) Kuethe A and Ohio A. "Investigation of the Turbulent Mixing Region formed by jet." JOURNAL OF APPL. MECH. Vol.(2) (1935)

36) Pai S. "Fluid Dynamics of jets". D VAN NOSTRAND CO. INC. London (1956).

37) Spalding D.B. "Lectures on jets and wakes". Imperial College of Science and Technology. (Feb. 1965)

38) Spalding D.B. "7th Symposium of Combustion" (1958)

39) Bradbury L.J.S. "An Investigation into the structure of a turbulent plane jet". (Ph.D. Thesis, Queen Mary College London) (1963)

40) Squire H.B. and Trouncer J. "Round Jets in a General Stream". R and M. No. (1976) ARC. TR (1944).

41) Szablewski W. "The Diffusion of Hot jet in Air in motion". NACA T.M. (1288)

42) Kuchemann and Webber — "Aerodynamics of Propulsion" MCGRAW HILL PUBLICATION IN AERONAUTICAL SCIENCE (1953)

43) Londis F. and Shapiro A.H. — "The Turbulent mixing of Co-axial gas jet." HEAT TRANSFER AND FLUID MECH. INST. (1951).

44) Crane L.J. and Pack D.C. — "The mixing of a jet of gas with an atmosphere of a different gas at a large distance from the orific". QUART. JOURNAL OF MECH. AND APPLIED MATHS. VOL.(14) (1961).

45) Schetz J.A. — "Supersonic diffusion flames". Supersonic flow, chemical processes and Radiative Transfer. PERGAMON PRESS LONDON (1964).

46) Bickley W.G. — Phil. Mag. (7) 23/727 (1937).

47) Ting L. and Libby P.A. — "Remarks on the Eddy viscosity in Compressible Mixing Flows." J.A.S. Vol.27 (No.10) (October 1960)

48) Hill J.A.F. and Nicholson J.E — "Compressibility effects on fluid entrainment by Turbulent mixing Layers". NASA CR - 131 (1964).

49) Craven A.H. — "The Effect of Density on Jet Flow at Subsonic Speeds." COLLEGE OF AERONAUTICS REPORT No.120 (1959).

50) Zerbe J. and Selna J. — "An Empirical Equation for the co-efficient of heat transfer to a plate surface from a plane heated air jet directed tangentially to the surface." NACA No. 1070 (1946).

51) Jakob M., Rose R. and Spilman M. "Heat Transfer from an air jet to a plane plate with entrainment of water vapour from the environment". TRANS. ASME. Vol.72 (1950).

52) Sigalla A. "Experimental data on a turbulent wall-jet." AIRCR. ENGR.30 (1958)

53) Seban R.A. and L.H. Back "Velocity and temperature profiles in a wall jet." INT. JOURNAL OF HEAT AND MASS TRANSFER Vol.3 No.4 (1961)

54) Eichelbrenner E.A. and Dumargue R. "The problem of the plane turbulent wall-jet with an external stream flow of constant velocity." JOURNAL DE MECANIQUE.I. (109) (1962).

55) Mathieu J. "Contribution a l'étude Aerothermique d'un jet plan evoluant en presence d'une paroi". PUBL. SCI. TECH. MINISTERE DE'L'AIR. No.376 (1961).

56) Gortshore I.S. "Jets and Wall jets in uniform streaming flow." McGILL UNIVERSITY REPORT (64-4) (1964).

57) Spalding D.B. "A unified theory of friction heat transfer and mass transfer in turbulent boundary-layer and wall jet". MECH. ENG. DEPT. IMPERIAL COLLEGE (1964).

58) Harris G.L. "The turbulent wall jet in a moving stream". RECENT DEVELOPMENT IN BOUNDARY LAYER RESEARCH ARGARDograph (97) (1965).

59) Myers G.E. Shauer J.J. and Eustis R.H. "The plane turbulent wall jet." STANFORD UNIVERSITY MECH. ENG. DEPT. Report No.I (1961)

60) Coles D. "The Law of the wake in the turbulent boundary layer". JOURNAL OF FLUID MECH. VOL.I (1956).

61) Foley W.H. "An experimental study of jet flap thrust recovery". Ph.D. thesis STANDFORD UNIVERSITY (1962).

62) Wygnanski I. "The effect of jet entrainment on loss of thrust for a two dimensional, symmetrical jet flap aerofoil". McGILL UNIVERSITY REPORT (64-13) (1964)

63) Eckert E.R.G. and Drake R.M. "Heat and Mass Transfer". McGRAW HILL (1954)

64) Hartnett J.P., Birkbak R.C. and Eckert E.R.G. "Velocity distribution, temperature distribution effectiveness and heat transfer for air injected through a tangential slot into a turbulent boundary-layer". J. HEAT TRANSFER TRANS. ASME C. 83 - 293 - 306 (1961).

65) Korst H.H. "Journal of Heat Transfer" Vol.84 (1962) (262-266)

66) Seban R.A. and Back L.H. "Effectiveness and heat transfer for a turbulent boundary-layer with tangential injection and variable free stream velocity". JOURNAL OF HEAT TRANSFER (Vol. 86) (1962).

Ph.D. 1965.

EL-EHWANY (A.A.M.N.)

Reprinted from

International Journal of
HEAT and MASS
TRANSFER

PERGAMON PRESS
OXFORD · LONDON · NEW YORK · PARIS

Int. J. Heat Mass Transfer. Vol. 8, pp. 55–65. Pergamon Press 1965. Printed in Great Britain

A NOTE ON THE USE OF A BOUNDARY-LAYER MODEL FOR CORRELATING FILM-COOLING DATA

J. L. STOLLERY and A. A. M. EL-EHWANY
Department of Aeronautics, Imperial College of Science and Technology, London, England

(*Received* 6 *March* 1964 *and in revised form* 3 *July* 1964)

Abstract—The boundary-layer model for correlating experimental data on film-cooled adiabatic walls is re-examined. Existing analyses are reviewed. A much simpler approach is given which can also cover the case of foreign gas injection. The utility and limitations of the boundary-layer model are emphasized by comparison with experimental data.

NOMENCLATURE

A, B, C, constants, see text;
C_f, local skin friction coefficient;
C_p, specific heat at constant pressure;
H, heat-transfer coefficient defined in text;
K, constant, see text;
L, unheated starting length, see equation (10);
M, Mach number;
Pr, Prandtl number;
Re, Reynolds number;
T, temperature;
T^*, reference temperature, see equation (10);
f, function of;
h, enthalpy;
k, coefficient of thermal conductivity;
k_e, eddy heat conductivity;
$\dot{m}$, mass flow rate;
m, $\rho_c u_c / \rho_m u_m$;
n, power law index;
p, pressure;
q, heat-transfer rate;
s, slot height;
t, time;
u, x component of velocity;
v, y component of velocity;
x_0, fictitious starting point of coolant boundary layer, see Fig. 1;
x, y, cartesian co-ordinates;
$\bar{x}$, $(x/ms).\{Re_c.(\mu_c/\mu_m)\}^{-1/4}$;
α, thermal diffusivity, $k/\rho C_p$;
β, eddy diffusivity, $k_e/\rho u C_p$;
α, β, constants, see text;
Γ, gamma function;
δ, boundary-layer thickness;
δ_1, boundary-layer displacement thickness;
δ_2, boundary-layer momentum thickness;
δ_T, boundary-layer thermal thickness;
η, $(T_{aw} - T_m)/(T_c - T_m)$;
η', $(h_{aw} - h_{om})/(h_{oc} - h_{om})$;
η'', $(T_{aw} - T_{om})/(T_{oc} - T_{om})$;
θ, $(T - T_w)/(T_m - T_w)$;
μ, coefficient of viscosity;
ξ, see equation (16);
ρ, density;
σ, $(T - T_m)$;
τ, skin friction.

Suffices

c, coolant;
m, mainstream;
o, total;
s, slot;
w, wall;
aw, adiabatic wall.

INTRODUCTION

WHEN A WALL is film cooled, by injecting a stream of gas between the surface and the hot external flow, three separate regions can be recognized, as shown in Fig. 1. A "potential core", wherein the wall temperature remains close to the coolant gas temperature, is followed by a zone where the velocity profile is similar to

that of a wall jet. Farther downstream, however, the flow must become similar to that in a fully developed turbulent boundary layer. For coolant and mainstream gases of similar density the relative length of the three regions is governed primarily by the velocity ratio u_c/u_m. When $u_c \gg u_m$ a simple jet model, as suggested by Spalding [1] for the second zone, may be valuable.

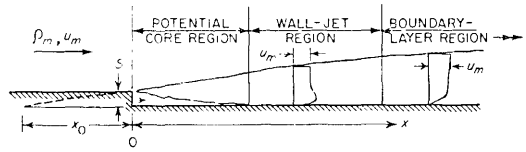

FIG. 1. The three possible regions for the flow past a film cooled surface.

For $u_c < u_m$ the second zone is non-existant and the boundary-layer model for correlating film cooling data should be useful. The re-derivation, critical examination and extension (to cover foreign gas injection and large density ratios, ρ_c/ρ_m) of the boundary-layer model is the subject of this note.

SURVEY OF PREVIOUS THEORETICAL WORK

Wieghardt [2] made one of the first investigations of slot injection in connexion with the problem of de-icing. He achieved an asymptotic solution of the turbulent boundary-layer equations of continuity and energy by assuming similarity for both the velocity and temperature profiles. His solution gave $T(y)$ and $T_{aw}(\delta)$ but not $T_{aw}(x)$. Wieghardt noted that the assumption $(\delta/x) \sim Re_x^{-1/5}$ would indicate $T_{aw} \sim x^{-4/5}$, a result in excellent agreement with his experiments, but he was unwilling to take this step. So although he was almost certainly aware of the simple expression for $T_{aw}(x)$ given in this note, he did not write it down, preferring instead to find $T_{aw}(x)$ experimentally.

Since his work provided a foundation for much that was to follow, it is worth considering in more detail. The basic assumptions in his analysis are:

(i) for $x/s \gg 1$ the flow near the wall resembles the flow in a boundary layer
(ii) low Mach number flow, the dynamic temperature rise is neglected
(iii) C_p is constant throughout the flow
(vi) the molecular heat conductivity is neglected in comparison with the eddy heat conductivity
(v) for large x/s the temperature profiles are similar, hence

$$\frac{\sigma}{\sigma_w(x)} = f\left[\frac{y}{\delta_T(x)}\right]$$

where $\sigma = T - T_m$

and $\delta_T(x) = \int_0^\infty (\sigma/\sigma_w)\, dy$

(vi) the mass-velocity profiles are also similar and may be written in power law form

$$\frac{\rho u}{\rho_m u_m} = \left(\frac{y}{\delta}\right)^n$$

(vii) k is a function of x only.

In the light of these assumptions the relevant equations may be written as

$$\frac{\partial(\rho u)}{\partial x} + \frac{\partial(\rho v)}{\partial y} = 0 \quad \text{continuity} \quad (1)$$

$$\rho u \cdot \frac{\partial \sigma}{\partial x} + \rho v \cdot \frac{\partial \sigma}{\partial y} = k \frac{\partial^2 \sigma}{\partial y^2} \quad \text{energy} \quad (2)$$

$$\int_0^\infty \rho u \sigma \, dy = \text{const.} = \rho_c u_c \sigma_c s \quad \text{conservation of energy for the case of an adiabatic wall} \quad (3)$$

By introducing assumptions (v) and (vi) into these equations and applying the boundary conditions

$$\frac{\partial T}{\partial y} = 0, \quad T = T_{aw} \quad \text{at} \quad y = 0$$

$$T = T_m \quad \text{at} \quad y = \infty$$

Wieghardt solves for $\sigma(y)$ obtaining

$$\frac{\sigma}{\sigma_{aw}} = \exp\left[-C_1 \left(\frac{y}{\delta_T}\right)^{n+2}\right] \quad (4)$$

where

$$C_1 = \left\{\Gamma\left(\frac{n+3}{n+2}\right)\right\}^{n+2}.$$

Substituting this result in the energy balance

equation (3), and defining δ by $y = \delta$ when $\sigma/\sigma_{aw} = 0{\cdot}1$, he finds that for $n = 1/7$

$$\frac{\sigma_{aw}}{\sigma_c} = \frac{T_{aw} - T_m}{T_c - T_m} = \eta = 2{\cdot}01\frac{ms}{\delta}. \qquad (5)$$

Wieghardt points out that further progress is impossible since the variation of δ with x is unknown. However, if the assumption is made that $\delta = 0{\cdot}37\, x\, Re_x^{-1/5}$ then one obtains the result

$$\eta = 5{\cdot}44\left(\frac{x}{ms}\right)^{-0{\cdot}8}\left(Re_c \cdot \frac{\mu_c}{\mu_m}\right)^{0{\cdot}2}. \qquad (6)$$

Hartnett *et al.* [3] adopted Wieghardt's analysis but simplified the mathematics by writing equation (4) as

$$\sigma/\sigma_{aw} = \exp\left[-C(y/\delta)^2\right] \quad \text{since} \quad n \ll 2 \qquad (7)$$

Expanding the right-hand side of (7), retaining only the first three terms and substituting in (3) gives

$$\int_0^1 \left(\frac{y}{\delta}\right)^{1/7}\left[1 - C_2(y/\delta)^2 + C_2^2(y/\delta)^4\right] \mathrm{d}(y/\delta) = \frac{\sigma_c}{\sigma_{aw}} \cdot \frac{ms}{\delta}.$$

The left-hand side is a constant and assuming now that $\delta = B\, x\, Re^{-1/5}$ and $\mu_c = \mu_m$ the authors obtain

$$\eta = \frac{\sigma_{aw}}{\sigma_c} = K\left(\frac{x}{ms}\right)^{-0{\cdot}8} Re_c^{0{\cdot}2}. \qquad (8)$$

In a graphical comparison of (8) with experiment the dependence of η on Re_c is omitted and a ± 40 per cent scatter noted. If $\mu_c \neq \mu_m$ and B is taken as 0·37 then (8) becomes

$$\eta = 3{\cdot}39\left(\frac{x}{ms}\right)^{-0{\cdot}8}\left(Re_c\frac{\mu_c}{\mu_m}\right)^{0{\cdot}2}. \qquad (9)$$

Rubesin [4] tackled the problem of the heat-transfer rate distribution along a flat plate with a step discontinuity in surface temperature. For a given unheated starting length L and wall temperature distribution $T_w(x)$ he found that the heat-transfer coefficient was

$$H(x, L) = \frac{q}{T_w - T_m} = 0{\cdot}0288\frac{k}{x} Re_x^{4/5}\, Pr^{1/3}\left[1 - \left(\frac{L}{x}\right)^{39/40}\right]^{-7/39}. \qquad (10)$$

His analysis used the integral form of the boundary-layer energy equation and among the assumptions were the following:

$$\frac{u}{u_m} = \left(\frac{y}{\delta}\right)^{1/7} \qquad (11a)$$

$$\delta = 0{\cdot}37\, x\, Re_x^{-1/5} \qquad (11b)$$

$$\theta = \frac{T - T_w}{T_m - T_w} = \left(\frac{y}{\delta_T}\right)^{1/7}. \qquad (12)$$

Klein and Tribus [5] solved the inverse problem of finding $T_w(x)$ when the heat flux $q(x)$ is prescribed. They show that if H can be written as

$$H(x, L) = f(x)\,(x^\alpha - L^\alpha)^{-\beta}$$

then

$$T_w(x) - T_m = \int_{L=0}^{x} \frac{q(L)\,(x^\alpha - L^\alpha)^{\beta-1}\,\alpha \cdot L^{\alpha-1}}{f(L)\,(-\beta)!\,(\beta - 1)!}\,\mathrm{d}L \qquad (13)$$

Using the work of Rubesin we have

$\alpha = 39/40$, $\beta = 7/39$,

$$f(x) = 0{\cdot}0288\frac{k}{x} Re_x^{4/5} \cdot Pr^{1/3}\, x^{7/40}.$$

At Eckert's suggestion Klein and Tribus considered the particular example of a line heat source placed at the leading edge of a flat plate and calculated the variation of adiabatic wall temperature along the plate. This example is similar to the film cooling problem, the source simulating the heat released from the coolant slot. Putting

$$q(L)\,\mathrm{d}L = \rho_c\, u_c\, s\, C_{p_c}(T_c - T_m)$$

at $x = 0$,

$$q = 0 \quad \text{for} \quad x > 0$$

and

$$L = 0$$

then equation (13) becomes

$$\eta = 5{\cdot}77\left(\frac{C_{p_c}}{C_{p_m}}\right) Pr_m^{2/3}\left(\frac{x}{ms}\right)^{-0{\cdot}8}\left(Re_c\frac{c}{\mu m}\right)^{0{\cdot}2} \qquad (14)$$

If $C_{p_c}/C_{p_m} = 1$ and $Pr_m = 0{\cdot}72$ then (14) reads

$$\eta = 4{\cdot}62\left(\frac{x}{ms}\right)^{-0{\cdot}8}\left(Re_c\frac{\mu_c}{\mu_m}\right)^{0{\cdot}2} \qquad (15)$$

In a more recent analysis Seban and Back [6] note the similarity between the approximate form of Wieghardt's temperature profile

$$\sigma/\sigma_{aw} = \exp[-C_2(y/\delta)^2] \quad \text{(see page 57)} \quad (7)$$

and a particular solution of the heat conduction equation,

$$\sigma/\sigma_w = \exp[-y^2/4\xi] \quad \text{where} \quad \xi = \int \alpha \, dt \quad (16)$$

The analogous equations are

$$\frac{\partial^2 T}{\partial y^2} = \frac{1}{\alpha(t)} \cdot \frac{\partial T}{\partial t} \quad \text{where} \quad \alpha = k/\rho C_p \quad (17)$$

and

$$\frac{\partial^2 T}{\partial y^2} = \frac{1}{\beta(x)} \cdot \frac{\partial T}{\partial t}, \quad \text{where} \quad \beta = k_e/\rho u C_p, \quad (18)$$

a rather gross contraction of the energy equation. Seban and Back, relying on the work of Hinze [6], take

$$\beta(x) = 0{\cdot}7 \, \delta_2 \sqrt{(C_f/2)}$$
$$\delta_2 = 0{\cdot}036 \, x \, Re_x^{-1/5}$$
$$C_f/2 = 0{\cdot}0296 \, Re_x^{-1/5}$$

Thus $\beta \sim x^{0{\cdot}7}$ and from the analogy we have $\delta^2 \sim \int \beta \, dx$, i.e.

$$\delta \sim x^{0{\cdot}85}$$

Use of the conservation of energy, equation (3), then leads to the final result

$$\eta = 11{\cdot}2 \left(\frac{x}{ms}\right)^{-0{\cdot}85} \left(Re_c \frac{\mu_c}{\mu_m}\right)^{0{\cdot}15} \quad (19)$$

There is one other theoretical model [8] for the film cooling process which, in contrast to the previous papers, begins by assuming that the coolant film exists as a discreet layer (no mixing). Two empirical modifications are then made to take care of the mixing phenomena. As might be expected this model provides a good basis for correlating experimental data [8] taken reasonably close to the coolant slot, ($0 < x/s < 150$). In view of the empirical nature of the modifications to the initial theory this model is not included here.

A MORE SIMPLE ANALYSIS

The assumptions here are:

(i) the flow is boundary-layer-like and $\delta = 0{\cdot}37 \, x \, Re_x^{-1/5}$

(ii) the coolant and mainstream gases have the same composition

(iii) the temperature differences are small enough for C_p to be constant

(iv) the pressure is constant throughout the flow field

(v) the temperature and velocity boundary layers have the same thickness

(vi) the stagnation enthalpy is uniform across any section therefore $T_o = f(x)$ only

(vii) the mass-velocity power law holds with $n = 1/7$, i.e.

$$\frac{\rho u}{\rho_m u_m} = \left(\frac{y}{\delta}\right)^{1/7} \quad (20)$$

From an energy (total enthalpy) balance with an adiabatic wall and $C_{p_m} = C_{p_c} = C_p$ we have

$$\dot{m}_{bl} \, C_p \, T_{aw} = \dot{m}_c \, C_p \, T_{oc} + \dot{m}_e \, C_p \, T_{om} \quad (21)$$

The mass flow rate in the boundary layer is

$$\dot{m}_{bl} = \int_0^{\delta} \rho u \, dy$$

which from (20) gives

$$\dot{m}_{bl} = (7/8) \, \rho_m \, u_m \, \delta$$

The mass entrained in the boundary layer $\dot{m}_e$ is then

$$\dot{m}_e = \dot{m}_{bl} - \dot{m}_c$$

where $\dot{m}_c$ is the coolant mass flow rate

$$\dot{m}_c = \rho_c \, u_c \, s.$$

Substitution in (21) gives immediately

$$\eta' = \frac{h_{aw} - h_{om}}{h_{oc} - h_{om}} = \frac{8}{7} \cdot \frac{\rho_c \, u_c \, s}{\rho_m \, u_m \, \delta}.$$

Using assumption (i) and introducing a slot Reynolds number as $Re_c = (\rho_c u_c s/\mu_c)$ we obtain

$$\eta' = 3{\cdot}09 \left(\frac{x}{ms}\right)^{-0{\cdot}8} \left(Re_c \frac{\mu_c}{\mu_m}\right)^{0{\cdot}2} \quad (22)$$

Foreign-gas injection

This simple analysis may be extended to cover the case of foreign gas injection by relaxing assumption (iii) and substituting

$$C_p(x) = \frac{\dot{m}_e \, C_{p_m} + \dot{m}_c \, C_{p_c}}{\dot{m}_{bl}} \quad (23)$$

The result then is

$$\left.\begin{aligned}\eta' = \frac{C_p T_{aw} - C_{p_m} T_{om}}{C_{p_c} T_{oc} - C_{p_m} T_{om}} = \\ \frac{1}{1 + \frac{C_{p_c}}{C_{p_m}}\left\{\frac{T_{oc} - T_{aw}}{T_{aw} - T_{om}}\right\}} = \\ 3{\cdot}09\left(\frac{x}{ms}\right)^{-0{\cdot}8} \times \left(Re_c \frac{\mu_c}{\mu_m}\right)^{0{\cdot}2}\end{aligned}\right\} \quad (24)$$

This may be rearranged to read

$$\eta'' = \frac{T_{aw} - T_{om}}{T_{oc} - T_{om}} = \frac{C_3 \eta'}{1 + (C_3 - 1)\eta'}$$

$$\text{where} \quad C_3 = C_{p_c}/C_{p_m} \qquad (25)$$

and η' is given by (22) or (24). For $C_3 = 1$, η' and η'' are identical. For $C_3 \neq 1$ equation (25) shows that, for large x/ms, $\eta'' \to C_3\eta'$. A result indicating the benefit of using a coolant with a large specific heat.

A comparison of the theoretical results

All but one [8] of the theories mentioned above are based on a boundary-layer model of the flow. They necessarily assume mixing of the coolant with the mainstream and are strictly asymptotic solutions valid only for large x/s. The precise definition of "large" can be found by correlating the experimental data. This is done later in the paper. It is interesting just to compare the theoretical results of Wieghardt, Hartnett *et al.* Tribus and Klein with the simple analysis presented here. The relevant expressions are

$$\eta = \eta' = 5{\cdot}44\,(\bar{x})^{-0{\cdot}8} \qquad \text{(reference 2)}$$

$$\eta = \eta' = 3{\cdot}39\,(\bar{x})^{-0{\cdot}8} \qquad \text{(reference 3)}$$

$$\eta = \eta' = 4{\cdot}62\,(\bar{x})^{-0{\cdot}8} \qquad \text{(reference 5)}$$

$$\eta' = 3{\cdot}09\,(\bar{x})^{-0{\cdot}8} \qquad \text{(this paper)}$$

where

$$\bar{x} = (x/ms)\,(Re_c\,\mu_c/\mu_m)^{-1/4}$$

For the case of foreign gas injection

$$\eta = 4{\cdot}62\,(C_{p_c}/C_{p_m})\,(\bar{x})^{-0{\cdot}8} \qquad \text{(reference 5)}$$

$$\eta' = 3{\cdot}09\,(\bar{x})^{-0{\cdot}8} \qquad \text{(this paper)}$$

where

$$\eta = \frac{C_{p_c}}{C_{p_m}}\eta' \Big/ \left[1 + \left(\frac{C_{p_c} - C_{p_m}}{C_{p_m}}\right)\eta'\right]$$

provided

$$T_o \simeq T.$$

The striking similarity between the various analyses is not surprising since they all use the 1/7th power law similarity solution for the velocity profile together with an energy balance equation. The different constants result from differing approximations to the temperature profile. For example Wieghardt obtains an exponential form, Rubesin assumes a 1/7th power law temperature profile and in the simple analysis of this paper the total temperature T_o is assumed constant across the boundary layer.

COMPARISON WITH SOME EXPERIMENTAL DATA

A selection of the available experimental data has been made covering the widest ranges of slot Reynolds number, density ratio ρ_c/ρ_m and velocity ratio u_c/u_m, and correlated using equations (22) and (24), in an attempt to test the validity of these equations. In particular it is important to know over what range of

$$m(= \rho_c u_c/\rho_m u_m)$$

a boundary-layer model of the flow is likely to be valid.

Data [2, 3, 9] obtained at three widely different slot Reynolds numbers are presented in Fig. 2(a) as a plot of η' against x/ms. Hartnett *et al.* [3] produced a similar picture and noted a ± 40 per cent scatter about their own experimental data. Figure 2(b) demonstrates now the three sets of data chosen are brought closer together by plotting η' against $\bar{x}$ as suggested by most of the theoretical treatments. The final slope of the best curve through the data correlated in this way is close to $-0{\cdot}8$ but the data suggests a value of the constant in equation (22) rather larger than 3·09. A further comparison is made in Fig. 3 using the data of Wieghardt [2] and Seban [9]. For $0 \leqslant m \leqslant 1{\cdot}5$ their data are all expressible in the form $\eta' = A(\bar{x})^{-0{\cdot}8}$. Table 1 and Fig. 3 give the value of the constant A and show that for $m \leqslant 1$ the constant is nearer 3·7. Beyond $m = 1$

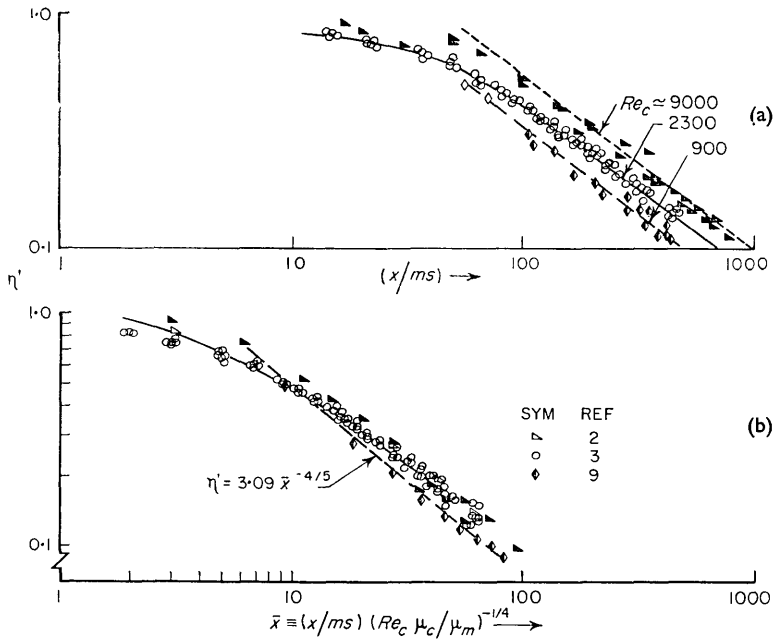

FIG. 2. The improvement of data correlation by inclusion of slot Reynolds number.

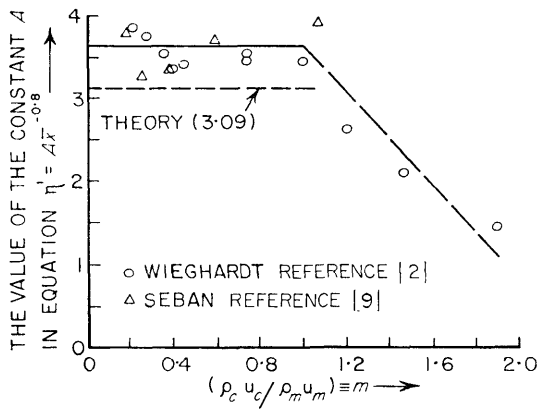

FIG. 3. The value of the constant A in the equation $\eta' = A(\bar{x})^{-4/5}$.

the constant falls rapidly and for $m > 1{\cdot}5$ the slope of the experimental curve changes as shown in Fig. 4, indicating the inadequacy of the boundary-layer model for this range of m.

The data of Chin *et al.* [10] for single and multiple slots were correlated empirically in the original paper. They are replotted in the way suggested by equation (22) in Fig. 5. Although the data do not fit the equation both the single and the ten-slot data correlate very well using the ordinates appropriate to the turbulent

Table 1. *The value of the constant A in the expression* $\eta' = A\bar{x}^{-0{\cdot}8}$

Ref. and Symbol	m	$Re_1(\mu_c/\mu_m)$	A
Wieghardt [2]	0·22	5300	3·85
●	0·28	7400	3·72
	0·36	8900	3·92
	0·40	11500	3·33
	0·40	5000	3·33
	0·45	1200	3·40
	0·74	9100	3·52
	0·74	9900	3·48
	1·01	12500	3·48
	1·20	12200	2·62
Seban [9]	1·45	12800	2·10
▲	1·90	13100	1·48
	0·18	7100	3·78
	0·26	1500	3·28
	0·39	3100	3·37
	0·59	7250	3·71
	1·08	6100	3·93

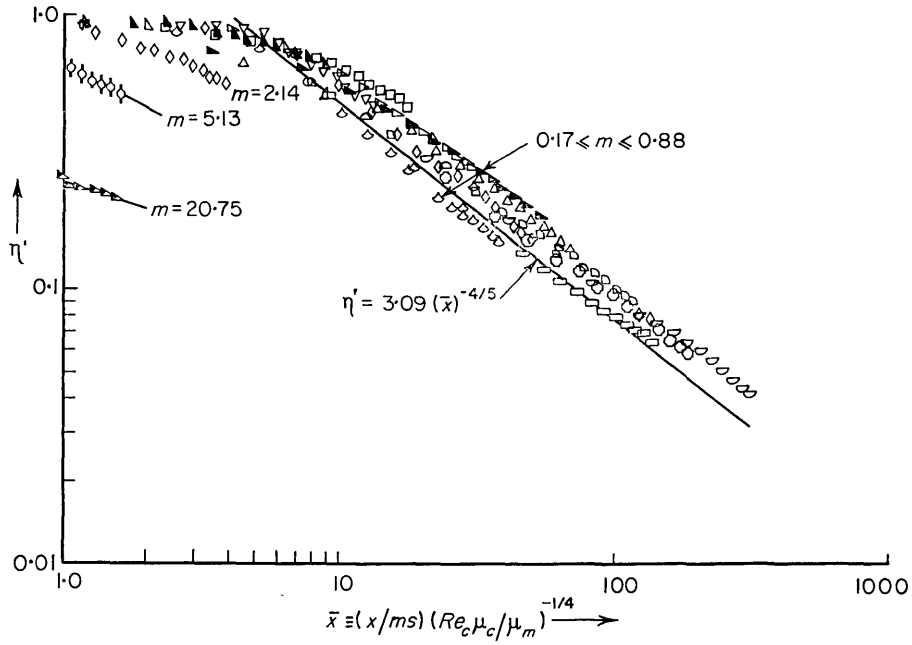

FIG. 4. Data taken from reference 9 to show the range of m for which the boundary-layer model is useful.

boundary-layer model. For the multi-slot case x is measured from the last slot and s is the height of an equivalent single slot through which all the cooling fluid passes. Finally the 20 row louvre data of Chin *et al.* is replotted, Fig. 5(b); again correlation is good. The negative slope of the correlated data tends towards 0·8, then decreases again for large (x/ms) because, according to reference 10, there was heat conduction through the plate.

In all the experimental data considered so far the density differences, temperature differences and flow velocities have been small so that ideas based on incompressible turbulent boundary layer theory might be expected to succeed. It is possible that the simple analysis given here may be useful under compressible flow conditions since experiments [12] have shown that the velocity profile on a flat adiabatic plate appears to be almost independent of Mach number and that the formula $\delta = 0{\cdot}37\, x\, Re_x^{-1/5}$ is usable up to $M = 2{\cdot}5$ at least. The highest Mach number data currently available is that of references 8 and 11. In reference 11 the values of η' are not unity at $x = 0$, the reason being [13] that the coolant temperature was measured well upstream of the slot and there was appreciable heat transfer between the measuring station and the slot exit. The results have therefore been corrected† and plotted in Fig. 6, they correlate very well on the basis of equation (22). The highest freestream Mach number used in the tests was 0·78. The coolant and freestream gas was air. In a later series of tests [8] helium was used as the coolant with injection velocities up to 3680 ft/s, $(M_c \simeq 1)$. Again the highest freestream Mach number was approximately 0·8. The data selected from reference 8 covered the whole range of test variables including the highest value of m (i.e. 1·57). At this value of m the velocity ratio u_c/u_m was 3·83. The results are compared with equation (24) in Fig. 7. Considering the simplicity of the analysis for foreign gas injection the agreement is encouraging but not good enough for design purposes. A more realistic approach is obviously needed for the compressible turbulent boundary-layer flow of a gas mixture.

† $\eta'(x)$ corrected $= \eta'(x)/\eta'(x=0)$.

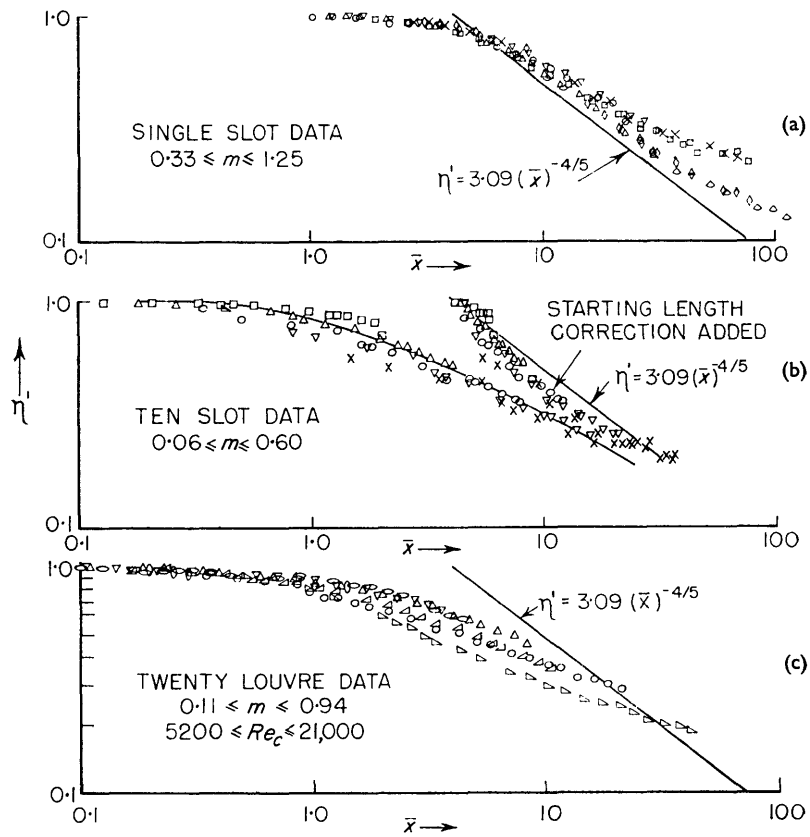

FIG. 5. The correlation of single, multi-slot and louvre data from reference 10.

POSSIBLE EXTENSIONS OF THE ANALYSIS

Corrections for finite δ *at* $x = 0$

Clearly the analyses presented here are only valid for large x/s. A "new" boundary layer is assumed to grow from the slot exit and to have zero thickness there. It should be possible to improve the analysis by taking account of the slot mass flow by equating one of its characteristics to that of a fictitious boundary layer growing from a point at a distance x_o ahead of the slot. For example, equating the mass flow in the fictitious boundary layer to that coming from the slot gives

$$\rho_c u_c s = \int_0^{\delta} \rho u \, dy = \rho_m u_m \int_0^1 (y/\delta)^{-1/7} \, d(y/\delta) =$$

$$= \tfrac{7}{8} \rho_m u_m \delta$$

Putting $\delta = 0{\cdot}37\, x_o\, Re_{x_o}^{-1/5}$ gives on re-arrangement

$$\frac{x_o}{ms}\left(Re_c \frac{\mu_c}{\mu_m}\right)^{1/4} = 4{\cdot}1 \qquad (26)$$

Adopting this correction in the analysis changes the relation (22) to

$$\eta' = 3{\cdot}09\,[\bar{x} + 4{\cdot}1]^{-0{\cdot}8} \qquad (27)$$

This result has the additional advantage that $\eta' \to 1$ as $x \to 0$. The correction is easy to apply and undoubtedly improves the agreement with "theory" as demonstrated in Fig. 5(b). However much useful experimental data in the region $0 < \bar{x} < 10$ is effectively "lost" if (27) is used moreover the *correlation* is not improved. The aim here is to demonstrate that the parameter $\bar{x}$ has theoretical justification and practical utility

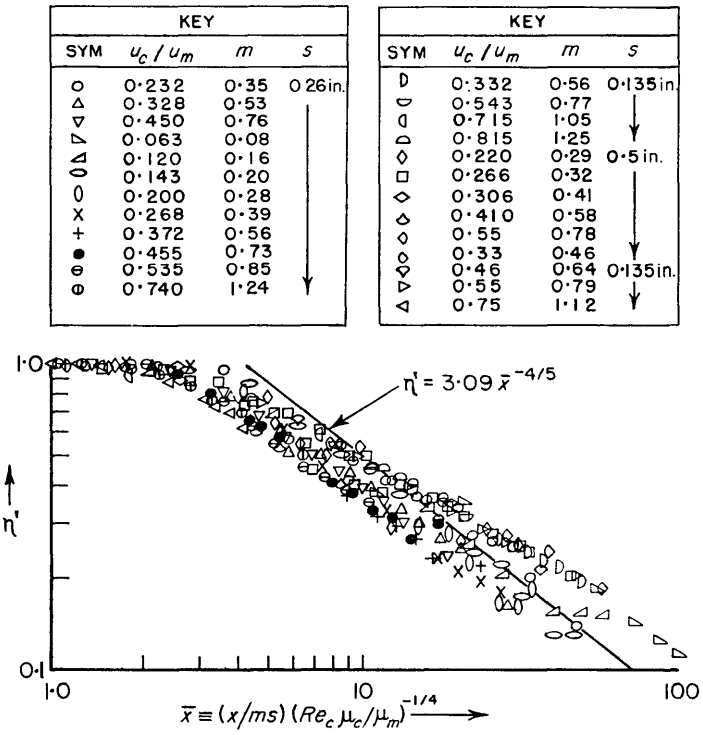

FIG. 6. The data of Papell and Trout [11] for air injection into a high temperature air mainstream.

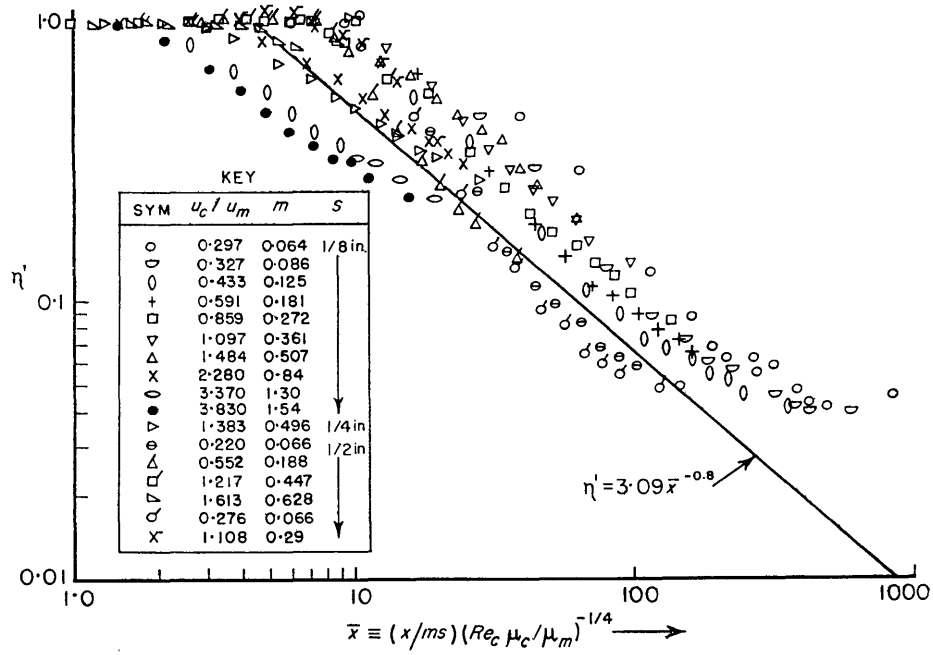

FIG. 7. The data of Hatch and Papell [8] for helium injection into air.

for correlating film cooling data, rather than to obtain the best possible fit between experiment and theory. The temptation to apply corrections has therefore been resisted.

The effect of pressure gradient

The simple analysis given here can obviously be extended to non-zero pressure gradient conditions provided $\delta(x)$ can be calculated. Numerous methods of calculation exist and in a correlation of some of these Stratford and Beavers [14] suggest

$$\left.\begin{aligned} &\delta = 0{\cdot}37\, X\, Re_X^{-1/5} \\ &\text{where} \\ &X = P^{-1} \int_0^x P\, \mathrm{d}x \\ &\text{and} \\ &P = \left[M \Big/ \left(1 + \frac{\gamma - 1}{2} M^2\right)\right]^4 \end{aligned}\right\} \quad (28)$$

for free stream Reynolds numbers of the order of 10^6. The substitution of X for x in the parameter $\bar{x}$ should then correlate film cooling data obtained in the presence of a pressure gradient.

Heat transfer

Hartnett *et al.* [3] have shown that the standard solid-wall heat-transfer relations between Stanton number and Re_x may be used for predicting the heat transfer in the presence of film cooling provided that

(a) the coefficient of film cooling is defined as

$$H = \frac{q}{T_w - T_{aw}} \quad (29)$$

where T_{aw} is now the local value determined, for example, from equation (22),

(b) the properties used to evaluate the Reynolds number and Stanton number are evaluated at the reference temperature T^* where

$$T^* = 0{\cdot}5\,(T_w + T_m) + 0{\cdot}22\,(T_{aw} - T_m) \quad (30)$$

Temperatures T_w and T_{aw} are again local values.

Seban [9] defined H in the same way and provided m was less than one he obtained good agreement with the Colburn equation

$$\frac{H}{\rho_m\, u_m\, C_p} = 0{\cdot}37\, Re_x^{-1/5} \quad (31)$$

for $x/s \geqslant 50$. These two pieces of data suggest that a knowledge of the adiabatic wall temperature plus the use of Eckert's reference enthalpy method might lead to a solution of the film-cooled-wall with heat-transfer problem. More experimental data are urgently needed to confirm or destroy this suggestion.

CONCLUSIONS

The boundary-layer model of a film-cooled surface has been used by a number of authors to derive an analytical expression for effectiveness in the form

$$\eta' = \text{const.} \left\{ \frac{x}{ms} \cdot \left(Re_c \frac{\mu_c}{\mu_m} \right)^{-1/4} \right\}^{-0{\cdot}8}$$

The present paper derives this result in a far simpler manner than has been used before. The paper emphasizes that the effectiveness should be based on enthalpy rather than temperature and that if this is done the same expression is theoretically valid for foreign gas injection.

The boundary-layer model correlates a wide range of data provided $0 \leqslant m \leqslant 1{\cdot}5$. It can be used for multi-slot or louvre cooling by postulating a single equivalent slot.

The analysis can be extended very simply to cover the effects of pressure gradient and heat transfer. More experimental data are needed to test the validity of such extensions.

It must be emphasized that the boundary-layer model is strictly an asymptotically correct solution of the film cooling problem. As such its accuracy improves as x/s increases and at infinity it must hold no matter what the initial conditions. However, the model is clearly inadequate for $m > 1{\cdot}5$ over the range of x/s currently of interest, and inaccurate close to the coolant slot when there are large density differences between the coolant and mainstream gases.

ACKNOWLEDGEMENTS

The authors wish to thank Professor D. B. Spalding for his encouragement and for his constructive criticism of this paper. The authors are also grateful to Mr. E. H. Cole, Dr. V. K. Jain and Mr S. J. Peerless for many helpful discussions.

REFERENCES

1. D. B. Spalding, Heat and mass transfer in boundary layers, Part 2. Film cooling. Northern Research and Engineering Corp. Report No. 1058–2 (September 1962).

2. K. WIEGHARDT, On the blowing of warm air for de-icing devices *F.B.* 1900 (1944). Reports and Translations No. 315.
3. J. P. HARTNETT, R. C. BIRKEBAK and E. R. G. ECKERT, Velocity distributions, temperature distributions, effectiveness and heat transfer for air injected through a tangential slot into a turbulent boundary layer, *J. Heat Transfer, Trans. A.S.M.E.* Series C, **83**, 293–306 (1961).
4. M. W. RUBESIN, The effect of arbitrary surface-temperature variation along a flat plate on the convective heat transfer in an incompressible turbulent boundary layer. *NACA TN* 2345 (April 1951).
5. J. KLEIN and M. TRIBUS, Forced convection from non-isothermal surfaces. Heat transfer, a symposium, University of Michigan Press, Ann Arbor, Michigan (1953).
6. R. A. SEBAN and I. H. BACK, Velocity and temperature profiles in turbulent boundary layers with tangential injection, *J. Heat Transfer, Trans. A.S.M.E.* Series C, **84**, 45–54 (1962).
7. J. O. HINZE, *Turbulence*, Figs. 7–17, p. 493. Mc-Graw Hill, New York (1959).
8. J. E. HATCH and S. S. PAPELL, Use of a theoretical flow model to correlate data for film cooling or heating an adiabatic wall by tangential injection of gases of different fluid properties. *NASA TN D*-130 (November 1959).
9. R. A. SEBAN, Heat transfer and effectiveness for a turbulent boundary layer with tangential fluid injection, *J. Heat Transfer, Trans. A.S.M.E.* Series C, **82**, 303–312 (1960).
10. J. H. CHIN, S. C. SKIRVIN, L. E. HAYES and F. BURGGRAF, Film cooling with multiple slots and louvres, *J. Heat Transfer, Trans. A.S.M.E.* Series C, **83**, 281–293 (1961).
11. S. S. PAPELL and A. M. TROUT, Experimental investigation of air film cooling applied to an adiabatic wall by means of an axially discharging slot. *NASA TN D*-9 (August 1959).
12. R. J. MONAGHAN and J. E. JOHNSON, The measurement of heat transfer and skin friction at supersonic speeds. Part II. Boundary layer measurements on a flat plate at $M = 2{\cdot}5$ and zero heat transfer. *A.R.C.* 18,490 (1956).
13. S. S. PAPELL, private communication.
14. B. S. STRATFORD and G. S. BEAVERS, The calculation of the compressible turbulent boundary layer in an arbitrary pressure gradient—A correlation of certain previous methods. *A.R.C. R. & M.* 3207.

Résumé—Le modèle de la couche limite pour corréler les données expérimentales sur les parois adiabatiques refroidies par film est réexaminé. Les analyses existantes sont passées en revue. Une approche beaucoup plus simple est donnée qui peut aussi couvrir le cas de l'injection d'un gaz étranger. L'utilité et les limitations du modèle de la couche limite sont mises en relief par comparaison avec les données expérimentales.

Zusammenfassung—Das Grenzschichtmodell, das experimentell ermittelte Werte mit Film-gekühlten adiabaten Wänden in Beziehung setzt, wird überprüft. Bestehende Analysen dazu werden durchgeseshen. Es wird eine viel einfachere Näherung gegeben, die auch den Fall der Fremdgaseinspritzung erfassen kann. Die Grenzen und die Verwendbarkeit des Grenzschichtmodells wird durch einen Vergleich mit experimentellen Ergebnissen gezeigt.

Аннотация—Вновь анализируется модель пограничного слоя для корреляции экспериментальных данных для стенок при пленочном охлаждении в адиабатических условиях. Снова рассматриваются существующие анализы. Дается более простой подход, который также включает случай вдува инородного газа. Применение и ограничения модели пограничного слоя показаны в сравнении с эксперимениальными данными.